

UC Davis

Research reports

Title

Pavement ME JPCP Transverse Cracking Model Calibration and Design Catalog Framework
(Version 2.5.5)

Permalink

<https://escholarship.org/uc/item/03p4h24f>

Authors

Saboori, Ashkan
Lea, Jeremy
Harvey, John
et al.

Publication Date

2021-09-01

DOI

10.7922/G26D5R8W

Pavement ME JPCP Transverse Cracking Model Calibration and Design Catalog Framework (Version 2.5.5)

Authors:

Ashkan Saboori, Jeremy Lea, John Harvey, Jon Lea,
Angel Mateos, and Rongzong Wu

Partnered Pavement Research Center Strategic Plan Element (PPRC SPE) 3.49 (DRISI Task 3199):
Implement Concrete ME Design Tools

PREPARED FOR:

California Department of Transportation
Division of Research, Innovation, and System Information
Office of Materials and Infrastructure

PREPARED BY:

University of California
Pavement Research Center
UC Davis, UC Berkeley




TECHNICAL REPORT DOCUMENTATION PAGE

1. REPORT NUMBER UCPRC-RR-2020-02	2. GOVERNMENT ASSOCIATION NUMBER	3. RECIPIENT'S CATALOG NUMBER
4. TITLE AND SUBTITLE Pavement ME JPCP Transverse Cracking Model Calibration and Design Catalog Framework (Version 2.5.5)		5. REPORT PUBLICATION DATE September 2021
		6. PERFORMING ORGANIZATION CODE
7. AUTHOR(S) Ashkan Saboori (ORCID 0000-0002-8318-3396), Jeremy Lea, (ORCID 0000-0003-3445-8661) John Harvey (ORCID 0000-0002-8924-6212), Angel Mateos (ORCID 0000-0002-3614-2858), and Rongzong Wu (ORCID 0000-0001-7364-7583)		8. PERFORMING ORGANIZATION REPORT NO. UCPRC-RR-2020-02 UCD-ITS-RR-22-23
9. PERFORMING ORGANIZATION NAME AND ADDRESS University of California Pavement Research Center, UC Davis and UC Berkeley Department of Civil and Environmental Engineering, UC Davis 1 Shields Avenue Davis, CA 95616		10. WORK UNIT NUMBER
		11. CONTRACT OR GRANT NUMBER
12. SPONSORING AGENCY AND ADDRESS California Department of Transportation Division of Research, Innovation, and System Information P.O. Box 942873 Sacramento, CA 94273-0001		13. TYPE OF REPORT AND PERIOD COVERED September 2017 to September 2020
		14. SPONSORING AGENCY CODE
15. SUPPLEMENTAL NOTES doi:10.7922/G26D5R8W		
16. ABSTRACT The <i>Mechanistic-Empirical Pavement Design Guide (MEPDG)</i> is a comprehensive method, including models and guidance, developed in 2002 by the American Association of State Highway and Transportation Officials (AASHTO) to analyze and design both flexible and rigid pavements. The <i>MEPDG</i> is implemented in a software called <i>Pavement ME</i> . The <i>MEPDG</i> models were calibrated using data from the Long-Term Pavement Performance (LTPP) sections from throughout the United States, including some from California. The <i>MEPDG</i> recommends that nationally calibrated models be validated using local data and, if necessary, recalibrated. This recommendation is particularly applicable to the Caltrans road network, considering the climate and materials differences between California and the rest of the nation. The first step in recalibrating <i>Pavement ME</i> is to perform a sensitivity analysis to identify which variables are most important and to look for results that do not match expected performance. This was the subject of a previous report titled <i>Pavement ME Sensitivity Analysis</i> . Based on the sensitivity analysis, the decision was made to perform a new calibration of the <i>MEPDG</i> models as implemented in <i>Pavement ME</i> software. A new approach was developed for the calibration. This new approach uses network-level performance data from the pavement management system (PMS) with orders of magnitude more observations and length of pavement than are used in the traditional approach and in the national calibration of the <i>MEPDG</i> models. The framework does not require sampling of materials from specific sections in the network. Rather, it uses the statewide median values from mechanistic testing from a representative sample of materials across the network. Variability of performance and reliability of design (probability that the design will meet or exceed the design life) is accounted for through separate consideration of within-project and between-project variability. The calibration reduced significant bias in the application of the nationally calibrated models to California. This report presents the results of the application of the new procedure to calibrate the <i>Pavement ME</i> transverse cracking model for jointed plain concrete pavements (JPCP). The California pavement management system (PaveM) database—with about 4600 lane-miles of JPCP built on 446 lane replacement projects completed between 1947 and 2017—was used to calibrate the transverse cracking model in <i>Pavement ME</i> . The nationally calibrated <i>Pavement ME</i> transverse cracking model prediction on the PaveM performance database has bias and standard error of 13.3% and 23.03%, respectively. After calibration, the bias and standard error of the locally calibrated model decreased to 0.039% and 5.69%, respectively.		
17. KEY WORDS Pavement ME, jointed plain concrete pavement, calibration, design catalog, transverse cracking, performance data		18. DISTRIBUTION STATEMENT No restrictions. This document is available to the public through the National Technical Information Service, Springfield, VA 22161
19. SECURITY CLASSIFICATION (of this report) Unclassified	20. NUMBER OF PAGES 110	21. PRICE None

Reproduction of completed page authorized

UCPRC ADDITIONAL INFORMATION

1. DRAFT STAGE Final	2. VERSION NUMBER 1				
3. PARTNERED PAVEMENT RESEARCH CENTER STRATEGIC PLAN ELEMENT NUMBER 3.49	4. DRISI TASK NUMBER 3199				
5. CALTRANS TECHNICAL LEAD AND REVIEWER(S) D. Rufino Feldman	6. FHWA NUMBER CA213199B				
7. PROPOSALS FOR IMPLEMENTATION					
8. RELATED DOCUMENTS UCPRC-RR-2019-02					
9. LABORATORY ACCREDITATION The UCPRC laboratory is accredited by AASHTO re:source for the tests listed in this report					
10. SIGNATURES					
A. Saboori FIRST AUTHOR	J.T. Harvey L. Khazanovich TECHNICAL REVIEW	D. Spinner EDITOR	J.T. Harvey PRINCIPAL INVESTIGATOR	D. Rufino Feldman CALTRANS TECH. LEAD	T.J. Holland CALTRANS CONTRACT MANAGER

Reproduction of completed page authorized

TABLE OF CONTENTS

LIST OF FIGURES	iv
LIST OF TABLES	v
PROJECT OBJECTIVES	vii
EXECUTIVE SUMMARY	ix
LIST OF ABBREVIATIONS.....	xii
1 INTRODUCTION.....	1
1.1 Previous Calibration and Design Catalog Development	1
1.2 Overview of New Calibration and Design Development.....	3
2 PAVEMENT MANAGEMENT SYSTEM AND JPCP CRACKING STATISTICAL PERFORMANCE MODEL	7
2.1 Introduction.....	7
2.2 Structural Distress Measures in JPCP	8
2.2.1 Concrete Slab Cracking.....	8
2.2.2 Transverse Joint Faulting	10
2.2.3 International Roughness Index (IRI).....	11
2.3 Pavement Structural (As-Built), Traffic, and Climate Data in PaveM Database	11
2.3.1 PCC Slab Thickness	14
2.3.2 PCC Joint Spacing.....	15
2.3.3 Base Type.....	18
2.3.4 Shoulder Type	20
2.3.5 Climate Region.....	23
2.3.6 WIM Spectra	24
2.3.7 Annual Average Daily Truck Traffic (AADTT).....	29
2.4 Statistical Performance Model for First- and Third-Stage Cracking.....	31
2.5 First-Stage-to-Transverse Cracking Model	41
3 PAVEMENT ME CALIBRATION.....	47
3.1 Introduction	47
3.2 Traditional Pavement ME Calibration Process	48
3.3 Variability Affecting Pavement Performance	50
3.4 Effects of Different Variabilities on Pavement ME Transverse Cracking Transfer Function	52
3.4.1 Monte Carlo Simulation Procedure.....	54
3.4.2 Within-Project Variability (WPV)	55
3.4.3 Between-Contractor Variability (BCV)	57
3.4.4 Between-Project Variability (BPV).....	60
3.5 Step-by-Step Procedure for Pavement ME Transverse Cracking Calibration Using PaveM Database	63
3.5.1 Step 1: Identify Roadway Segment	68
3.5.2 Step 2: Prepare PMS Data.....	68
3.5.3 Step 3: Develop Statistical Performance Model.....	69
3.5.4 Step 4: Estimate Median Values for Non-Design Variables	69
3.5.5 Step 5: Run Pavement ME for Each Cell of Data	69
3.5.6 Step 6: Analyze Nationally Calibrated Model Error	72
3.5.7 Step 7: Identify WPV and BCV and Find Calibrated C_5	76
3.5.8 Step 8: Identify Between-Project Variability and Find Calibrated C_4	79
3.5.9 Step 9: Find C_4 Corresponding to 95% Reliability	83
3.5.10 Step 10: Analyze Calibrated Model Error.....	86
4 SUMMARY, CONCLUSIONS, AND RECOMMENDATIONS.....	89
4.1 Summary	89
4.2 Conclusions	91
4.3 Recommendations	92
5 REFERENCES.....	93

LIST OF FIGURES

Figure 2.1: Pavement section length distribution.....	12
Figure 2.2: JPCP project construction year distribution.....	12
Figure 2.3: JPCP pavement age distribution.	13
Figure 2.4 PCC slab thickness distribution.	14
Figure 2.5: JPCP total cracking for different PCC slab thicknesses.	15
Figure 2.6: PCC slab pattern distribution.	16
Figure 2.7: PCC slab pattern history distribution.....	17
Figure 2.8: JPCP total cracking for different PCC slab patterns.....	18
Figure 2.9: Base type distribution.	19
Figure 2.10: JPCP total cracking for different base types.....	20
Figure 2.11: Shoulder type distribution.....	21
Figure 2.12: JPCP total cracking for different shoulder types.	22
Figure 2.13: Probability of different distress types versus slab length for WRF shoulders.....	23
Figure 2.14: Climate region distribution.	23
Figure 2.15: JPCP total cracking for different climate regions.....	24
Figure 2.16: Single equivalent axle load distributions of the different WIM spectra.	28
Figure 2.17: WIM spectra distribution.	29
Figure 2.18: JPCP total cracking for different WIM spectra.	29
Figure 2.19: AADTT per lane distribution.....	30
Figure 2.20: JPCP total cracking for different AADTTs per lane.....	31
Figure 2.21: Mixed-effects cracking performance model predictions for different PCC slab thicknesses.....	36
Figure 2.22: Mixed-effects cracking performance model predictions for different PCC slab patterns.	37
Figure 2.23: Mixed-effects cracking performance model predictions for different base types.	38
Figure 2.24: Mixed-effects cracking performance model predictions for different shoulder types.....	39
Figure 2.25: Mixed-effects cracking performance model predictions for different climate regions.	39
Figure 2.26: Mixed-effects cracking performance model predictions for a cell of data.	41
Figure 2.27: First-stage cracking to transverse cracking model predictions for different shoulder types.	43
Figure 2.28: First-stage cracking to transverse cracking model predictions for different climate regions.	44
Figure 3.1: <i>Pavement ME</i> transverse cracking transfer function.	53
Figure 3.2: Accumulated damages versus number of load repetitions for 1,000 pavement segments.....	55
Figure 3.3: Transverse cracking (percent of slabs transverse cracked) versus number of load repetitions for 1,000 pavement segments.	56
Figure 3.4: Transverse cracking histories for projects with different standard deviation in modulus of rupture.	58
Figure 3.5: Transverse cracking histories for projects with different standard deviation in applied stress.	59
Figure 3.6: Transverse cracking histories for projects with different standard deviations in modulus of rupture and applied stress.	59
Figure 3.7: Transverse cracking histories for projects with different mean values and zero standard deviation in modulus of rupture and applied stress.	60
Figure 3.8: Transverse cracking histories for projects with different mean values in modulus of rupture and applied stress in a semi-log plot.....	61
Figure 3.9: Accumulated damage histories for projects with different mean values in modulus of rupture and applied stress in a log-log plot.	63
Figure 3.10: Effects of C_4 coefficient on <i>Pavement ME</i> transfer function.....	66
Figure 3.11: Schematic representation of BPV.....	67
Figure 3.12: Effects of C_5 coefficient on <i>Pavement ME</i> transfer function.....	68
Figure 3.13: A cell of data of cracking performance used for <i>Pavement ME</i> calibration in PaveM database.	70
Figure 3.14: An example of a cell of data with limited observations.	71

Figure 3.15: Decision tree fitted on the nationally calibrated <i>Pavement ME</i> transverse cracking model prediction error for all data.	73
Figure 3.16: Decision tree fitted on the nationally calibrated <i>Pavement ME</i> transverse cracking model prediction error for only short slab pattern 12,13,14,15 ft.	74
Figure 3.17: An example of long slab pattern performance data compared with <i>Pavement ME</i> transverse cracking model prediction showing overprediction error.	74
Figure 3.18: An example of short slab pattern performance data compared with <i>Pavement ME</i> transverse cracking model prediction showing overprediction error.	75
Figure 3.19: An example of short slab pattern performance data along with <i>Pavement ME</i> transverse cracking model prediction showing underprediction error.	75
Figure 3.20: An example of a Monte Carlo simulation on a cell of data.	77
Figure 3.21: An example of Monte Carlo simulation on a cell of data grouped by slab length.	78
Figure 3.22: Schematic representation of cracked slabs and fitted logistic regression model.	79
Figure 3.23: Mixed-effects cracking performance model predictions for a cell of data.	80
Figure 3.24: The expected (average) performance of the pavement after removing BPV.	82
Figure 3.25: Distribution of random effect variable in mixed-effects cracking performance model.	84
Figure 3.26: Example of locally calibrated <i>Pavement ME</i> transverse cracking model prediction with 50% and 95% reliabilities for long slab pattern for one cell.	85
Figure 3.27: Example of locally calibrated <i>Pavement ME</i> transverse cracking model prediction with 50% and 95% reliabilities for short slab pattern for all cells as seen applied to one cell.	86
Figure 3.28: Predicted transverse cracking from nationally calibrated <i>Pavement ME</i> transverse cracking model versus measured transverse cracking.	87
Figure 3.29: Predicted transverse cracking from locally calibrated <i>Pavement ME</i> transverse cracking model versus measured transverse cracking.	88

LIST OF TABLES

Table 2.1: Truck Class Distribution	25
Table 2.2: Hourly Distribution	26
Table 2.3: Axles-Per-Truck Distribution (Common to all WIMs).....	27
Table 2.4: Mixed-Effects Cracking Performance Model Random Effect Parameter.....	34
Table 2.5: Mixed-Effects Cracking Performance Model Location (Fixed) Parameters.....	35
Table 2.6: Mixed-Effects Cracking Performance Model Threshold Parameters	36
Table 3.1: Calibrated C_4 for 50% Reliability	83
Table 3.2: Calibrated C_4 for 95% Between-Project Reliability	84

DISCLAIMER

This document is disseminated in the interest of information exchange. The contents of this report reflect the views of the authors who are responsible for the facts and accuracy of the data presented herein. The contents do not necessarily reflect the official views or policies of the State of California or the Federal Highway Administration. This publication does not constitute a standard, specification, or regulation. This report does not constitute an endorsement by the Department of any product described herein.

For individuals with sensory disabilities, this document is available in alternate formats. For information, call (916) 654-8899, TTY 711, or write to California Department of Transportation, Division of Research, Innovation and System Information, MS-83, P.O. Box 942873, Sacramento, CA 94273-0001.

ACKNOWLEDGMENTS

The authors would like to acknowledge the support, assistance, and direction of Dr. Dulce Rufino Feldman and Dr. T. Joseph Holland of Caltrans, and Prof. Lev Khazanovich, who provided advice and technical review. They would also like to acknowledge the help from UCPRC Senior Editor David Spinner in producing and publishing this report.

PROJECT OBJECTIVES

The goal of Partnered Pavement Research Center Strategic Plan Element (PPRC SPE) 3.49, titled “Implement Concrete ME Design Tools,” is to calibrate *Pavement ME* software for traffic, climate, materials, and construction practices in California and then, based on the calibrated software, update the rigid pavement design catalog in the Caltrans *Highway Design Manual*. An additional goal, if Caltrans decides to pursue it, is to develop a simplified user interface for operating the calibrated version of *Pavement ME*. The following tasks are to be completed to accomplish these goals:

1. Conduct an analysis of the sensitivity of the current version of *Pavement ME* to design variables.
2. Assemble the data needed to calibrate *Pavement ME* for California traffic and climate conditions, materials, and construction practices.
3. Identify any issues with the current version of *Pavement ME* that will have an effect on local calibration or preparation of the design catalog.
4. Calibrate *Pavement ME* for California conditions using calibration data.
5. Develop a design catalog.
6. If Caltrans chooses to develop a simplified user interface:
 - a. Design the experimental factorial and reliability approach for *Pavement ME* runs to create the neural networks necessary for the simplified user interface.
 - b. Develop a simplified web-based user interface using locally calibrated *Pavement ME*.
7. Prepare documentation for the calibration, catalog, and, if developed, the simplified user interface.
8. Assist Caltrans in developing design guidance.

The results in this report demonstrate the new calibration procedure for the *Pavement ME* transverse cracking model for jointed plain concrete pavements (JPCP) using PaveM, California’s pavement management system (PMS) database. The work presented is used to obtain a set of calibrated model coefficients that will be used to develop the Caltrans JPCP design catalog for California.

(This page intentionally blank)

EXECUTIVE SUMMARY

The *Mechanistic-Empirical Pavement Design Guide (MEPDG)*, released in 2002 by the American Association of State Highway and Transportation Officials (AASHTO), details a comprehensive system to analyze and design both flexible and rigid pavements. The *MEPDG* is implemented in a software program called *Pavement ME*. The *MEPDG* models were calibrated using Long-Term Pavement Performance (LTPP) sections from throughout the United States, including some from California. The *MEPDG* recommends that nationally calibrated models be validated using local data and, if necessary, recalibrated. This makes sense for California because of differences between the state's climate and materials and those in the majority of the sections used for the national calibration. The first step in the recalibration process is to perform a sensitivity analysis study to check the reasonableness of the models' predictions, to identify potential software issues, and to help identify and understand the inputs that significantly affect the models' outputs. This was the subject of an earlier University of California Pavement Research Center (UCPRC) research report, *Pavement ME Sensitivity Analysis (Version 2.5.3)*. The next step is to conduct the calibration, which is documented in this report.

In 2006, the UCPRC performed a research study that included an initial sensitivity analysis of jointed plain concrete pavement (JPCP) distress prediction models in the *MEPDG*. That study identified the most important variables affecting predicted performance, including concrete stiffness, concrete coefficient of thermal expansion (CTE), and time to loss of bonding between the concrete and the base. The research study also included the evaluation of *MEPDG* predictions based on the cracking and faulting measured in a limited number of JPCP sections on the California state highway network. The study showed that using the nationally calibrated coefficients resulted in reasonable cracking and faulting predictions and concluded that the default model parameters could be used, but only with appropriate inputs for stiffness and loss of bond. After that research study, the *MEPDG* with nationally calibrated coefficients was used to produce a preliminary design catalog for the Caltrans *Highway Design Manual (HDM)*; Caltrans adjusted that catalog further to produce the one in the current *HDM*.

In 2010, Caltrans developed the capacity for Automated Pavement Condition Survey (APCS) data collection from the state highway network. As a result, a much larger and more reliable pavement condition database is now available in *PaveM*, the California pavement management system (PMS). Due to considerable effort on the part of Caltrans, the database now includes as-built data such as pavement structure, base type, shoulder type, slab length, and construction year—items that were scarce in the previous study but are now available for almost every project built since 1990. These data provide the capability to validate and calibrate *Pavement ME* using thousands of performance data observations and to use the explanatory data in the as-built database. The UCPRC has

collected, in addition to the data in Pavem, detailed data for Caltrans for tens of projects sampled in the early 2000s and 2010s. Those data are for variables not in the as-built database in Pavem, such as concrete materials properties and the stiffnesses of underlying layers.

Updates and improvements in *Pavement ME*, combined with the increased amount and higher quality of data now in Pavem, have created the opportunity to perform a new JPCP prediction model sensitivity analysis and calibration specifically for California. In this study, the latest version of *Pavement ME* (v2.5.5) is used. It should be noted that an earlier version of *Pavement ME* (v2.5.3) was used for the sensitivity analysis. However, after careful investigation, it was found that the *Pavement ME* model predictions remained unchanged.

The traditional approach for validating and calibrating mechanistic-empirical design methods is to collect all data—including performance, as-built, and detailed materials data from tens of sections within a state—and to compare the predicted and measured performance for those few sections. For the national calibration of *Pavement ME*, this was done on the scale of several hundred LTPP sections across the United States. The next *Pavement ME* calibration for California will take advantage of a combination of hundreds of times more performance and as-built data from Pavem as well as detailed materials data collected from tens of sections in the state and validate and calibrate *Pavement ME* with a much more extensive dataset than can be used following the conventional approach. A new approach will be used for the calibration process, and the results will be checked further using the data for the tens of sections in the state that have complete sets of detailed data. This new approach recognizes that in the design-bid-build (low-bid) contracting environment used in California, a designer does not actually know the detailed materials properties when a design is being created. Therefore, the calibration will use median values of the detailed materials properties and recognize the variability caused by different contractors' materials when a design is built. The calibration will also use the detailed information available from Pavem regarding layer types, thicknesses, slab dimensions, shoulder types, dates of construction, and performance data, along with detailed climate and traffic data.

In the previous study that was part of this research, a sensitivity analysis was performed on *Pavement ME* software to check the reasonableness of the models' predictions, to identify potential software issues, and to help identify and understand the inputs that significantly affect the models' outputs. The results of that study are used in this calibration process.

This report provides a detailed description of the new calibration procedure. Pavem data were analyzed and cleaned to make them ready for the calibration. The International Roughness Index (IRI) of doweled concrete pavement is primarily dependent on the initial as-constructed IRI, and it increases very slowly. However, in 1998

Caltrans decided to use dowels in its JPCP construction projects, and this solved the faulting and smoothness issues for those pavements. Consequently, the calibration undertaken in this study focused on the transverse cracking model only.

The MEPDG calibration's first step included the development of a statistical model for predicting JPCP cracking performance. To have a sound calibration even with scattered cracking data, a mixed-effects cracking performance model was developed to account for variability within the pavement. A mixed-effects cracking performance model was developed on first- and third-stage cracking. However, the cracking model in *Pavement ME* predicts transverse cracking. Therefore, to make the cracking performance data suitable for *Pavement ME* calibration, a model was developed based on per-slab data available from APCS 2010–2011 to predict the portion of first-stage cracking that is transverse cracking. This portion of transverse cracking was added to the third-stage cracking data (since third-stage cracking has at least one transverse crack), and the result was used as the total amount of transverse cracking to calibrate the *Pavement ME* transverse cracking model.

Conventional *Pavement ME* calibration has limitations that do not allow for use of the huge amount of performance data in PaveM. Further, the conventional procedure does not consider the variabilities involved in pavement performance. Therefore, models calibrated following that method may predict reasonable average performance while also underestimating variability. Moreover, one of the traditional calibration procedure's other limitations is that it requires project-specific inputs, meaning that field sampling and material testing are needed to calibrate its models. This requirement imposes limits on the number of roadway segments that can be included in a calibration, which can lead to underestimation of model and input errors.

The new calibration procedure described in this report remediates these limitations and accounts for different variabilities involved in pavement performance, while also making use of a huge PMS database with some unknown project-specific variables. This report also includes recommendations on how to implement the study outcomes, including the calibration coefficients and the first-stage-to-transverse cracking model, in the development of the Caltrans JPCP design catalog.

LIST OF ABBREVIATIONS

AADTT	Average annual daily truck traffic
AASHTO	American Association of State Highway and Transportation Officials
AB	Aggregate base
APCS	Automated Pavement Condition Survey
ATPB	Asphalt-treated permeable base
BCV	Between-contractor variability
BPV	Between-project variability
CDF	Cumulative distribution function
CLMM	Cumulative link mixed model
CTB	Cement-treated base
CTE	Coefficient of thermal expansion
FLX	Untied flexible (shoulder type)
HDM	Highway Design Manual
HMA	Hot mix asphalt
IRI	International Roughness Index
JPCP	Jointed plain concrete pavements
LCB	Lean concrete base
LTPP	Long-Term Pavement Performance
MEPDG	Mechanistic-Empirical Pavement Design Guide
MR	Modulus of rupture
NAP	Not applicable (no shoulder)
PCC	Portland cement concrete
PCS	Pavement condition survey
PMS	Pavement management system
RIG	Tied concrete (shoulder type)
SEE	Standard error of estimate
SHS	State highway system
UCPRC	University of California Pavement Research Center
WIM	Weigh-in-motion
WPV	Within-project variability
WRF	Widened concrete (shoulder type)

SI* (MODERN METRIC) CONVERSION FACTORS

APPROXIMATE CONVERSIONS TO SI UNITS				
Symbol	When You Know	Multiply By	To Find	Symbol
LENGTH				
in.	inches	25.40	millimeters	mm
ft.	feet	0.3048	meters	m
yd.	yards	0.9144	meters	m
mi.	miles	1.609	kilometers	km
AREA				
in ²	square inches	645.2	square millimeters	mm ²
ft ²	square feet	0.09290	square meters	m ²
yd ²	square yards	0.8361	square meters	m ²
ac.	acres	0.4047	hectares	ha
mi ²	square miles	2.590	square kilometers	km ²
VOLUME				
fl. oz.	fluid ounces	29.57	milliliters	mL
gal.	gallons	3.785	liters	L
ft ³	cubic feet	0.02832	cubic meters	m ³
yd ³	cubic yards	0.7646	cubic meters	m ³
MASS				
oz.	ounces	28.35	grams	g
lb.	pounds	0.4536	kilograms	kg
T	short tons (2000 pounds)	0.9072	metric tons	t
TEMPERATURE (exact degrees)				
°F	Fahrenheit	(F-32)/1.8	Celsius	°C
FORCE and PRESSURE or STRESS				
lbf	pound-force	4.448	newtons	N
lbf/in ²	pound-force per square inch	6.895	kilopascals	kPa
APPROXIMATE CONVERSIONS FROM SI UNITS				
Symbol	When You Know	Multiply By	To Find	Symbol
LENGTH				
mm	millimeters	0.03937	inches	in.
m	meters	3.281	feet	ft.
m	meters	1.094	yards	yd.
km	kilometers	0.6214	miles	mi.
AREA				
mm ²	square millimeters	0.001550	square inches	in ²
m ²	square meters	10.76	square feet	ft ²
m ²	square meters	1.196	square yards	yd ²
ha	hectares	2.471	acres	ac.
km ²	square kilometers	0.3861	square miles	mi ²
VOLUME				
mL	milliliters	0.03381	fluid ounces	fl. oz.
L	liters	0.2642	gallons	gal.
m ³	cubic meters	35.31	cubic feet	ft ³
m ³	cubic meters	1.308	cubic yards	yd ³
MASS				
g	grams	0.03527	ounces	oz.
kg	kilograms	2.205	pounds	lb.
t	metric tons	1.102	short tons (2000 pounds)	T
TEMPERATURE (exact degrees)				
°C	Celsius	1.8C + 32	Fahrenheit	°F
FORCE and PRESSURE or STRESS				
N	newtons	0.2248	pound-force	lbf
kPa	kilopascals	0.1450	pound-force per square inch	lbf/in ²

*SI is the abbreviation for the International System of Units. Appropriate rounding should be made to comply with Section 4 of ASTM E380. (Revised April 2021)

(This page intentionally blank)

1 INTRODUCTION

1.1 Previous Calibration and Design Catalog Development

The American Association of State Highway and Transportation Officials (AASHTO) 2002 *Mechanistic-Empirical Pavement Design Guide (MEPDG)* was calibrated using Long-Term Pavement Performance (LTPP) sections throughout the United States, including some from California (1). However, the *MEPDG* recommends that nationally calibrated models be validated using local data and, if necessary, recalibrated. This makes sense for California because nearly all the state's climate zones are drier and warmer than those of most of the sections in the national calibration set. In addition, the aggregate used in the state's concrete is primarily of igneous origin, while that of much of the national dataset is concrete with limestone aggregate; these igneous aggregates often have a greater coefficient of thermal expansion (CTE) than limestone aggregates. The dry climate increases the drying shrinkage, and the igneous aggregates increase the effects of thermal gradients. The two effects result in increasing tensile stresses that cause cracking. California also does not have the prolonged periods of freezing and thawing that are accounted for in the national calibration.

Therefore, there was a need to validate the models in the *MEPDG* based on the performance of California pavements and to recalibrate the models if necessary. In addition, the reliability approach used in *Pavement ME* is based on the national calibration and does not explicitly address typical local deviations of important variables. (Note: In this report the design guide is referred to as *MEPDG* and the software as *Pavement ME*.) Once models are locally calibrated, updated design tools then need to be developed based on the calibrated software. The first step in this process is to perform a sensitivity analysis study to check the reasonableness of the models' predictions, to identify potential software issues, and to help identify and understand the inputs that significantly affect the models' outputs.

In 2006, the University of California Pavement Research Center (UCPRC) performed a research study that included an initial sensitivity analysis of jointed plain concrete pavements (JPCP) distress prediction models in the *MEPDG* (2). That study identified the most important variables affecting predicted performance and studied a design variable that was found to be the most important for the predicted performance of JPCP in California—the time to loss of bonding between the concrete and the base (3). After that calibration, the software was used to produce a preliminary design catalog for the Caltrans *Highway Design Manual (HDM)*; Caltrans adjusted that catalog further to produce the one in the current *HDM*. The assumptions and results for that preliminary design catalog are documented in *Sample Rigid Pavement Design Tables Based on Version 0.8 of the Mechanistic-Empirical Pavement Design Guide* (4). In 2019, the UCPRC performed another sensitivity analysis study of JPCP distress prediction models in *Pavement ME* (v2.5.3) (5). In this study, the important variables affecting the

predicted transverse cracking performance were found to be portland cement concrete (PCC) slab thickness, built-in curl-warp temperature, PCC coefficient of thermal expansion, PCC shortwave absorptivity, and PCC compressive strength.

Pavement ME is the current version of the software developed from the MEPDG models. This software uses the MEPDG models to produce transverse cracking, faulting, and International Roughness Index (IRI) predictions.

PaveM, the California pavement management system (PMS), manages jointed plain concrete pavement based on third-stage cracking, rather than transverse cracking. *First-stage cracking* is defined as the first crack that divides a slab into two pieces. A first-stage crack can be a transverse crack, the only type of cracking modeled by *Pavement ME*, or a longitudinal crack, which also occurs on Caltrans JPCP (6). *Third-stage cracking* is defined as a state of cracking that divides a slab into three or more pieces. In California, a transverse crack is one of the cracks that commonly creates a third-stage crack along with a longitudinal crack—although, less frequently, third-stage cracking is also created by two transverse cracks or two longitudinal cracks.

The traditional approach for validating and calibrating mechanistic-empirical design methods is to collect all input data—including performance, as-built, and detailed materials data—from tens of sections within a state and to compare the predicted and measured performances for those few sections. For the national calibration of *Pavement ME*, this was done on the scale of several hundred LTPP sections across the United States.

The previous California calibration of an early version of *Pavement ME* (3) followed the traditional approach to ME method calibration and involved only 52 JPCP and 43 crack, seat, and overlay sections. On those sections, the amounts of first-stage transverse and longitudinal cracking and third-stage cracking were measured at the time of coring and deflection testing for those sections that had not been overlaid with asphalt. To develop better transverse cracking histories for those sections and for the overlaid sections, whether the measured third-stage cracking had begun as a first-stage transverse crack or longitudinal crack had to be estimated to produce a transverse cracking history starting from each section's time of construction. Because there were insufficient data and the locations of the sections did not cover the entire state well, a model predicting whether a third-stage crack began as a transverse or longitudinal crack could not be developed. Instead, a range of potential transverse cracking histories was produced for each section, with the maximum of the range assuming that all third-stage cracks began as transverse cracks and the minimum assuming that they all began as longitudinal cracks. This added uncertainty to the calibration.

Soon after that calibration, Caltrans asked for a transfer function that could predict third-stage cracking from transverse cracking predictions; this function was developed and used in the creation of the preliminary design tables that were the basis for the design tables included in the 2007 *HDM*. The development of that transfer function has not been published.

1.2 Overview of New Calibration and Design Development

In 2010, Caltrans developed a capacity for Automated Pavement Condition Survey (APCS) data collection from the state highway network, and, as a result, a much larger and more reliable pavement condition database is now available in *PaveM*. Due to considerable effort on the part of Caltrans, the database now includes as-built data such as pavement structure, base type, shoulder type, slab length, and construction year—items that were scarce in the previous study but are now available for almost every project built since 1990 and many built prior to that year. These data provide the capability to validate and calibrate *Pavement ME* using thousands of performance data observations and to use the explanatory data in the as-built database. In addition to the data in *PaveM*, the UCPRC has collected detailed data for Caltrans for more than 100 projects sampled in the early 2000s and 2010s. Those data are for variables—such as concrete materials properties and the stiffnesses of underlying layers—not in the as-built database in *PaveM*.

Since 2006, new versions of the *Pavement ME* software have been released with many improvements both in models and software implementation. These updates and improvements, combined with the increased amount and higher quality of data now in *PaveM*, have created the opportunity to perform a new JPCP prediction model sensitivity analysis and calibration specifically for California. In this study, the latest version of *Pavement ME* (v2.5.5) was used. It should be noted that an earlier version of *Pavement ME* (v2.5.3) was used for the sensitivity analysis study. However, after careful investigation, it was found that the *Pavement ME* model predictions remained unchanged.

A new approach was used for the calibration process, and the results were checked against all the data available in *PaveM*. This new approach recognizes that in the design-bid-build (low-bid) contracting environment used in California, a designer does not actually know the detailed materials properties when a design is being created. Therefore, the calibration used median values of the detailed materials properties and recognized the variability caused by different contractors' materials when a design is built. The calibration also used the detailed information available from *PaveM* regarding layer types, thicknesses, slab dimensions, shoulder types, dates of construction, and performance data, along with detailed climate and traffic data, to find the coefficients in *Pavement ME* that on average produce the best match between predicted performance and observed performance. The distribution

of differences between the predicted and observed performance also provide information needed for introducing reliability into the future design tools.

In this research, *Pavement ME* was calibrated to the transverse cracking estimated from first-stage cracking. To achieve this, a new model was developed that gives the probability that the first-stage crack is longitudinal or transverse. This effort used the APCS 2011–2012 data, which accurately separated transverse and longitudinal cracking on all JPCP across the entire state and thus provided sufficient data to produce a model. This model was then used to predict the rate of transverse and longitudinal cracking development for all JPCP performance data in the historic PMS database. The model included consideration of explanatory variables such as shoulder type, climate region, and slab thickness and dimensions.

The model was able to relate the development of transverse cracking to the subsequent development of third-stage cracking. This can be used to set transverse cracking failure levels for the development of design tools and to relate predicted transverse cracking from *Pavement ME* to the third-stage cracking used in Pavem.

The calibration of the *Pavement ME* empirical model transverse cracking coefficients C_4 and C_5 was made using the predicted portion of transverse cracking in the observed first-stage cracking. The model was also able to identify situations where longitudinal cracking was expected. Associated design guidance will be developed from this model to help designers limit the possibility of early failure. That guidance is not included in this report. *Pavement ME* was not developed to predict longitudinal cracking because it seldom occurs outside of the dry climate regions that are predominant in California and some other western states, a condition that is not typical of the rest of the United States.

The steps followed in the calibration process are as follows:

1. Identify roadway segments.
2. Prepare PMS data.
3. Develop statistical performance model.
4. Estimate median values for unknown variables.
5. Run *Pavement ME* for each cell of data.
6. Analyze nationally calibrated model error.
7. Identify *within-project variability* (WPV) and *between-contractor variability* (BCV) and find calibrated C_5 .
8. Identify *between-project variability* (BPV) and find calibrated C_4 .
9. Find C_4 corresponding to 95% reliability.
10. Analyze calibrated model error.

The results presented in this report demonstrate the new calibration procedure for the *Pavement ME* JPCP transverse cracking model based on use of the extensive data in the pavement management system database. The set of calibrated model coefficients will be used to develop the Caltrans JPCP design catalog.

In Chapter 2, JPCP cracking performance data from the PaveM database are analyzed and a performance model for first- and third-stage cracking is developed. Also, a transfer model is developed to predict the portion of first-stage cracking data being transversely cracked. In Chapter 3, the new calibration procedure is presented. Chapter 4 presents the summary and conclusions of the study and recommendations for future studies.

(This page intentionally blank)

2 PAVEMENT MANAGEMENT SYSTEM AND JPCP CRACKING STATISTICAL PERFORMANCE MODEL

2.1 Introduction

Pavement management is the process of using available financial resources as efficiently as possible to ensure the highest overall functional performance of a road network, both spatially and over time, while maintaining the structural condition of the pavements to protect the initial investment in construction. As such, to perform pavement management, it is necessary to capture the current functional and structural condition of the network and to predict its future condition for different management scenarios. Historically, a team of Caltrans pavement raters conducted a pavement condition survey (PCS) at various locations along the state highway system (SHS) once a year as part of a manual pavement condition survey. The pavement raters visually inspected the outer highway lanes for both directions of travel using systematic sampling techniques. Pavement condition assessments were extrapolated for each section of the entire SHS based on those sample locations.

The boundaries of pavement management sections across the network changed annually, as did the locations where surveys occurred. Because the same location was not sampled each year, building performance histories was difficult for the 2006 *Pavement ME* calibration. Changing section boundaries from year to year also meant that a given pavement location could be included in different sections in any year. On jointed plain concrete pavements (JPCP) the sections were typically around one mile long.

Between 2011 and 2012, Caltrans began testing and transitioning from the manual PCS to the Automated Pavement Condition Survey (APCS). The APCS can efficiently collect, evaluate, and analyze pavement conditions for all lanes on the SHS. It utilizes vehicles equipped with an array of on-board high-definition cameras, laser sensors, Global Positioning System trackers, and other measurement devices that quickly collect pavement data at highway speeds. The information collected includes geographical locations of the highways, downward-looking pavement surface images, forward right-of-way images, and pavement surface profiles. The data are collected for every 26.4 ft. section, referred to as an *element*, for asphalt pavement and continuously reinforced concrete pavement and every concrete slab for JPCP. Data are aggregated to calculate a weighted average of the pavement condition of larger segments for management or reporting purposes.

Because evaluating condition, especially functional condition, can be subjective, agencies have generally settled on trying to identify and quantify specific distresses. A *distress* is a measurable phenomenon on the surface of a pavement, such as observable cracking, changes in ride quality (smoothness/roughness), or rutting. Distress is the result of internal deterioration within the pavement, typically either cracking or permanent deformation of materials, or, in the case of JPCP, permanent changes in vertical alignment on the two sides of joints.

Deterioration, in turn, is the result of internal damage within the materials, which is not observable. This might include particle movement, breaking of bonds, or other atomic/microscopic changes. These damage processes take place at different rates at different locations in the pavement because of many possible causes, including variability in the materials, construction processes, traffic, drainage, and underlying subgrade soil type. As a result, observed distress accumulates at different rates along the road surface, even within a section that is nominally uniform due to the variables previously mentioned.

This chapter outlines the pavement structure, climate, and traffic variables along with distress measures available in California's pavement management system (PMS) (known as *PaveM*) database. It also briefly discusses the qualitative effects of different variables on the performance of the JPCP over its service life. The condition survey distress data from both the PCS and APCS were used to develop empirical performance models for *PaveM*, and these models were in turn used to calibrate *Pavement ME*, as shown in the next chapter. An *empirical performance model* is a statistical model based on the data obtained through the pavement condition surveys. The model predicts the future performance (condition) of the pavement—which in this study is the percentage of cracking—based on input variables such as pavement structure (i.e., portland cement concrete [PCC] slab thickness, PCC slab length, base type, and shoulder type) and nonstructural variables such as climate and truck traffic spectra category. In Section 2.5, a model (transfer function) was developed that gives the probability that a first-stage crack is longitudinal or transverse. This model was later used to determine the portion of first-stage cracked pavements having transverse cracking. The result added to third-stage cracking data was used to calibrate the *Pavement ME* transverse cracking model.

2.2 Structural Distress Measures in JPCP

2.2.1 Concrete Slab Cracking

Cracking is the primary distress in JPCP due to traffic loading and environmental conditions. Each pass of traffic loading results in damage-causing stress in the concrete slabs. The minor damage from each load accumulates with thousands to hundreds of millions of load passes until eventually it results in failure in the form of fatigue cracking. Environmental conditions, such as curling caused by vertically differential temperatures in the slab and warping caused by vertically differential shrinkage, also create stresses that contribute to damage in the concrete slab.

Cracking in concrete slabs can be categorized into three main types: (1) transverse cracking, (2) longitudinal cracking, (3) and corner cracking. Transverse cracks appear perpendicular to the pavement centerline and extend across the entire slab from one longitudinal edge to the other. Longitudinal cracks appear parallel to the pavement centerline and extend along the entire slab from one transverse joint to the other. Corner cracks occur in one

quadrant of a slab and have one endpoint on a longitudinal joint and the other on a transverse joint. Other types of cracking are also possible, such as diagonal cracks or “deformed” transverse or longitudinal cracks, but these are uncommon and are caused by localized issues, such as subsidence.

Typically, a combination of repeated loads combined with thermal and shrinkage stresses causes transverse cracking in concrete slabs. There are two mechanisms for initiation and progression of transverse cracking, referred to as bottom-up and top-down cracking. When truck axles are near the longitudinal edge of a slab, midway between the transverse joints, a critical tensile stress occurs at the bottom of the slab with its maximum value in the longitudinal direction. The presence of a high positive vertical temperature gradient (the top of the slab is warmer than the bottom of the slab) through the slab thickness causes additional tensile stress at the bottom of the concrete slab and loss of slab support near its longitudinal edges, midway between transverse joints. Both of these stresses contribute to bottom-up cracking.

Alternatively, the combined effect of two heavy truck axles, frequently steering and drive axles, simultaneously loading the opposite ends of a slab results in tensile stresses at the top of the slab that may cause top-down fatigue transverse cracking. Top-down transverse cracking is accelerated by high negative temperature gradients (the top of the slab cooler than the bottom of the slab) and differential drying shrinkage (the top of the slab has contracted more than the bottom), which cause tensile stress at the top of the slab and loss of slab support at its corners.

Longitudinal cracking in California is primarily caused by high differential drying shrinkage that causes high tensile stresses at the top of the slab and loss of slab support at its corners, which (with the combined effect of the left and right wheels of the truck axles) result in top-down cracking.

Corner cracking is also caused by a top-down mechanism, where load repetitions at the corner of the slab combine with poor joint and shoulder load transfer, loss of slab support from the underlying layers, and curling (cooler on top than the bottom of the slab) and warping stresses. The lack of support and poor load transfer may be due to the pumping of underlayer material or loss of load transfer between the adjacent concrete slabs, such as undoweled concrete pavement that does not have tied concrete shoulders.

Once a slab has cracked, its geometry changes and the locations of critical loads and distress on it changes. Because cracks are more random than constructed joints, the process of cracking from this point onward becomes more chaotic and difficult to analyze. In some cases, a first-stage transverse crack might act as an additional joint, and the slab will show little further distress. In other cases, a first-stage crack might result in a cascading failure as the slab transitions to a more aggressive failure mode.

Caltrans has traditionally categorized the cracking in JPCP in terms of its severity into two main groups: (1) first-stage cracking and (3) third-stage cracking. In the official Caltrans definition, *first-stage cracking* is a crack that breaks the concrete slab into two pieces; this crack can be a transverse, longitudinal, or diagonal crack. *Third-stage cracking* is defined as a set of two or more intersecting longitudinal or transverse cracks that divide the concrete slab into two or more pieces. However, despite these written definitions, Caltrans raters have long used the simpler definitions that a slab has first-stage cracking if it is divided into two pieces and it has third-stage cracking if it is divided into three or more pieces. Corner cracking is not considered in either of these two definitions, and it is defined and measured separately.

Caltrans measures cracking as the percent of cracked slabs in a pavement section. Caltrans historically has collected data on first- and third-stage cracking only, without defining whether the first-stage cracking is transverse or longitudinal. However, as part of the APCS data collection in 2011–2012 and 2018, transverse and longitudinal cracking data were also collected as individual measures. Therefore, the amount of transverse and longitudinal cracking data in the APCS database comes only from these years and is much less than the amount of data that consists of only first- and third-stage cracking.

2.2.2 *Transverse Joint Faulting*

Faulting is the difference in elevation across a transverse joint between two adjacent concrete slabs or across a transverse crack. It is primarily caused by poor load transfer, and it is therefore usually an issue with undoweled JPCP.

The main mechanism that causes faulting is movement of fine material from under the leave concrete slab to under the approach slab. This is caused by large differences in deflection between the loaded slab and the unloaded slab, which reverse as wheels travel across the joint and create a pumping action. Dowel bars significantly decrease relative deflections across transverse joints under load, thus reducing faulting development and further deterioration of joints and corner cracks.

Caltrans measures both average fault height and faulting as the percent of transverse joints in a pavement section with faults greater than a threshold value of 0.15 in. Average fault height is used in the *Mechanistic-Empirical Pavement Design Guide (MEPDG)* and other federal pavement management metrics, but it is difficult to measure because small fault heights cannot be measured reliably and are rounded down to zero in the averaging. There is some disagreement over the measurement of faulting at transverse cracks and whether these should be included in these metrics. Typically, they are included in MEPDG and similar metrics by the automated algorithms that analyze and report faulting from the measured data.

2.2.3 *International Roughness Index (IRI)*

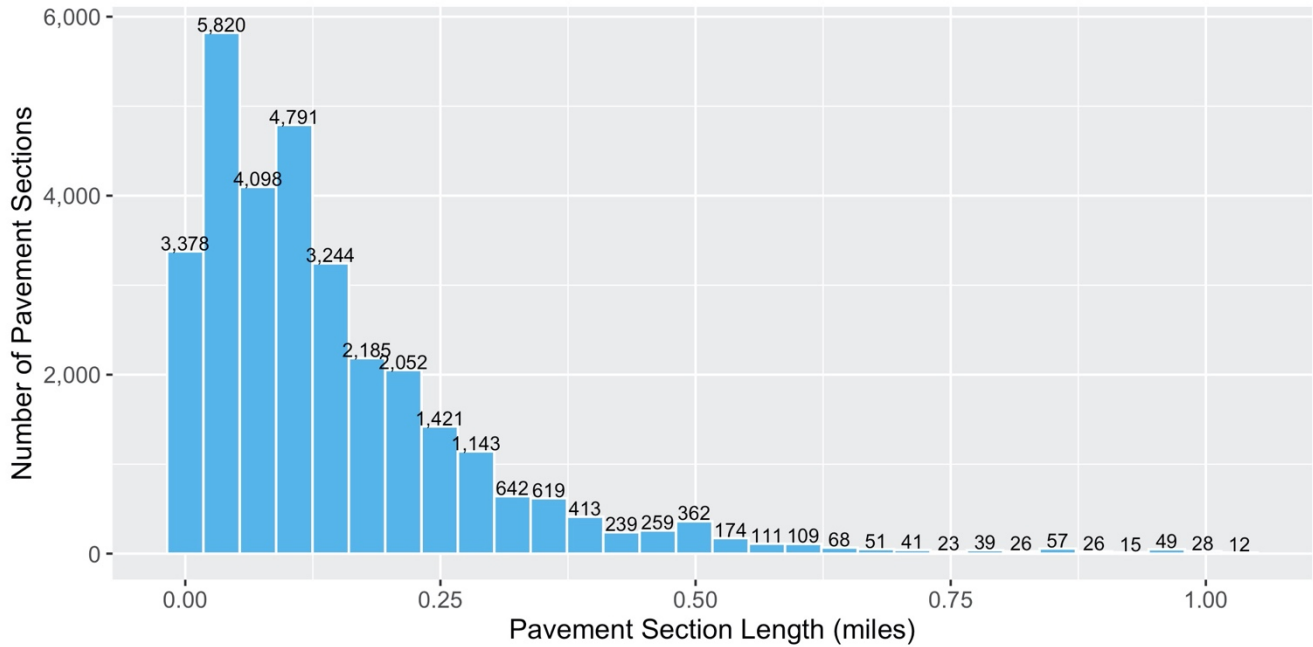
Pavement roughness is generally defined as an expression of irregularities in the pavement surface that adversely affect the ride quality of a vehicle and thus the user. Roughness is an important pavement characteristic because it affects not only ride quality but also vehicle maintenance costs, fuel consumption, and freight damage. Roughness in Pavem data is quantified using the International Roughness Index (IRI), which defines a characteristic of the longitudinal profile of a traveled wheel track. IRI constitutes a standardized roughness measurement and is measured in units of in./mi. in Pavem.

2.3 Pavement Structural (As-Built), Traffic, and Climate Data in Pavem Database

The development of the performance modeling database summarized below is covered in detail in a report about the performance models (7). The process of computing the traffic and assigning traffic repetitions and weigh-in-motion (WIM) spectra is also covered in a previous report (8). There are about 260,000 observations of first- and third-stage cracking performance data in the current Caltrans condition survey database, which includes data collected from 30,000 JPCP sections, totaling about 4,300 lane-miles built on 446 lane replacement projects completed between 1947 and 2017. (All new JPCP projects are recorded as “lane replacement” in the database.) Performance data in the database were obtained from the manual PCS from 1978 to 2013 and the APCS done in 2011–2012 and 2018. APCS 2015–2016 cracking data could not be used because they were measured using automated algorithms that did not produce reliable results. Each observation in the condition survey data corresponds to the performance condition of a pavement section in the highway network at the time the survey was done.

These data for each construction section within a project were divided into approximately uniform sections as part of the performance modeling effort. Section boundaries were kept constant through time and all uniform construction sections within a project were defined as having the same pavement structure or treatment. This altered the available history of each section so that it had the same traffic loading and the same climate condition as all other sections in the project. Figure 2.1 shows the variability in the resulting lengths of these sections in the dataset. For simplicity, uniform construction sections within a project (which is a legal and financial construct) are referred to as “projects,” because one contract might have multiple different pavement sections or even treat different routes.

Figure 2.2 shows the distribution of yearly JPCP project construction from 1947 to 2017. Since the first condition survey data were collected in 1978, the oldest available time histories begin in that year.



Note: 0.00 indicates sections with lengths less than 0.08 mi.

Figure 2.1: Pavement section length distribution.

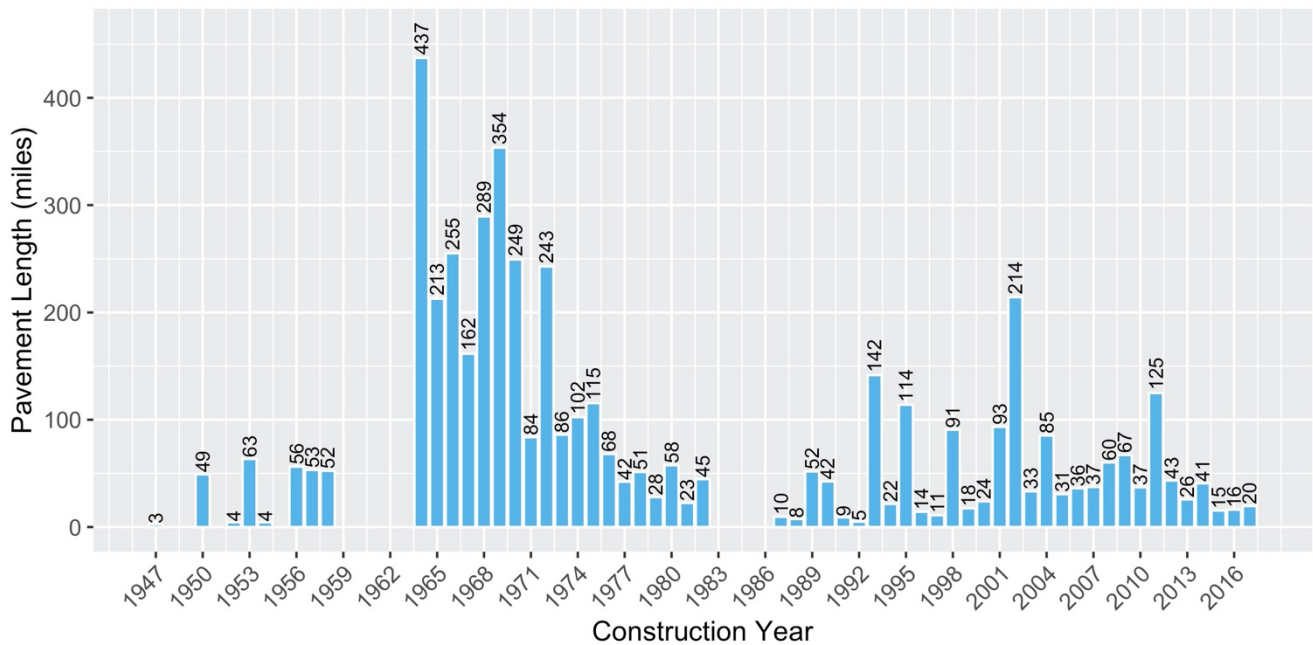


Figure 2.2: JPCP project construction year distribution.

Figure 2.3 shows the JPCP pavement age distribution based on condition survey observations. The age of each pavement section is the difference between the construction date and the pavement condition survey date. Most of the pavement condition observations in the condition survey dataset are on pavements that are less than 40 years old.

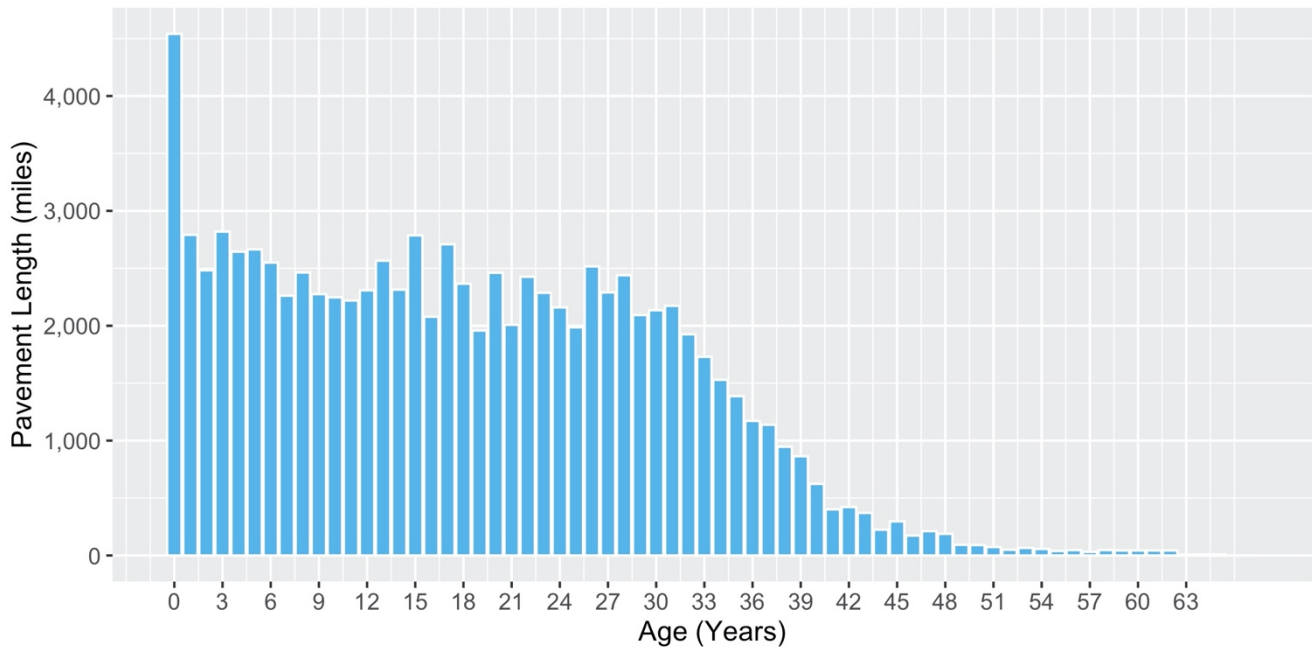


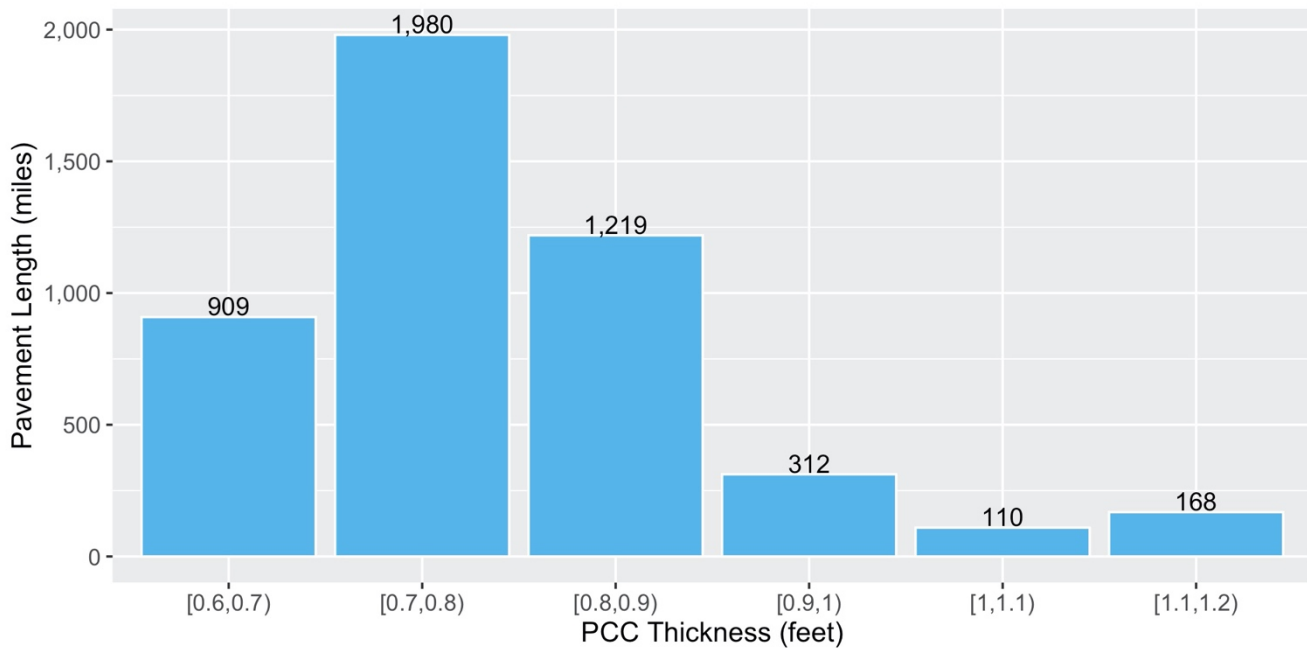
Figure 2.3: JPCP pavement age distribution.

The Caltrans as-built database includes only information on PCC slab thickness and base type. It does not record whether JPCP projects were doweled, and no other sources were found to obtain that information. Projects with completion dates after 2000 were assumed to be doweled JPCP, as Caltrans standard plans mandated using dowels in JPCP projects starting in 1998. In Sections 2.3.1 through 2.3.7 of this report, the distribution of each of the as-built variables is presented, and a qualitative evaluation of their effects on the measured cracking performance of JPCP is discussed.

Slab lengths and shoulder types were derived from APCS 2011–2012 data for slabs within each section. It is unlikely that the slab lengths changed with time, but the shoulder type may have changed over their long histories, particularly because adjacent lanes might have been added that were tied to the existing lanes. If the section was not observed in 2011–2012, then these variables are missing.

2.3.1 PCC Slab Thickness

Figure 2.4 shows the distribution of PCC slab thicknesses in the database. PCC slab thickness is categorized into increments of 0.1 ft. The distribution shows that the majority of the PCC slabs were constructed with thicknesses between 0.6 and 0.9 ft.



Note: 0.6 ft. = 7.2 in., 0.7 ft. = 8.4 in., 0.8 ft. = 9.6 in., 0.9 ft. = 10.8 in., 1.0 ft. = 12 in., 1.1 ft. = 13.2 in., 1.2 ft. = 14.4 ft.

Figure 2.4 PCC slab thickness distribution.

Figure 2.5 shows the cracking performance of the JPCP with different thicknesses over the years. The Y-axis represents the total cracking (first-stage plus third-stage) percentage, the X-axis represents the age of the pavement, and each panel corresponds to a PCC slab thickness. The black points in each plot are the observations of cracking in each thickness range, with the size of each point representing the amount of data in lane-miles; the gray-shaded points show all data in the complete dataset for reference. From Figure 2.5, it can be seen that thicker slabs perform better than thinner ones, despite the fact that truck traffic data is not controlled in the plot. This seems to indicate that despite the intention of previous design methods to account for truck traffic in a manner that results in similar functional lives regardless of traffic level, the sections designed for low traffic levels (thin slabs) fail faster than those designed for high traffic levels (thick slabs). It is not certain how much of the difference is due to underestimation or overestimation of truck traffic or to the design method not accounting well for the traffic. There may also be other variables—such as slab length; base type; shoulder type; and material properties, including

concrete strength and CTE—causing differences in performance because factor levels of these variables are unequally distributed within the thickness categories.

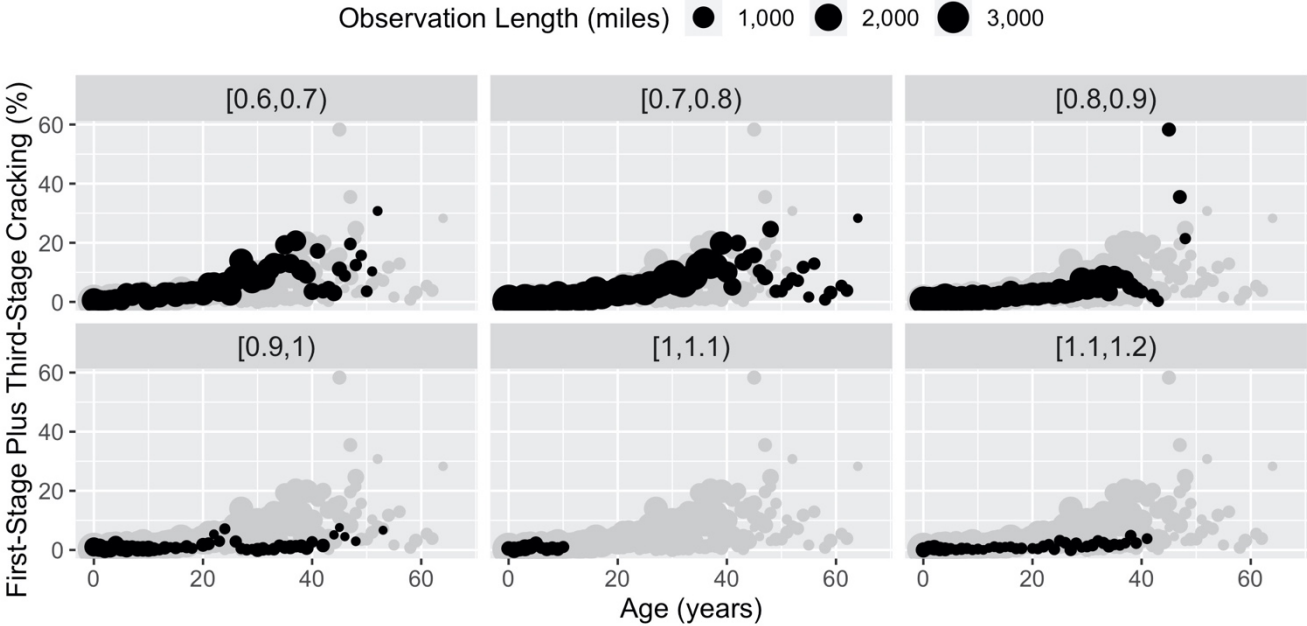


Figure 2.5: JPCP total cracking for different PCC slab thicknesses.

2.3.2 PCC Joint Spacing

Figure 2.6 shows the slab patterns for JPCP constructed in California. It is clear from the figure that historically, the three most common slab patterns constructed in California are 12,13,14,15 ft.; 12,13,18,19 ft.; and 15 ft.

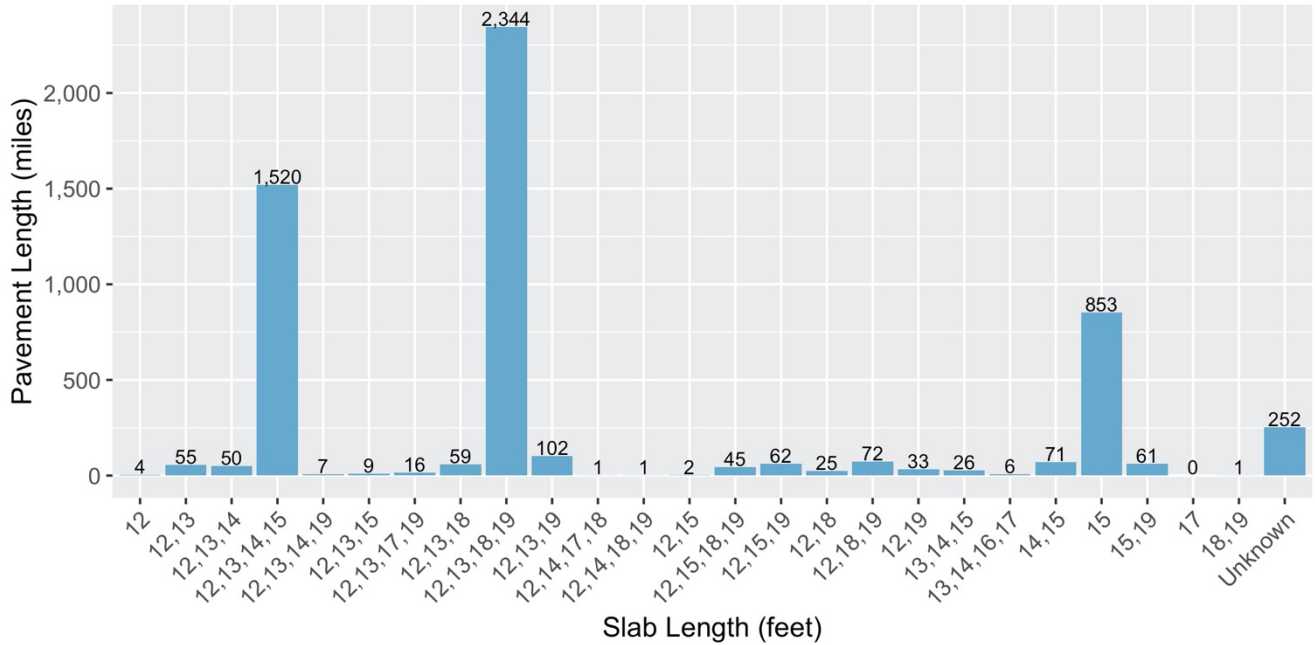


Figure 2.6: PCC slab pattern distribution.

Figure 2.7 shows the history of slab pattern construction over the years. Each panel in the figure corresponds to a 10-year interval. Up to about 1990, the 12,13,18,19 ft. slab pattern was the most common, whereas after 1990, the 12,13,14,15 ft. slab pattern was prevalent. For the calibration, a decision was made to categorize the slab patterns into two groups, with 12,13,14,15 ft. being the short pattern and 12,13,18,19 ft. being the long one. Data from the other patterns were not discarded; they were included in either the short or long pattern.

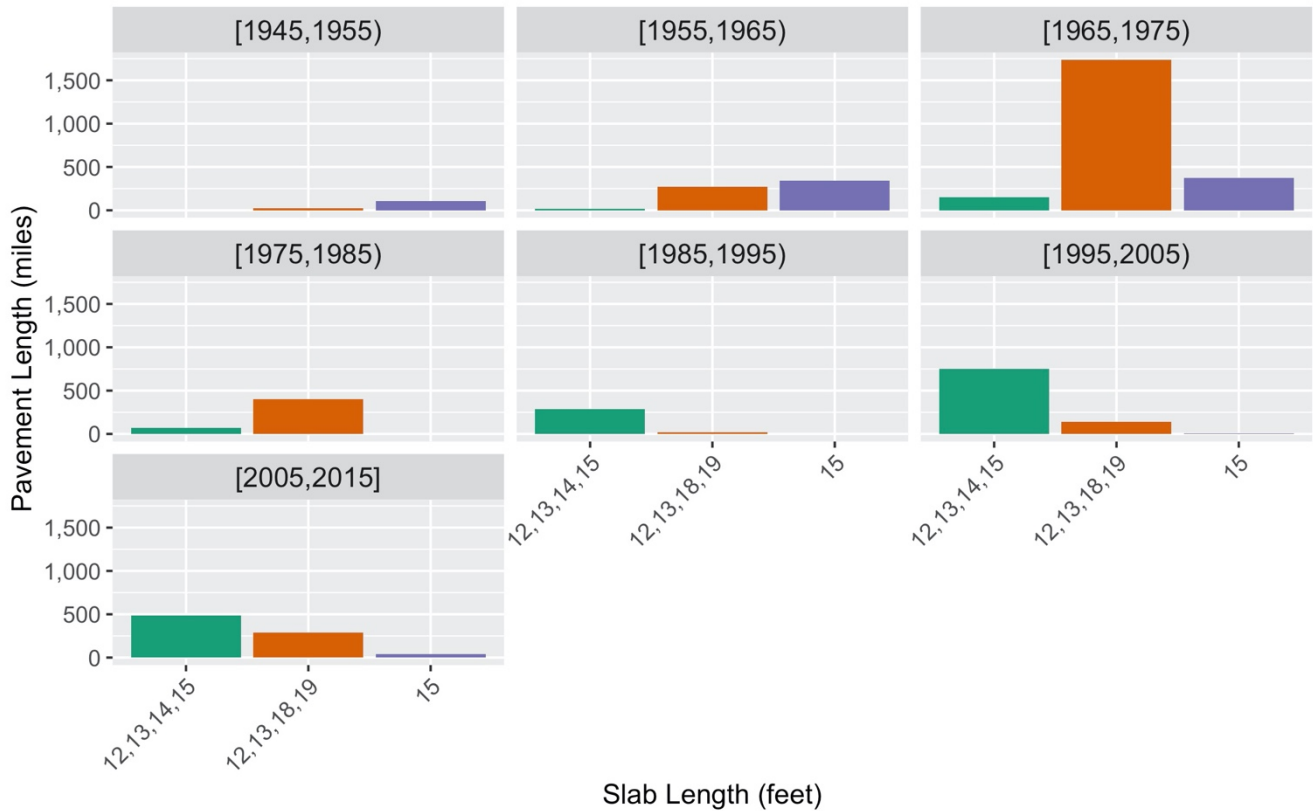


Figure 2.7: PCC slab pattern history distribution.

Figure 2.8 shows that the longer slab pattern has a higher rate of cracking over the years. The performance data of the non-alternating 15 ft. slabs are included in the 12,13,14,15 ft. slab pattern. However, the difference in performance between the different slab patterns is not as significant as suggested in the *Pavement ME* sensitivity analysis conducted as a preliminary step in this calibration (5).

It should be noted that the pattern of increased cracking over time, followed by lower cracking with fewer observations at greater ages, is common in this type of data. The main cause is right censoring of the data caused by sections with high distress being maintained or replaced, so only sections with good performance remain.

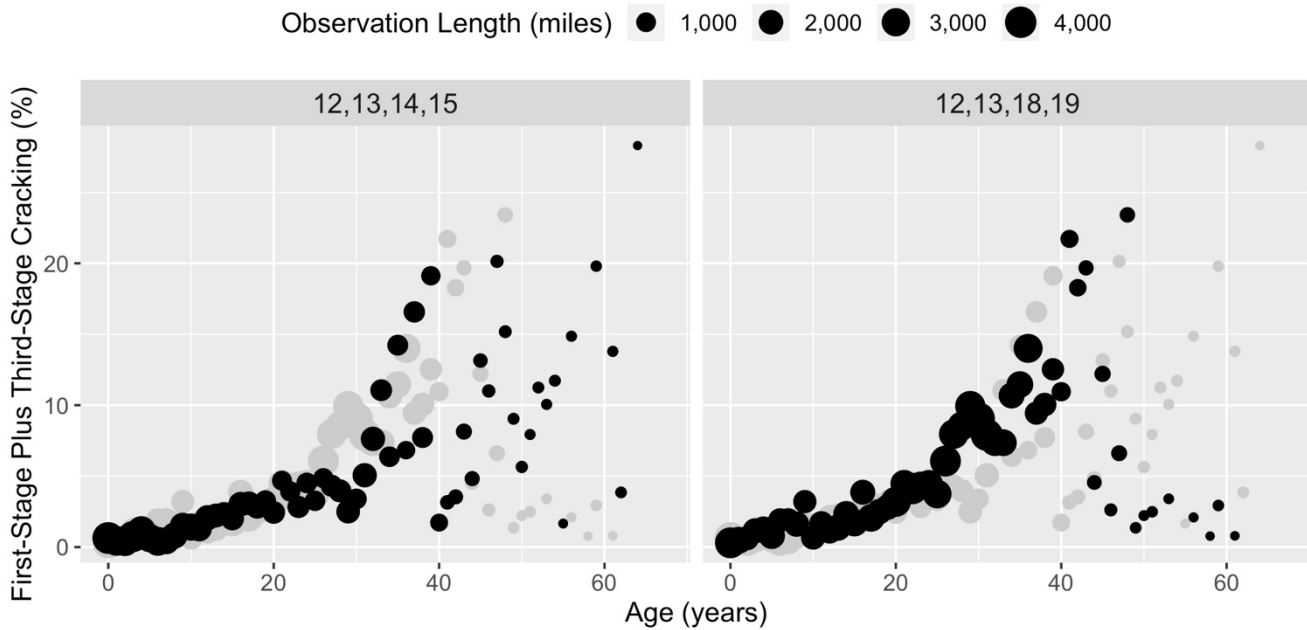


Figure 2.8: JPCP total cracking for different PCC slab patterns.

2.3.3 Base Type

There are five different base types available in the Caltrans pavement management system performance database: (1) aggregate base (AB), (2) asphalt-treated permeable base (ATPB), (3) cement-treated base (CTB), (4) hot mix asphalt (HMA), and (5) lean concrete base (LCB). Figure 2.9 shows that the majority of JPCP was constructed with CTB and that ATPB was used the least.

It should be noted that Caltrans CTB specifications have changed considerably over the years, which is reflected in the performance database (6). They have included CTB mixed both on grade and in plant, and they have included different minimum required compressive strengths. From 1952 to 1967, Caltrans used different CTB specifications at the same time; the choice of specification depended on the designed average annual daily truck traffic (AADTT).

From a first glance at Figure 2.10, one would infer that CTB has the worst performance among the selected base types. However, this is not necessarily a correct conclusion, since Figure 2.10 considers only one variable (base type) that affects the performance of JPCP and does not account for other variables such as PCC slab thickness, PCC slab length, shoulder type, traffic, and climate.

To consider all the variables with their interactions at the same time on the cracking performance of JPCP, a statistical model was developed based on the performance data. In its predictions, the statistical model considers PCC slab thickness, PCC slab pattern, base type, shoulder type, climate, and AADTT variables. The model

considers PCC slab thickness, PCC slab pattern, base type, shoulder type, climate, and AADTT as input variables, but the model does not consider concrete materials properties, including strength and CTE, because no in-network data on them were available. Predictions from this statistical model and a more in-depth discussion on the effects of each variable on the performance of JPCP using the statistical model are provided later in this report.

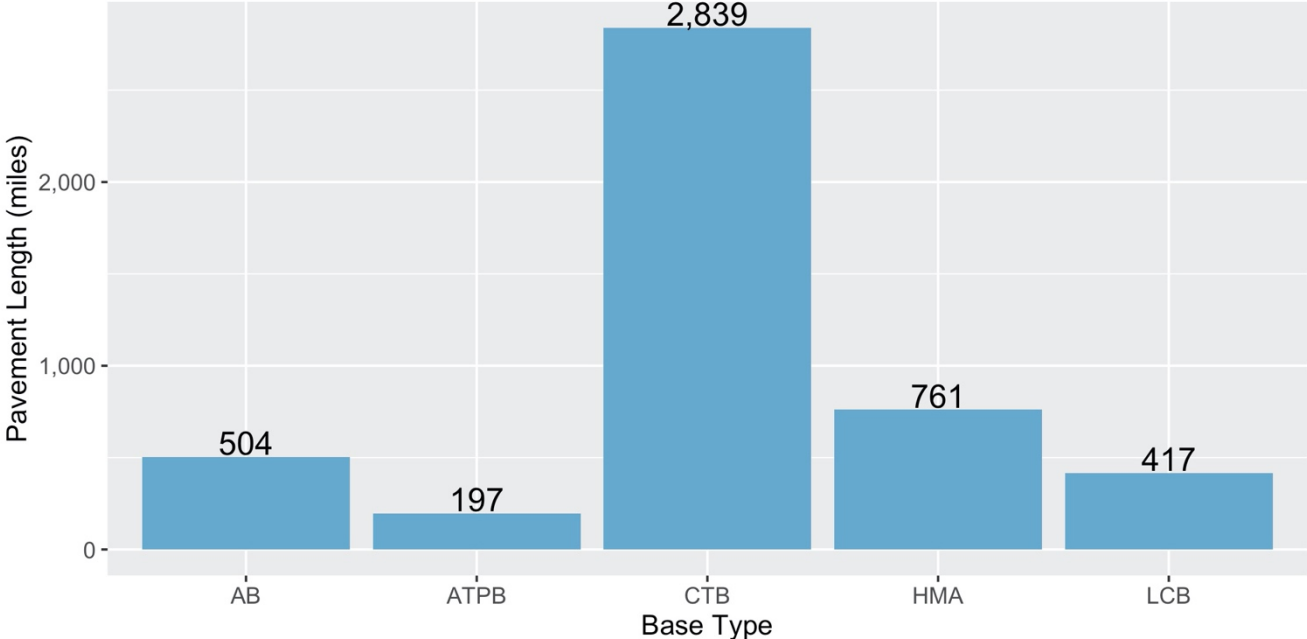


Figure 2.9: Base type distribution.

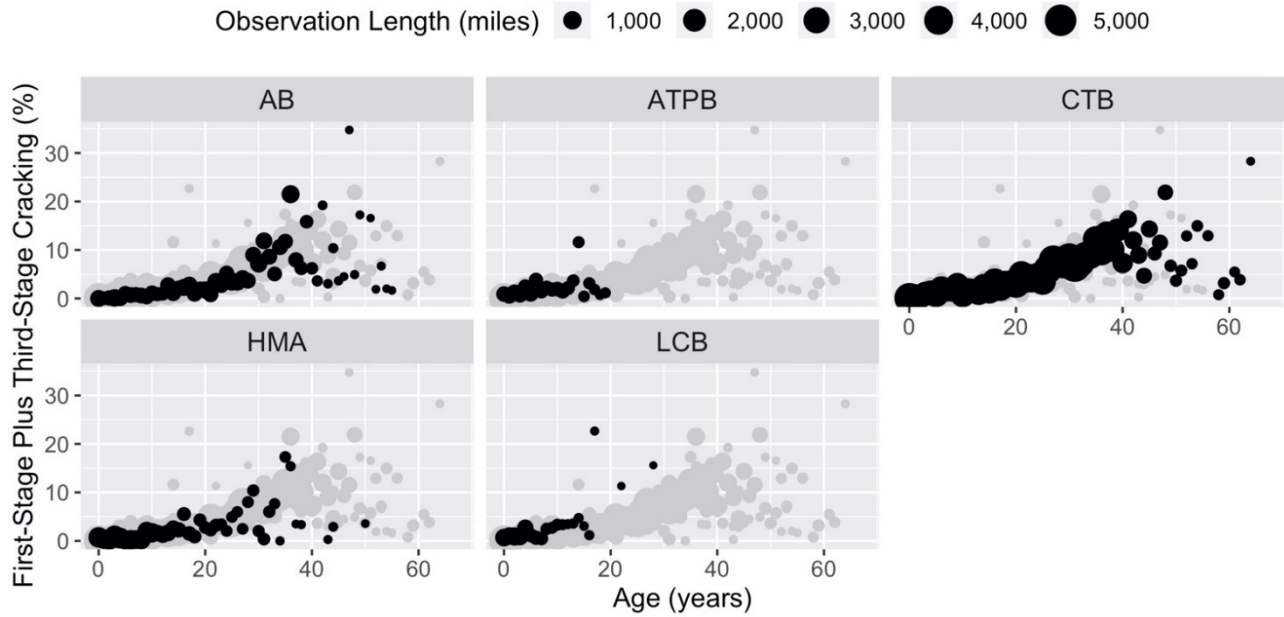


Figure 2.10: JPCP total cracking for different base types.

2.3.4 Shoulder Type

There are four different shoulder types defined in the database: (1) not applicable (NAP) for interior lanes without a shoulder, (2) untied flexible (FLX) shoulder, (3) tied concrete (RIG) shoulder, and (4) widened concrete (WRF) shoulder. It should be noted that the WRF shoulder type represented in the database is a 2 ft. wide rigid shoulder. Figure 2.11 shows the distribution of each of these shoulder types in the database. WRF has the fewest constructed lane-miles of all the shoulder types in the database, and it is included in the newest sections since it has only been used since 2000.

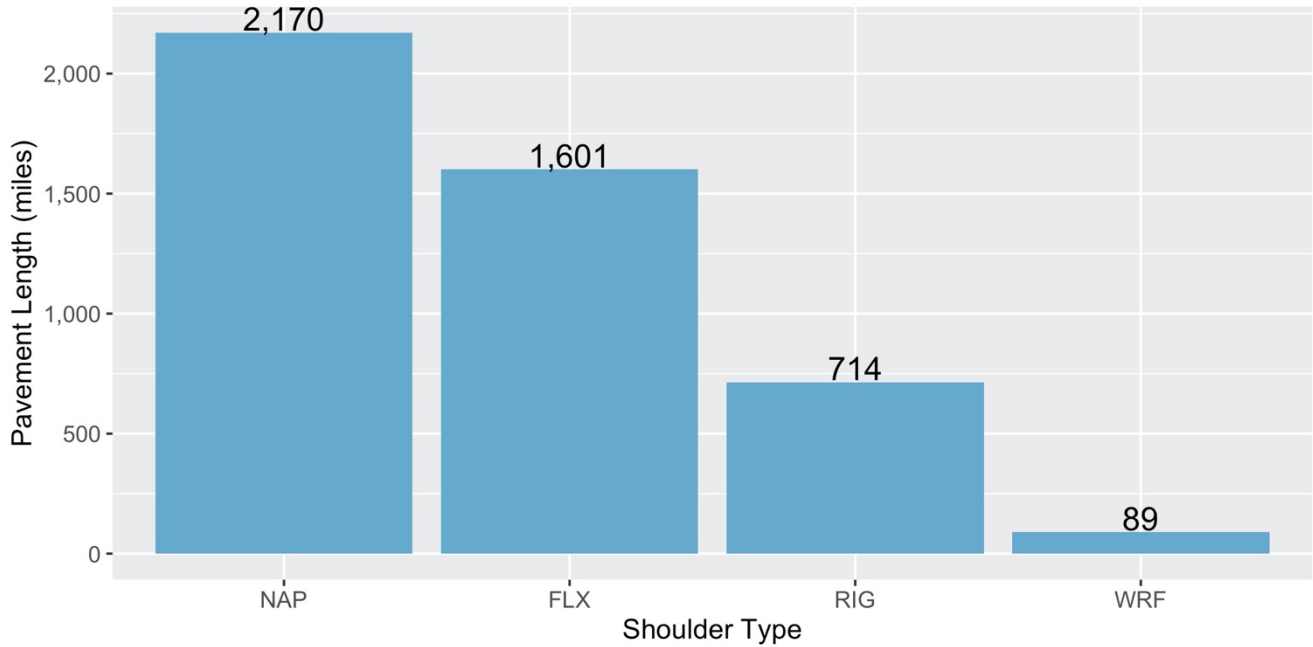


Figure 2.11: Shoulder type distribution.

Figure 2.12 shows that pavements with no shoulders or flexible shoulders have the poorest performance and pavements with the rigid shoulder type have the best performance. Pavements with widened concrete shoulders show a considerable amount of cracking, although they were used because they were considered more resistant to transverse cracking than other shoulder types.

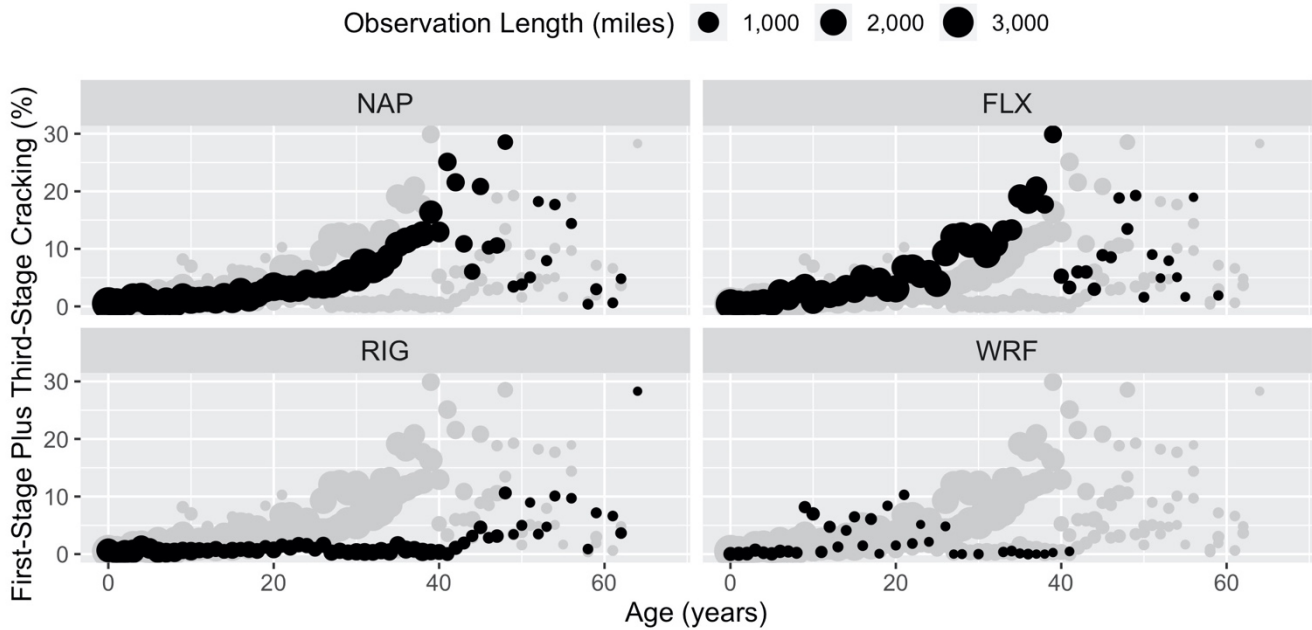


Figure 2.12: JPCP total cracking for different shoulder types.

To investigate the poor performance of WRF, APCS 2011–2012 per-slab performance data were studied. Figure 2.13 shows the amounts of different types of cracking for JPCPs with the WRF shoulder type categorized into panels with different base types and PCC slab thicknesses. The *X*-axis represents the PCC slab length and the *Y*-axis represents the probability of cracking. Each color shows a different distress type, and the points on top of each panel represent the amount of data available at each PCC slab length. By looking at the two bottom center panels, it can be seen that WRF mitigates the transverse cracking problem for shorter slabs. However, it can also be seen that a considerable portion of shorter slabs (less than 16 ft.) have significant amounts of longitudinal cracking. This explains poorer overall cracking performance of WRF shoulders, which is driven by their susceptibility to longitudinal cracking in shorter slabs.

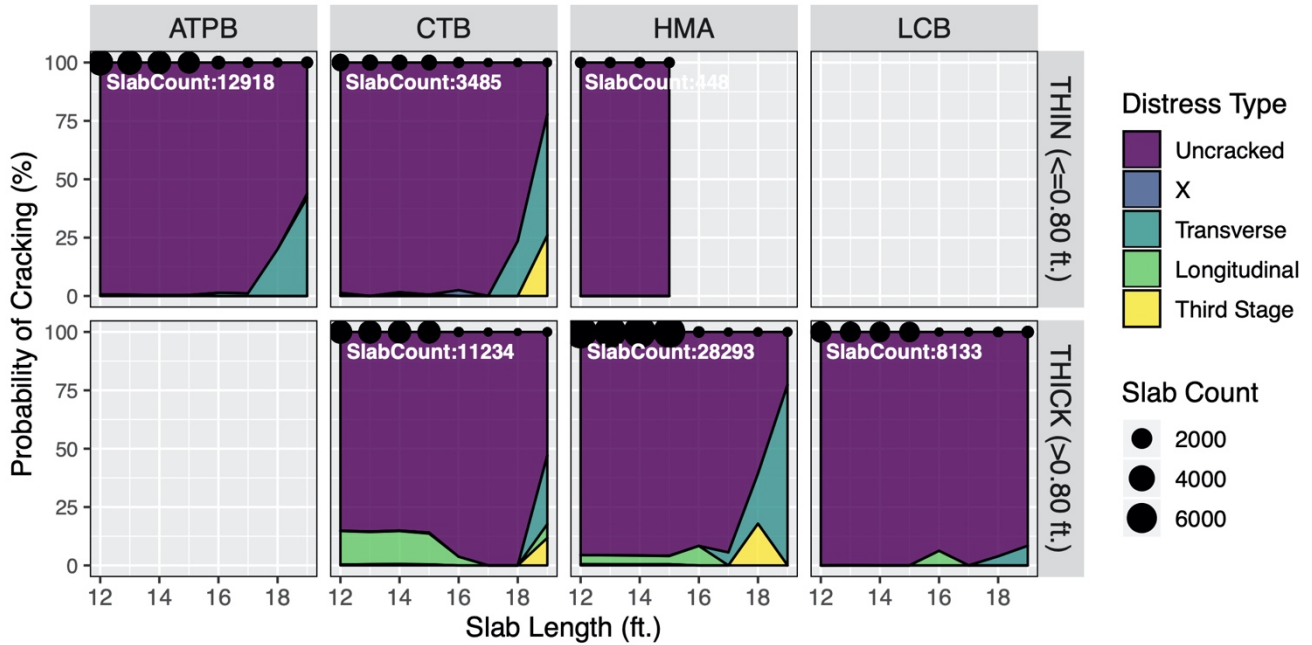


Figure 2.13: Probability of different distress types versus slab length for WRF shoulders.

2.3.5 Climate Region

Figure 2.14 shows the climate region distribution in the data. Most of the JPCP is in California’s Inland Valley and South Coast, while the state’s High Desert and Low Mountain climate regions have the fewest lane-miles of JPCP.

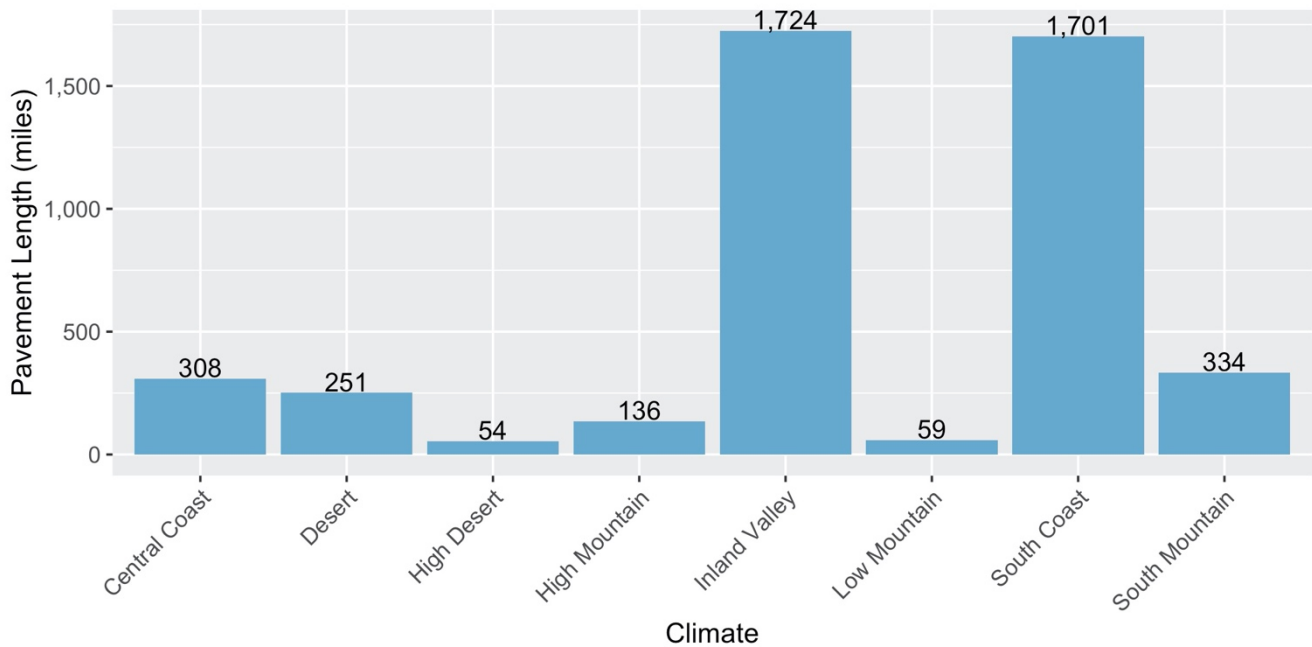


Figure 2.14: Climate region distribution.

Figure 2.15 shows the JPCP performance in different climate regions. The High Desert (small amount of data), Inland Valley, Low Mountain (small amount of data), and South Mountain have poorer performance compared to the other climate regions.

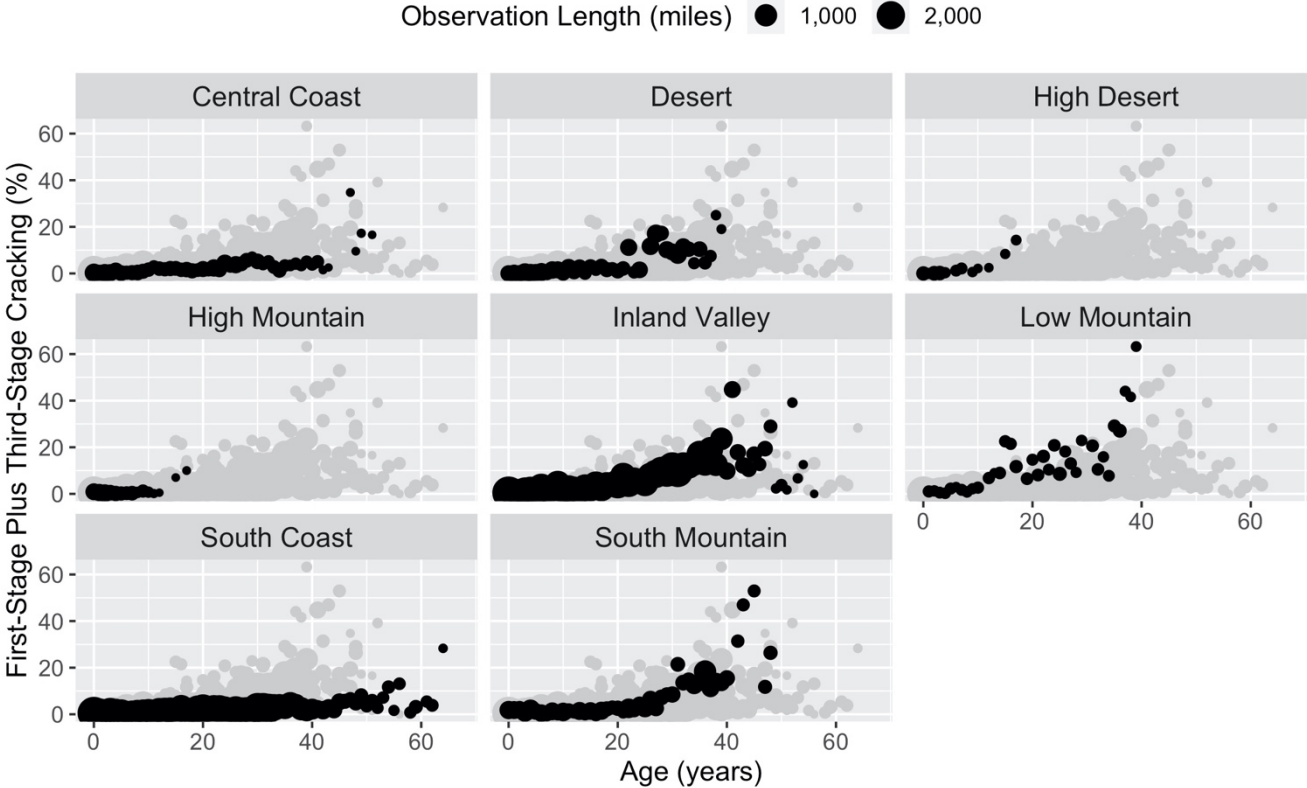


Figure 2.15: JPCP total cracking for different climate regions.

2.3.6 WIM Spectra

Caltrans considers five different truck traffic spectra for pavement design and management: WIM Spectra 1, WIM Spectra 2, WIM Spectra 3, WIM Spectra 4, and WIM Spectra 5. These five spectra represent the truck traffic characteristics found in the Caltrans road network, with the higher spectra numbers corresponding to heavier truck traffic loads. In *Pavement ME*, the WIM spectra can be regarded as a regional-level characterization of the truck traffic variables.

Each WIM spectra is defined by the distribution of truck classes (Table 2.1); the distribution of hourly traffic (Table 2.2); and the weight distributions of single, tandem, and tridem axles (these weight distributions are not shown in this report). Table 2.3 shows the distribution of axles per truck, which is the same for all the WIM spectra. To simplify the process of finding similarities between the different spectra, a variable called Single

Equivalent Axle Load was chosen for this study. This variable’s frequency is the value that results from splitting tandem axles into two and tridem axles into three (e.g., one tandem axle becomes two singles, each with half the load), and the variable is used on the Y-axis for the different WIM spectra in Figure 2.16. It should be noted, however, that use of this variable has no effect on the actual spectra used in *Pavement ME*.

Table 2.1: Truck Class Distribution

Truck Class	WIM1	WIM2	WIM3	WIM4	WIM5
Class4	1.87	2.05	1.73	1.32	3.24
Class5	59.63	52.71	28.05	20.88	37.07
Class6	3.52	3.34	2.37	11.93	4.18
Class7	0.08	0.1	0.12	0.11	0.2
Class8	8.6	8.1	8.01	6.85	6.94
Class9	23.24	27.82	53.83	54.41	45.09
Class10	0.06	0.12	0.52	0.9	0.27
Class11	2.34	5.24	3.97	2.42	2.29
Class12	0.66	0.48	1.3	1.15	0.69
Class13	0	0.04	0.1	0.03	0.03
Total	100	100	100	100	100

Table 2.2: Hourly Distribution

Hour	WIM1	WIM2	WIM3	WIM4	WIM5
1	4.55	3.82	4.14	4.21	4.84
2	3.48	3.13	3.56	3.83	4.42
3	2.63	2.67	3.08	3.47	4.04
4	2.03	2.3	2.68	3.17	3.7
5	1.67	2.07	2.41	2.93	3.38
6	1.44	1.95	2.22	2.78	3.04
7	1.29	1.85	2.04	2.59	2.66
8	1.24	1.72	1.96	2.5	2.49
9	1.21	1.67	1.93	2.45	2.36
10	1.24	1.73	1.98	2.5	2.19
11	1.39	1.98	2.25	2.73	2.18
12	1.89	2.67	2.88	3.21	2.34
13	3	3.94	3.9	3.97	2.73
14	4.62	5.29	4.83	4.52	3.32
15	5.95	5.79	5.23	4.74	4.04
16	6.83	6.02	5.57	5.02	4.77
17	7.34	6.53	6.1	5.4	5.37
18	7.38	6.89	6.47	5.75	5.79
19	7.25	7	6.61	5.92	6.02
20	7.09	6.9	6.57	5.95	6.07
21	6.99	6.74	6.42	5.87	6.1
22	6.9	6.47	6.21	5.76	6.2
23	6.65	5.88	5.79	5.55	6.12
24	5.94	4.99	5.17	5.18	5.83
Total	100	100	100	100	100

Table 2.3: Axles-Per-Truck Distribution (Common to all WIMs)

Truck Class	Single	Tandem	Tridem	Quad
Class4	1.34	0.649	0	0
Class5	2	0	0	0
Class6	1	1	0	0
Class7	1.89	0.893	0.107	0
Class8	2.58	0.494	0	0
Class9	1	2	0	0
Class10	1	1	1	0
Class11	5	0	0	0
Class12	4	1	0	0
Class13	2.6	2.4	0.2	0

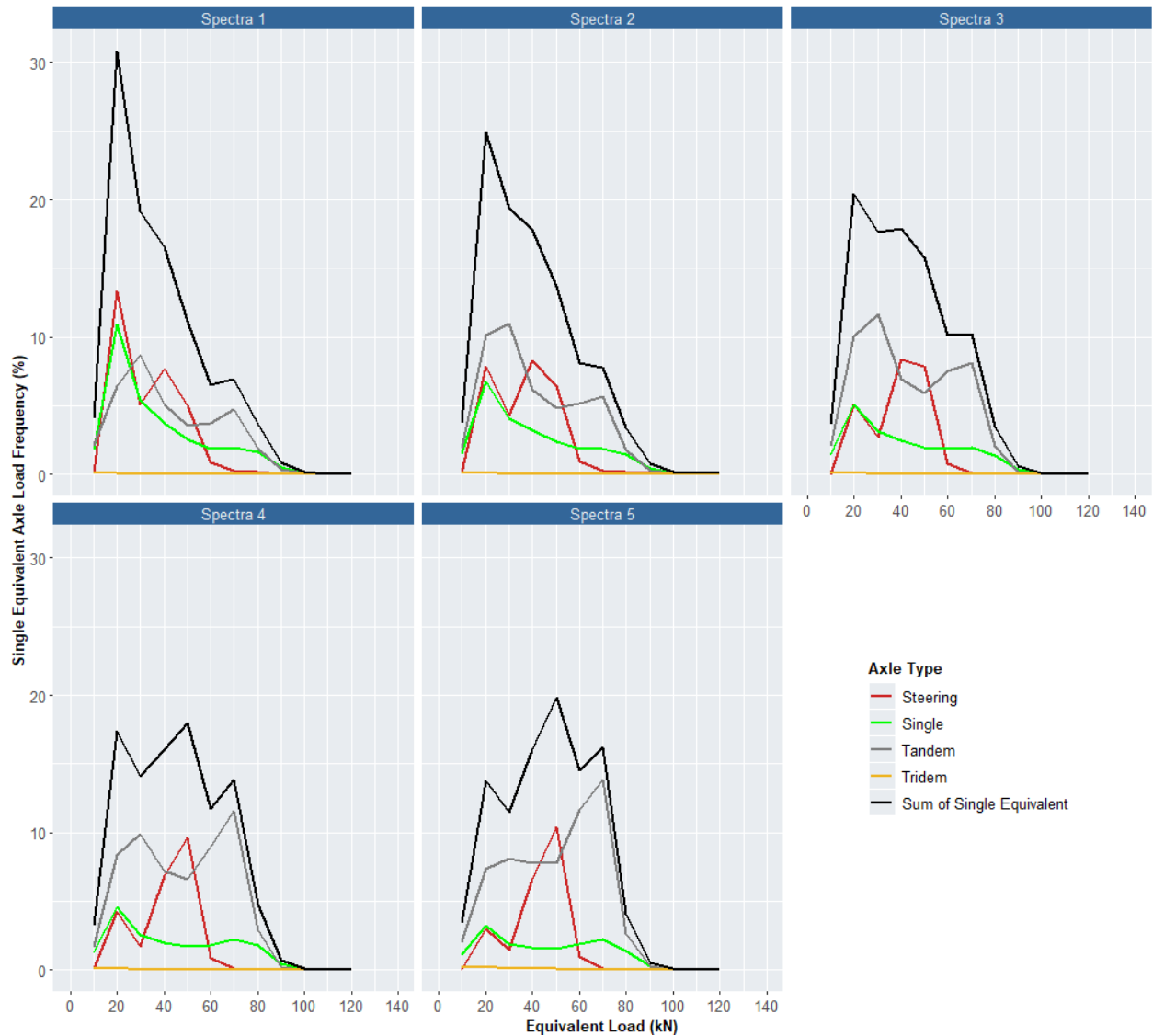


Figure 2.16: Single equivalent axle load distributions of the different WIM spectra.

Figure 2.17 shows the distribution of the pavement length (in lane-miles) for the five weigh-in-motion (WIM) spectra in the database. Most of the JPCP have WIM Spectra 1 and 2. This is certainly weighted by the extensive lane-miles of the network’s inner lanes, which have fewer trucks and whose trucks tend to be smaller and lighter.

Figure 2.18 shows the JPCP performance for the different WIM spectra. As the WIM spectra increase from 1 to 3, the amount of first-stage cracking increases, as expected. However, this is not the case for the heavier WIM Spectra 4 and 5, which have similar performance; this outcome was unexpected.

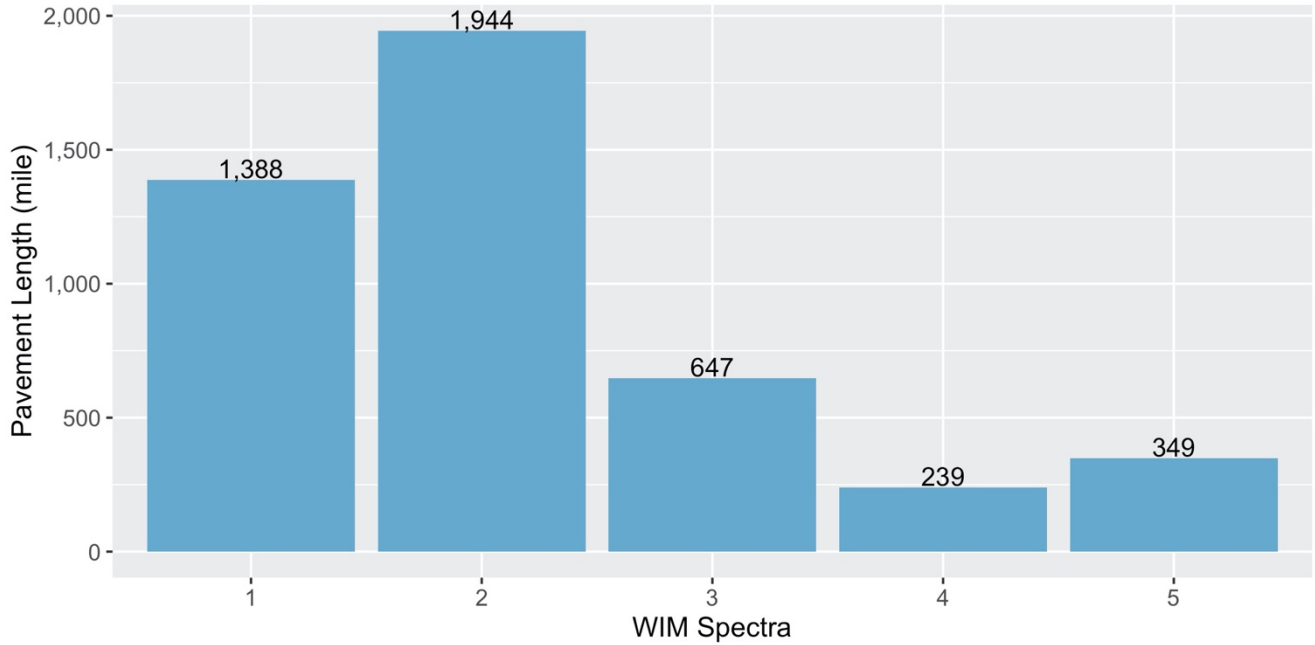


Figure 2.17: WIM spectra distribution.

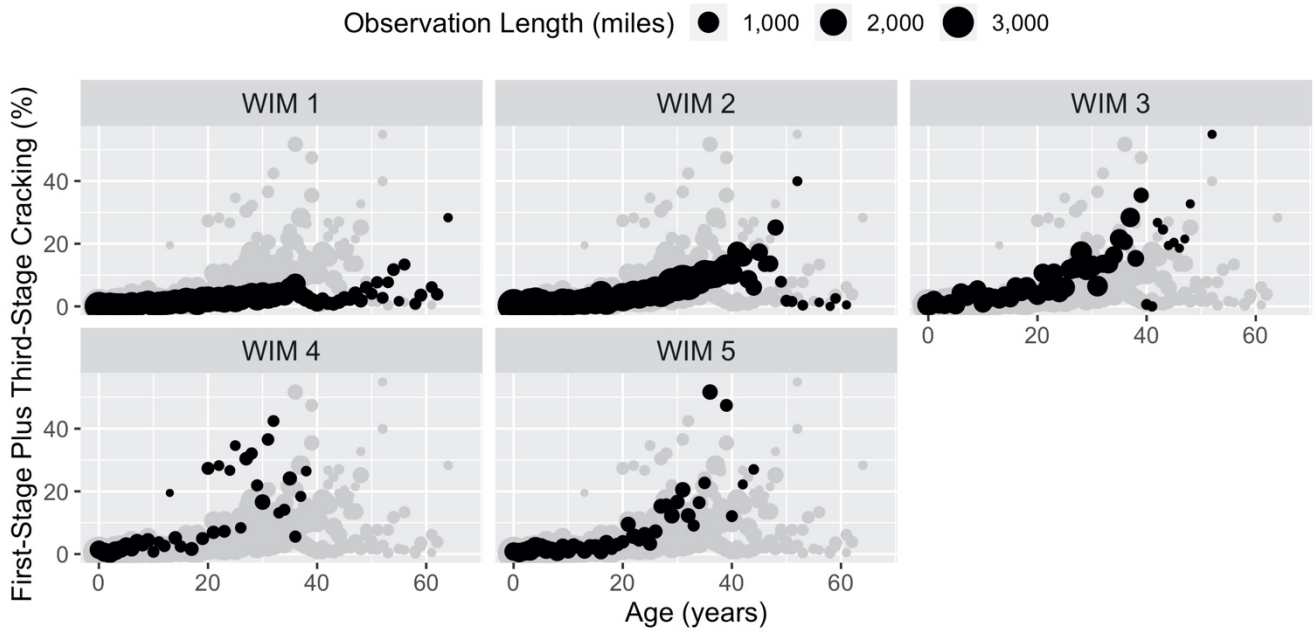


Figure 2.18: JPCP total cracking for different WIM spectra.

2.3.7 Annual Average Daily Truck Traffic (AADTT)

Figure 2.19 shows the distribution of unidirectional per lane AADTT. The X-axis shows the AADTT in thousands of trucks in increments of 3,000 trucks per day.

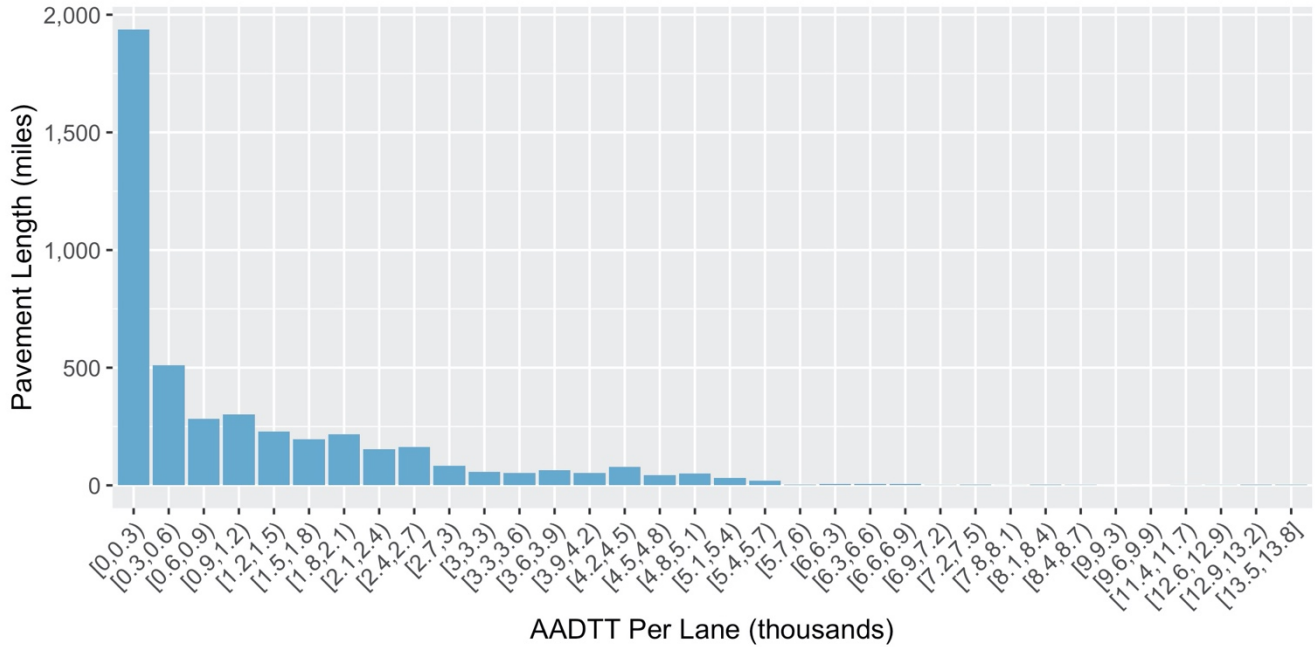


Figure 2.19: AADTT per lane distribution.

Figure 2.20 shows the performance of JPCP for different AADTTs. Each panel corresponds to a range of AADTT. As the amount of truck traffic increases, the amount of first-stage cracking increases. The last four panels have sparse data, and therefore drawing conclusions from them is not advised. However, predictions by the performance model support the visual observation in the data that greater AADTT causes more cracking, which was expected and will be discussed in the next section.

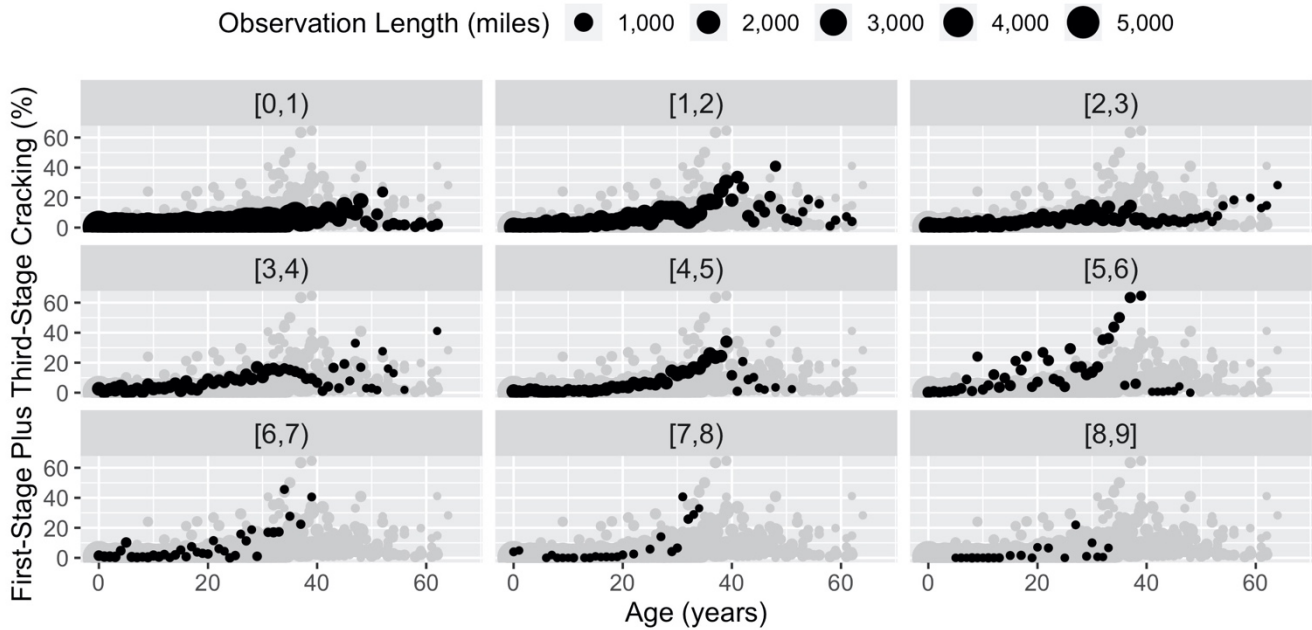


Figure 2.20: JPCP total cracking for different AADTTs per lane.

2.4 Statistical Performance Model for First- and Third-Stage Cracking

JPCP performance data can be considered a time series panel dataset, where the panels are the individual pavement sections that are defined as discrete lengths of pavement with similar factor levels for all the variables at different locations within projects. The variable of interest is the *pavement state*, an ordinal variable. There are three cracked pavement states: (1) undamaged, (2) first stage, and (3) third stage. This variable obviously is not a continuous, normally distributed variable. A generalized linear model is thus required, and in this case an ordered logit model (or ordered logistic regression) seems appropriate. In addition, because the data are nested panel data, a mixed-effects model is required, which allows each panel to have different regression parameters (the intercept in this model) to account for unexplained variability. The nested panel data (longitudinal data) are multidimensional data involving measurements over time, which in this case are cracking performance measures obtained from condition surveys in different years. In this context, this unexplained variability is called *between-project variability* (BPV), and it is caused by parameters such as material properties (e.g., PCC compressive strength, PCC thermal conductivity, and PCC coefficient of thermal expansion) that are unknown to designers prior to construction and variables that are not included in the database, such as subgrade soil stiffness. This type of model is known as a cumulative link mixed model (CLMM), a specialized form of a generalized linear mixed model accounting for ordinal data, whose generalized form is:

$$g(p(y < j)) = \eta = \theta_j + \mathbf{X}\boldsymbol{\beta} + \mathbf{Z}\boldsymbol{\gamma} + \epsilon \quad (2.1)$$

where: \mathbf{y} = vector of outcomes
 $\mathbf{g}(\cdot)$ = link function
 $\boldsymbol{\eta}$ = latent predictor $\sim N(\mathbf{0}, \mathbf{I})$
 θ_j = threshold for level j
 \mathbf{X} = matrix of predictor variables
 $\boldsymbol{\beta}$ = vector of fixed effect regression parameters
 \mathbf{Z} = matrix of design variables (panel variables)
 $\boldsymbol{\gamma}$ = vector of random effects $\sim N(\mathbf{0}, \mathbf{I}\boldsymbol{\xi})$
 $\boldsymbol{\epsilon}$ = vector of random errors

In this case, the link function is the logistic function, which is the natural logarithm of the odds that an event occurs, and the probability distribution of the outcomes is treated as a binomial distribution at each transition. Because the outcomes have a known distribution, the error of the latent variable must be scaled to have a unit normal distribution. Without scaling the latent variable to a unit normal distribution, there will be infinite solutions (fitted models). Notice that the only variable that changes with each threshold is θ_j , so that the transitions from one level to the next are not independent. The major advantage of this structure is that it accounts for the fact that the first-stage cracking evolution can inform the growth of third-stage cracking. This is particularly useful in this study because, for most JPCP sections, the first-stage cracking percentage reaches values that are much larger than those of third-stage cracking.

To fit the CLMM, the data were first structured so that each pavement section was a single sample, with the project level variables (e.g., PCC slab thickness, PCC slab length, shoulder type, base type, and climate) repeated for each section. In this approach, each observation (pavement section) can have any of three conditions—undamaged, first-stage cracked, or third-stage cracked—with a column determining the length of the section. Equivalently, the data within each project can be treated as a percentage of pavement sections that are in each of the three categories, and the fit weighted by the number of pavement sections. These two approaches are equivalent and produce identical results.

Several different predictor variables were tried in the fitting process. Based on the results from different models and visual inspection of the data, the following CLMM was used for calibration of the transverse cracking model:

$$\begin{aligned} \text{logit}(p(Y_i < j)) = & \theta_j - \beta_1 * \log(\text{age}_i) - \beta_2 * \log(\text{age}_i) * \text{AADTT_lane}_i \\ & - \beta_3 * \text{slab_pattern}_i * \text{PCC_thickness}_i - \beta_4 * \log(\text{age}_i) * \text{slab_pattern}_i - \beta_5 * \text{base_type}_i \\ & - \beta_6 * \text{shoulder_type}_i - \beta_7 * \text{climate}_i * \text{slab_pattern}_i - u(\text{project}_i) \end{aligned} \quad (2.2)$$

The proposed model includes a \log_{10} transform of age (in years), which is consistent with the observed effect of age and has been used in many other pavement models (9,10). This selection results automatically in zero probability of cracking when age is zero. Because Caltrans pavement design thicknesses are expressed in US feet,

the thickness variable was not changed to millimeters. During the model's development, it was found that the doweled/undoweled variable had no impact on the cracking status of the pavement, and therefore the variable was discarded. The WIM spectra variable did not have the expected effect (i.e., WIM4 and WIM5, greater percentages of heavier axle loads for a given amount of truck traffic, did not cause more cracking), and hence were not considered in the model. This likely points to issues with the WIM spectra assignment rather than the cracking data and will be investigated in future research.

This model estimates the probability of the i^{th} observation falling in the j^{th} category or below, where i is the index for observations (pavement section) and j is the index for the response categories, which in this model are undamaged, first-stage, and third-stage cracking. The explanatory variables are:

- *age*: age of the pavement section in years
- *AADTT_lane*: average annual daily truck traffic in thousands
- *slab_pattern*: slab length that is a categorical variable with levels 12,13,14,15 ft. or 12,13,18,19 ft.
- *PCC_thickness*: PCC slab thickness in feet
- *base_type*: type of base that is a categorical variable with levels aggregate base (AB), hot mix asphalt (HMA), asphalt-treated permeable base (ATPB), lean concrete base (LCB), and cement-treated base (CTB)
- *shoulder_type*: type of pavement shoulder that is a categorical variable with levels not applicable (NAP), meaning an inner lane, untied flexible shoulder (FLX), tied concrete shoulder (RIG), and widened concrete shoulder (WRF)
- *climate*: one of the climate regions that exists in California

θ_j is the threshold coefficient or cut point between either uncracked and first-stage cracking or first- and third-stage cracking. $\beta_1, \beta_2, \beta_3, \beta_4, \beta_5, \beta_6,$ and β_7 are model coefficients. Project effects were considered to be random with normal distribution $u(project_i) \sim N(0, \sigma^2)$. The random effect is considered on a project level and represents the BPV that is due to variables, such as material properties, that are unknown to a designer prior to construction. The difference between these unknown variables—while all the other design variables, traffic, and climate are the same—will lead to different pavement performance. This is unexplained by the variables that could be included in the model and accounted for by random effects in the CLMM. The random effect for each project is initially chosen randomly; however, final results are obtained by iteratively maximizing the log of the likelihood function. The CLMM2 function in the ordinal package in R was used to fit the model (11). Table 2.4 to Table 2.6 show the results of the model fit to the data. Looking at the p-values, some variables became insignificant; however, their interactions with other variables are significant. In the statistical model fitting, each individual

variable is an intercept term and should be included in the model, as ignoring an intercept term may cause the fitting process to force the model through zero, which is not necessarily correct.

Table 2.4: Mixed-Effects Cracking Performance Model Random Effect Parameter

Random Variable	Variance	Standard Deviation
Project	1.32856	1.152632

Table 2.5: Mixed-Effects Cracking Performance Model Location (Fixed) Parameters

Coefficient	Estimate	Std. Error	z-value	p-value
log10(Age)	1.1134	0.0650	17.1332	< 2.22e-16
slab_pattern (12,13,18,19) ¹	-0.2141	1.5338	-0.1396	0.889000
pcc_thickness	-1.8864	1.4091	-1.3387	0.180682
base_type (ATPB) ²	0.9241	0.3956	2.3357	0.019508
base_type (CTB)	-0.1939	0.2486	-0.7800	0.435400
base_type (HMA)	0.3148	0.3330	0.9453	0.344484
base_type (LCB)	1.9887	0.3675	5.4111	6.2636e-08
shoulder_type (FLX) ³	0.2841	0.0372	7.6288	2.3697e-14
shoulder_type (RIG)	-1.4978	0.0772	-19.3954	< 2.22e-16
shoulder_type (WRF)	0.2849	0.1499	1.9007	0.057336
climate (Desert) ⁴	0.2200	0.6973	0.3155	0.752355
climate (High Desert)	0.2256	1.3702	0.1646	0.869229
climate (High Mountain)	1.1428	0.7080	1.6140	0.106527
climate (Inland Valley)	1.2008	0.5376	2.2337	0.025505
climate (Low Mountain)	0.8263	1.3733	0.6017	0.547389
climate (South Coast)	0.2657	0.5388	0.4931	0.621925
climate (South Mountain)	1.3493	0.6532	2.0657	0.038857
log10(age)*AADTT_lane	0.1224	0.0035	35.2560	< 2.22e-16
slab_pattern (12,13,18,19)*pcc_thickness	-0.1833	1.7065	-0.1074	0.914476
log10(age)*slab_pattern (12,13,18,19)	0.4582	0.0762	6.0121	1.8316e-09
slab_pattern (12,13,18,19)*climate (Desert)	-0.6564	0.8341	-0.7870	0.431281
slab_pattern (12,13,18,19)*climate (High Desert)	0.4981	1.7792	0.2800	0.779515
slab_pattern (12,13,18,19)*climate (High Mountain)	-1.2651	1.5402	-0.8214	0.411417
slab_pattern (12,13,18,19)*climate (Inland Valley)	-1.1382	0.6472	-1.7587	0.078623
slab_pattern (12,13,18,19)*climate (Low Mountain)	0.7469	1.4870	0.5023	0.615480
slab_pattern (12,13,18,19)*climate (South Coast)	-1.2499	0.6633	-1.8845	0.059503
slab_pattern (12,13,18,19)*climate (South Mountain)	-1.7031	0.7515	-2.2662	0.023436

¹ Reference category: 12,13,14,15 ft.

² Reference category: AB

³ Reference category: NAP

⁴ Reference category: Central Coast

Table 2.6: Mixed-Effects Cracking Performance Model Threshold Parameters

Threshold Coefficients	Estimate	Standard Error	z-value
Undamaged >> First-Stage	6.7784	1.2109	5.5980
First-Stage >> Third-Stage	8.7319	1.2113	7.2090

Since the model is fairly complicated and has many interactions between different variables, it is difficult to understand the effect of each variable (coefficient in the model) on the cracking performance of the JPCP. Therefore, a sensitivity analysis on the model predictions is presented below. The predictions from the model are presented for a set of input variables so that reasonableness of the model’s predictions and the effects of each variable on the JPCP performance can be evaluated.

Figure 2.21 shows the effects of PCC slab thickness on the cracking performance of JPCP. Each panel represents a PCC slab thickness. Panels are plotted for 0.6, 0.9, and 1.2 ft. thick slabs with the short slab pattern (12,13,14,15 ft.). The X-axis represents age of the pavement, and the Y-axis represents the probability of each state (undamaged, first-stage cracking, and third-stage cracking). This graph is plotted for the Central Coast climate region, with no shoulder, LCB, and AADTT per lane of 4,000. As the PCC slab thickness increases (looking from left to right in the panels), the green area becomes bigger and yellow and red areas shrink. This means that the thicker PCC slabs show less first- and third-stage cracking, which matches what was expected from the qualitative analysis of the data presented at the beginning of this chapter.



Figure 2.21: Mixed-effects cracking performance model predictions for different PCC slab thicknesses.

Figure 2.22 shows the effects of slab pattern on the JPCP cracking performance. This graph is plotted for the Central Coast climate region, with no shoulder, LCB, 0.9 ft. PCC slab thickness, and AADTT per lane of 4,000. The performance model predicts much more first- and third-stage cracking for the long slab pattern (12,13,18,19 ft.) than for the short one (12,13,14,15 ft.).

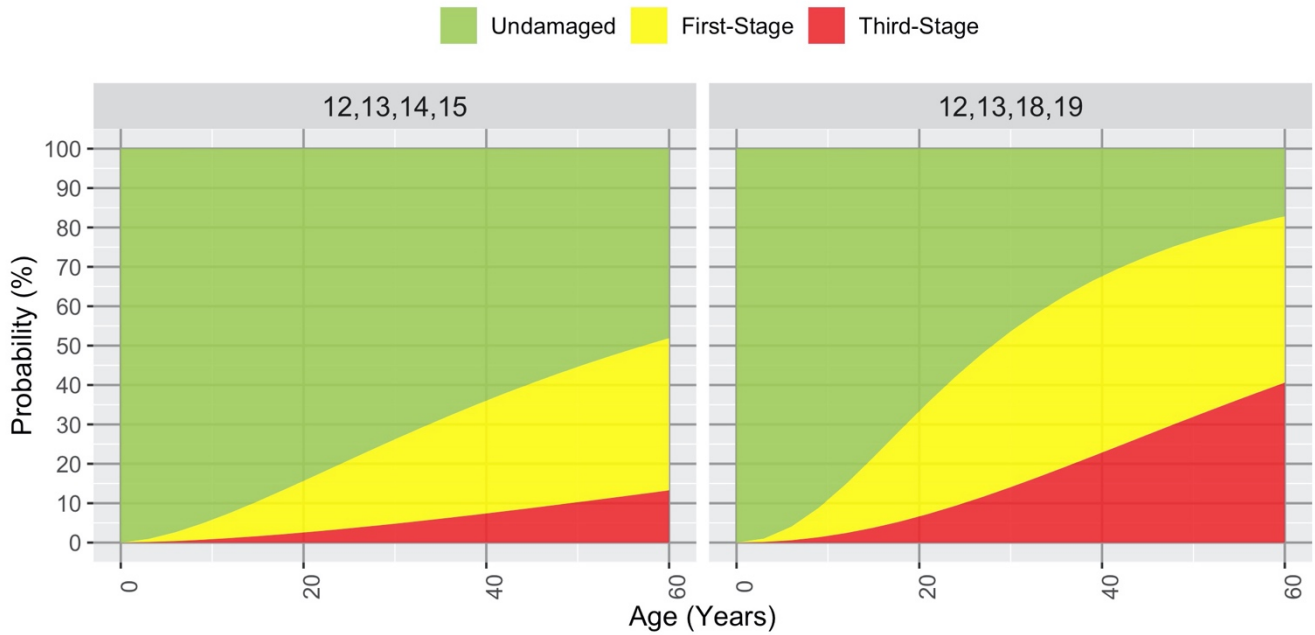


Figure 2.22: Mixed-effects cracking performance model predictions for different PCC slab patterns.

Figure 2.23 shows the effects of different base types on the cracking performance of JPCP. This graph is plotted for the Central Coast climate region, with no shoulder, 0.9 ft. PCC slab thickness, short slab pattern (12,13,14,15 ft.), and AADTT per lane of 4,000. This graph shows that the conclusion drawn from Figure 2.10, which shows that CTB has the worst cracking performance of the five base types considered, was not correct as it considered only one variable (base type) on the performance of JPCP. The performance model used for Figure 2.23 considers all the variables and their interactions at the same time and predicts that the JPCP with LCB has the worst cracking performance, while the JPCP with CTB and HMA bases have the best cracking performances. (In the *Pavement ME* calibration process, the ATPB and HMA base types will be combined into one category, as ATPB has not been defined in *Pavement ME* software.)

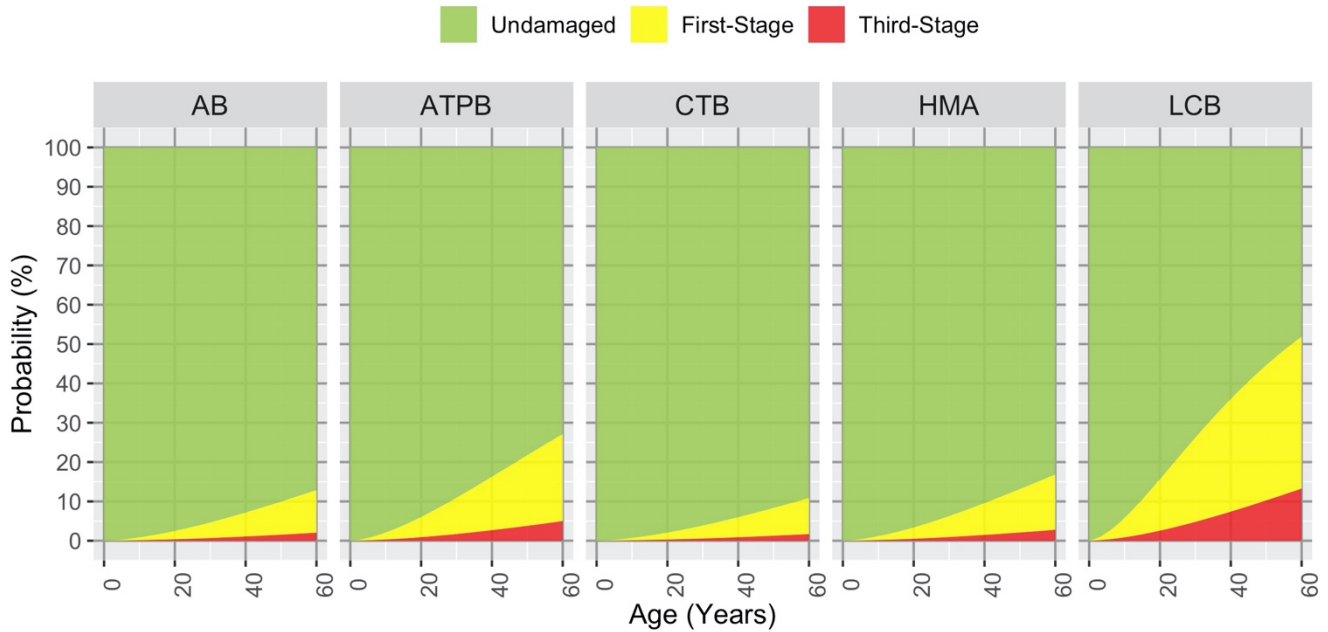


Figure 2.23: Mixed-effects cracking performance model predictions for different base types.

Figure 2.24 shows the effects of shoulder type on JPCP cracking performance. This graph is plotted for the Central Coast climate region, with LCB, 0.9 ft. PCC slab thickness, short slab pattern (12,13,14,15 ft.), and AADTT per lane of 4,000. In the figure below, NAP represents no shoulder (i.e., interior lanes), FLX is untied flexible shoulder, RIG is tied concrete shoulder, and WRF is widened concrete shoulder. The graph shows that the JPCP with tied concrete shoulder performs the best and the JPCP with flexible and widened shoulders equally perform poorly. The widened slabs were historically constructed with 14 ft. slabs (2 ft. of shoulder) to mitigate the problem with transverse cracking; however, as shown in Figure 2.13, this shoulder type results in nearly the same JPCP cracking performance as the flexible shoulder.

Figure 2.25 shows the effects of climate region on JPCP cracking performance. This graph is plotted for JPCP pavement with no shoulder, LCB, 0.9 ft. PCC slab thickness, short slab pattern (12,13,14,15 ft.), and AADTT per lane of 4,000. The JPCP in the Inland Valley, High Mountain, and South Mountain climate regions have the worst performances among all climate regions. The best performances occur in the South Coast, Central Coast, High Desert, and Desert regions, with the Low Mountain region falling in between. (The North Coast climate region does not appear in Figure 2.25, as the database used for the development of the statistical performance model does not contain JPCP for that region.)

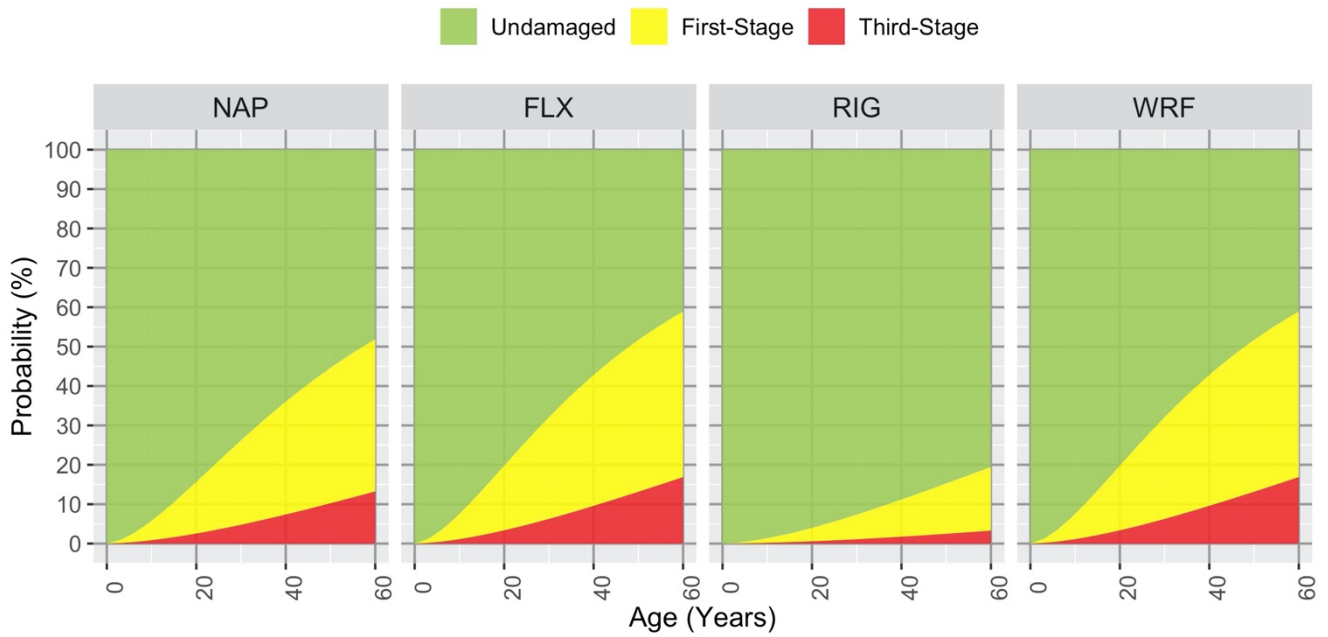


Figure 2.24: Mixed-effects cracking performance model predictions for different shoulder types.

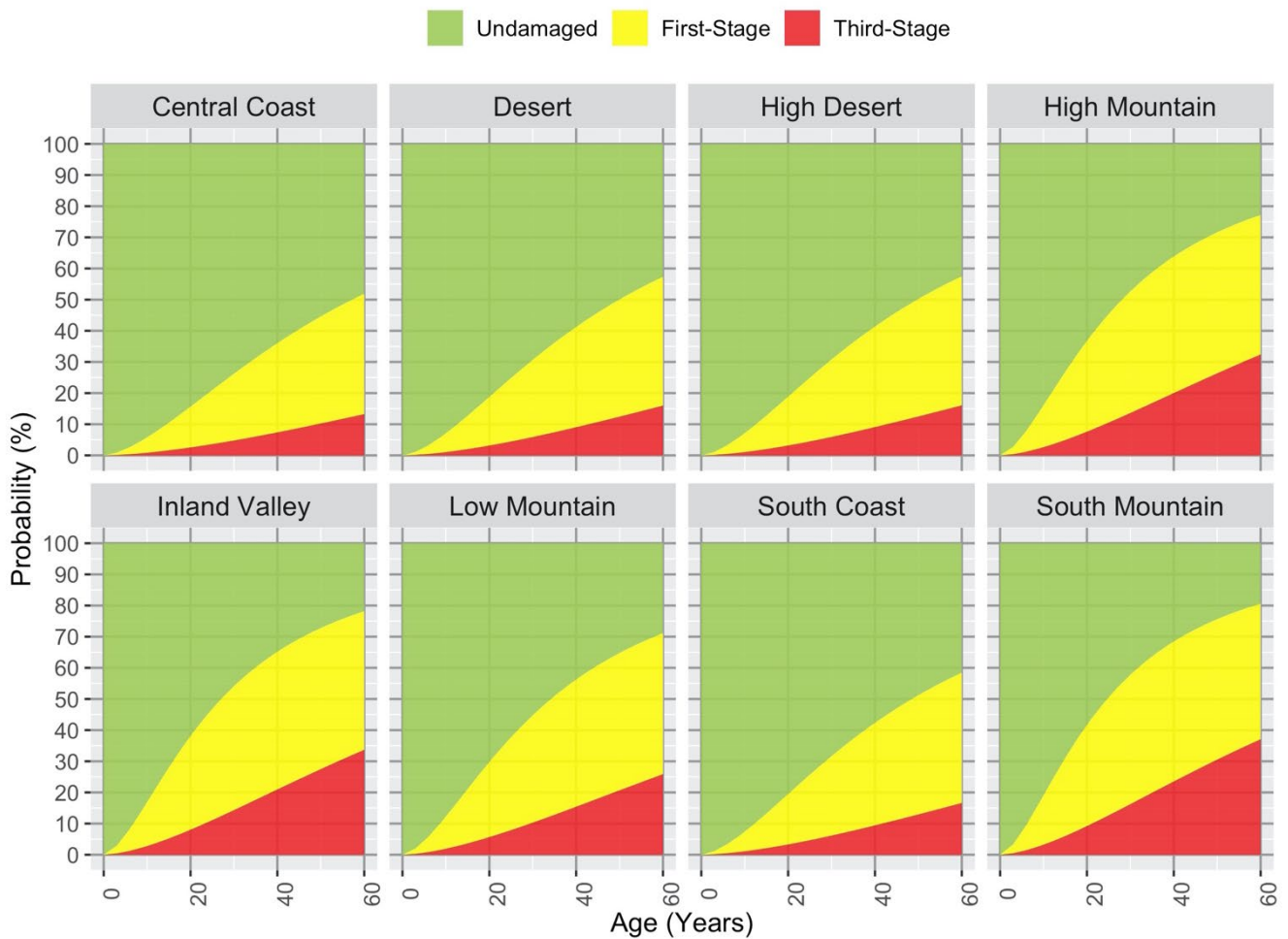


Figure 2.25: Mixed-effects cracking performance model predictions for different climate regions.

Another informative output from the model, besides the coefficients, is the *between-project variability* (BPV) parameter, which has a standard deviation of 1.15. BPV is defined as the random effects in the CLMM model. To understand the concept of BPV and how it is accounted for in the CLMM, Figure 2.26 includes actual performance data and corresponding model predictions for three projects in a cell of data in the Pavem pavement management system (PMS) database. A *cell of data* is a set of performance data that could be collected from different projects but that have the same values for all design variables (pavement structure, traffic, and climate). The cell of data presented in Figure 2.26 corresponds to the Desert climate zone, CTB, FLX shoulder, long slab pattern (12,13,18,19 ft.), 0.75 ft. PCC slab thickness, and AADTT per lane of 1,000. The Y-axis represents the total cracking (first- plus third-stage cracking) percentage and the X-axis represents the time under service (age) of the JPCP. The faded gray data points are the actual raw performance data. The data points in color show the results after data aggregation.

The performance data for this cell have been collected from three different projects, and all data points corresponding to a specific project are distinguished with a specific color. Although all these projects have the same pavement structure, traffic, and climate, they have shown different cracking performance. This difference in performance is due to other sources of variability that are unavailable (unknown to the designer) such as material properties (i.e., PCC compressive strength and CTE), model limitations, and error in input parameters. The dashed line is the model prediction (expected/average) without considering BPV, and the colored lines correspond to model predictions for each project (sharing the same color as its data points) considering BPV. Therefore, it is expected that after removing the BPV parameter from each project, the colored lines lie on the dashed line. In the example shown in Figure 2.26, the individual project lines are all above the cell model average. In other cells, the project lines may be above or below the cell model average, and across all cells and ages the cell model average should match the median performance of the entire database. This is an important concept that will be used in the next chapter in order to calibrate the *Pavement ME* transverse cracking model.

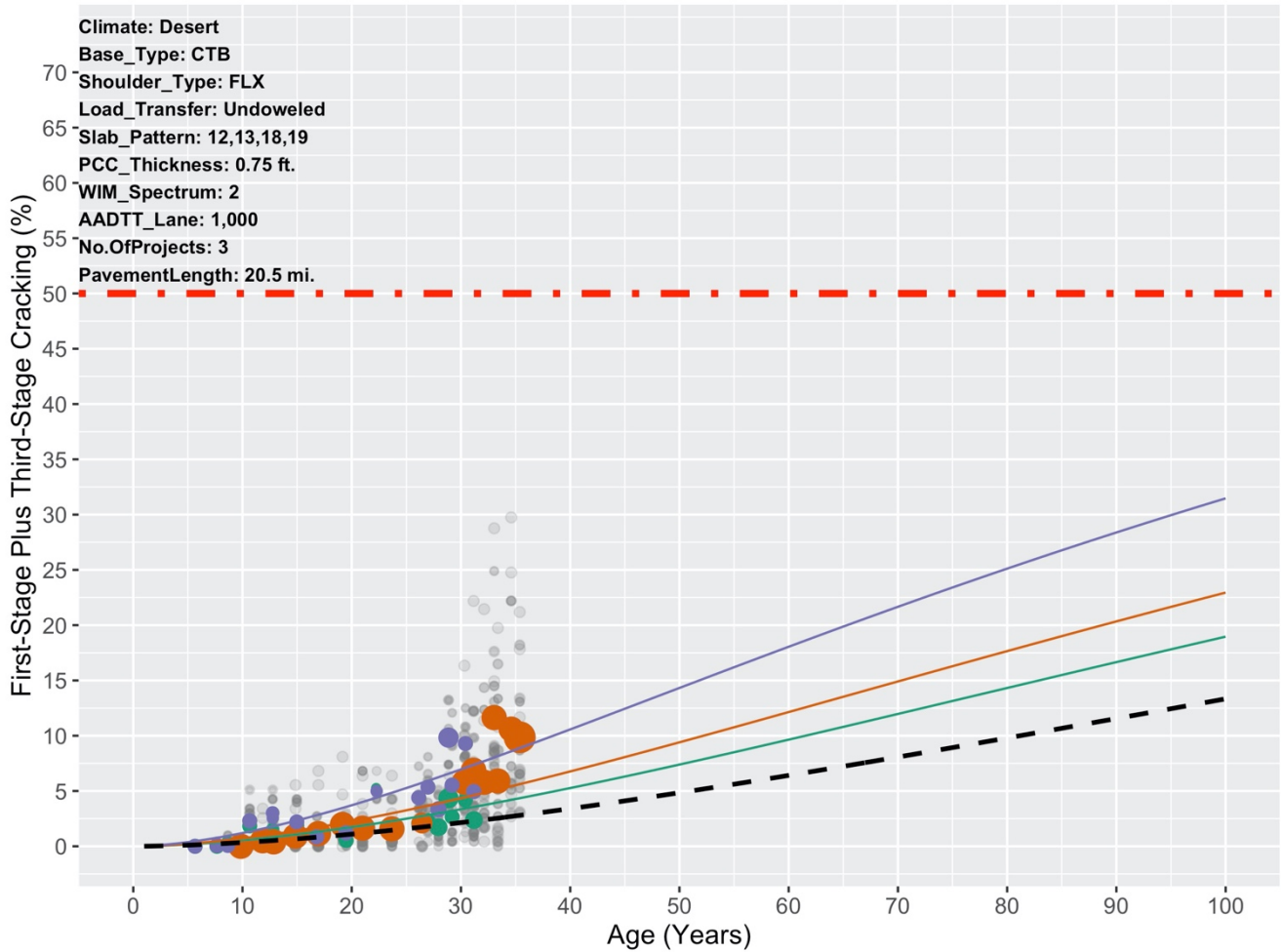


Figure 2.26: Mixed-effects cracking performance model predictions for a cell of data.

2.5 First-Stage-to-Transverse Cracking Model

As detailed above, Caltrans has historically collected JPCP cracking data in terms of first-stage and third-stage cracking. However, the *Pavement ME* transverse cracking model predicts only the percentage of transverse cracking in JPCP. Since there are only a few years of first-stage cracking data in the *PaveM* database that separate transverse and longitudinal cracking, a model was developed that can predict the portion of first-stage cracking that is transverse cracking. In this study, it is assumed that 100% of the slabs with third-stage cracking have at least one transverse crack. This assumption together with the model allow the use of the *PaveM* performance database for *Pavement ME* calibration.

APCS 2011–2012 is the only survey that currently has per-slab data in the *PaveM* database. This database contains information on pavement structure, traffic, climate, and slab condition (undamaged, transversally cracked, longitudinally cracked, or X-cracked, defined as cracks that did not meet the definitions of transverse, longitudinal,

or corner cracks) needing separation to identify transverse cracking (corner cracking was recorded separately). These data have been used to develop a model that can predict the portion of first-stage cracking that is transverse cracking, which was then applied to all of the APCS and PCS data Caltrans has collected since 1978 to create a transverse cracking database for *Pavement ME* calibration.

The data were first structured so that each slab is a single sample. The dependent variable (outcome) is a binary variable stating whether or not the slab is cracked transversely. The goal was to develop a model with the highest accuracy possible. Many different models were developed—from those that are highly interpretable but low in accuracy (such as a logistic regression model) to machine-learning black-box models with high accuracy and low interpretability (such as random forest, gradient boosting, and neural network). Of these models, the gradient boosting model had the best performance, more reasonable predictions, and least time for fitting. Performance was evaluated by the percentage of transverse cracked slabs that were predicted correctly (recall) and the overall accuracy. To develop the model, 80% of the data was randomly chosen, and the model predictions were evaluated on the remaining 20% (unseen to the model) of the data. *Recall* is the ratio of the total number of transverse cracked slabs predicted by the model to the total number of transverse cracked slabs available in the data, and *overall accuracy* is the ratio of total number of correct model predictions to total number of instances.

The idea of boosting comes from the question of whether a weak learner can be modified to become better. A *weak learner* is defined as one whose performance is at least slightly better than random chance. Boosting is the idea of filtering observations, leaving those observations that the weak learner can manage and focusing on developing new weak learners to manage the remaining difficult observations. The gradient boosting model involves three elements:

1. Loss function: The loss function should be optimized. The loss function depends on the type of problem being solved. For regression problems, the squared error is used, and for classification problems, the log loss function is used. In this model, the log loss function was used, as it is a binary classification problem.
2. Weak learner: Weak learners are mathematical (parametric or non-parametric) simple models that make predictions. Decision trees are used as the weak learner in gradient boosting.
3. Additive model: This model is used to add up the weak learners to minimize the loss function. Trees are added one at a time, and existing trees in the model are not changed. The output for each new tree is then added to the output of the existing sequence of trees in an effort to correct or improve the final output of the model. A fixed number of trees are added, or training stops once loss reaches an acceptable level or no longer improves on an external validation dataset.

A gradient boosting model was developed with the following predictors and parameters:

$$\text{condition} \sim f(\text{PCC_thickness}, \text{PCCSlab_length}, \text{shoulder_type}, \text{base_type}, \text{climate}, \text{doweled}, \text{WIM}) \quad (2.3)$$

- Max depth: 31
- Number of leaves: 137
- Number of trees: 4,000
- Learning rate: 0.005

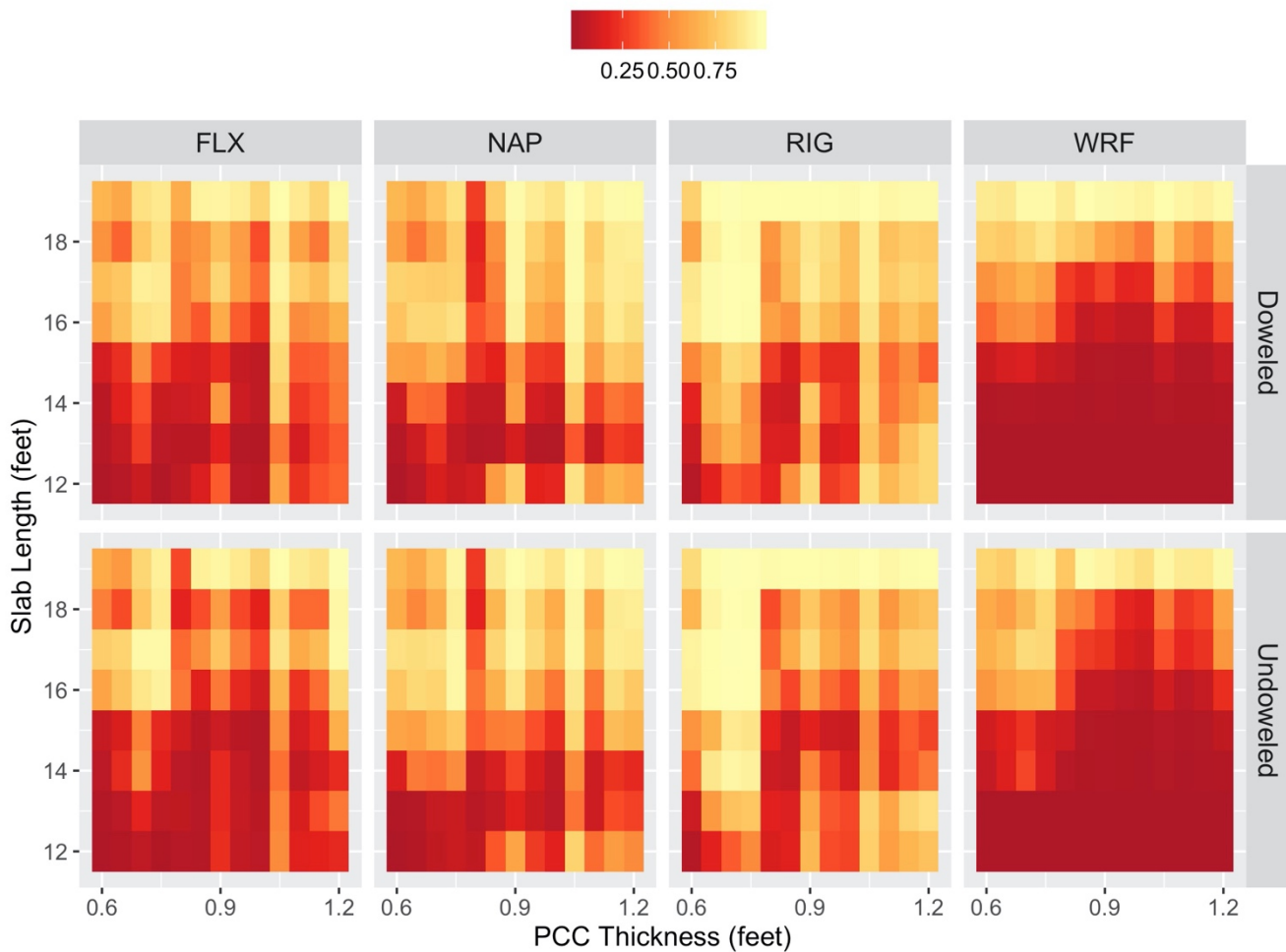


Figure 2.27: First-stage cracking to transverse cracking model predictions for different shoulder types.

This model has a recall of 87.5%, which means that 87.5% of slabs with transverse cracking were identified correctly. The precision is 81.8%, which means out of all transverse cracking predictions done by the model, 81.8% were correct. Figure 2.27 shows model predictions for different pavement variables. These plots correspond to pavements in the Inland Valley climate zone, with HMA base, and under WIM Spectra 1. Each

panel in the graph corresponds to a shoulder type with either doweled or undoweled load transfer. The Y-axis represents the PCC slab length in feet, the X-axis represents the PCC slab thickness in feet, and the color shows the transverse cracking percentage (a lighter color indicates more transverse cracking, and a darker color indicates more longitudinal cracking). This graph shows that the model adequately predicts greater percentages of transverse cracking as the slab length increases. It also shows that the model predicts less transverse cracking for shorter slabs with widened concrete shoulder, which is in accordance with what was discussed in Section 2.3.4. It is also clear that for widened shoulders, the doweled pavement shows more longitudinal cracking than the undoweled pavement, which verifies a study done on the development of a longitudinal cracking fatigue damage model for JPCP (12).

Figure 2.28 shows model predictions for doweled pavements, with CTB, FLX shoulder, and WIM Spectra 1. Each panel in the graph corresponds to a different climate region. The model predicts that the Desert climate region has more transverse cracking, whereas the South Mountain region has more longitudinal cracking.

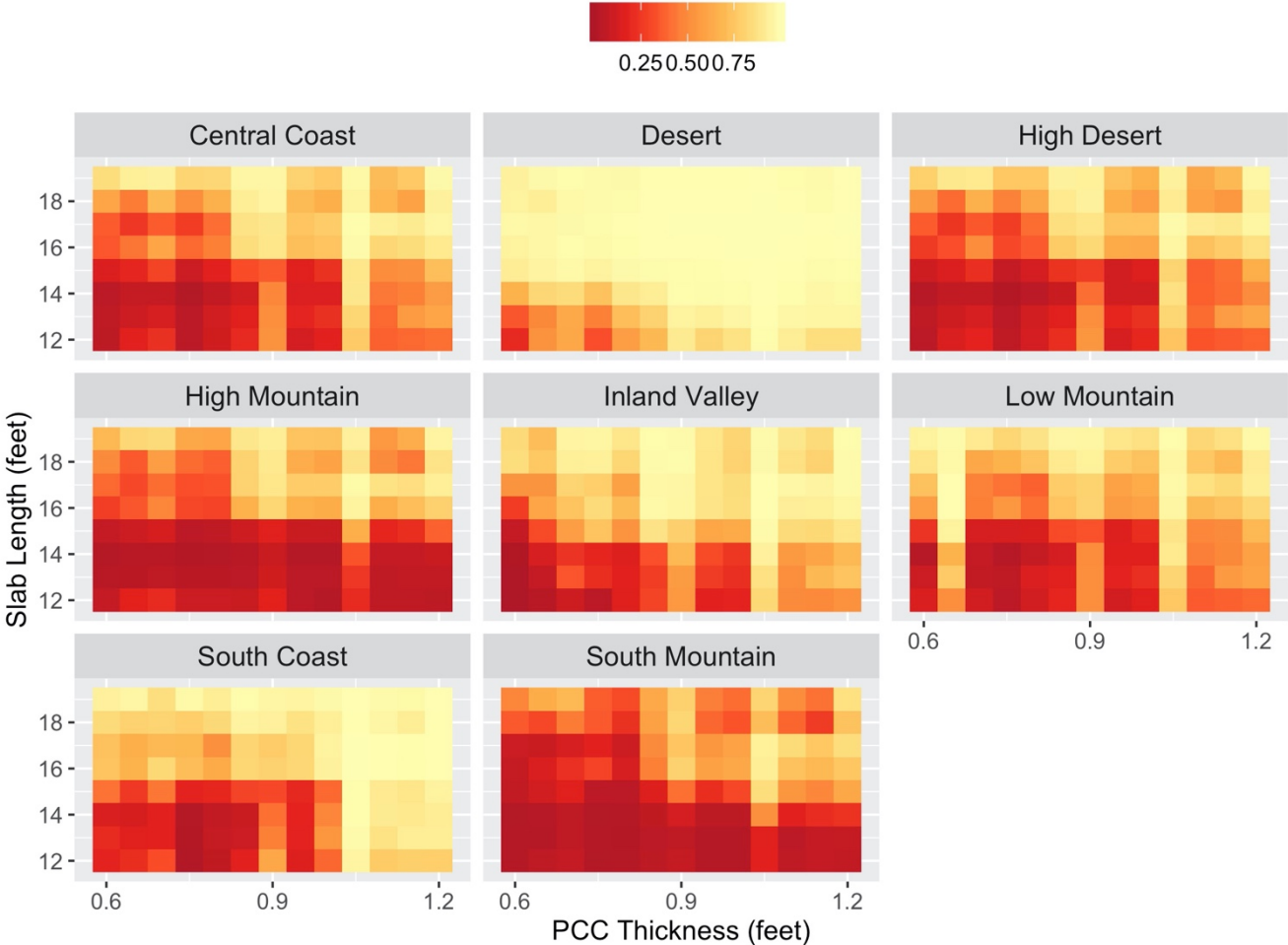


Figure 2.28: First-stage cracking to transverse cracking model predictions for different climate regions.

This model separates the first-stage cracking into an estimate of transverse cracking data. Separating the first-stage cracking is done by multiplying the outcome of this model by the percentage of first-stage cracking, which results in the best estimate of the amount of transverse cracking in the JPCP. However, this amount represents the start of transverse cracking and should be added to third-stage cracking to obtain the total amount of transverse cracking over the full history, because third-stage cracking has at least one transverse crack. Finally, the total amount of transverse cracking is the performance measure that will be used for *Pavement ME* calibration. The next chapter discusses the calibration process in detail.

(This page intentionally blank)

3 PAVEMENT ME CALIBRATION

3.1 Introduction

Pavement ME software uses three distress models for jointed plain concrete pavements (JPCP) analysis and design under traffic and environmental loads. These three distress models are (1) transverse cracking, (2) transverse joint faulting, and (3) International Roughness Index (IRI). The transverse cracking and transverse joint faulting models are stand-alone models that have been developed based on the principles of mechanics and statistical models and are therefore called mechanistic-empirical models. The IRI model was developed by fitting a statistical model to the predictions of the transverse cracking and transverse joint faulting models.

The goal of this chapter is to calibrate the *Pavement ME* transverse cracking model with the performance data available in the Pavement Management System (PMS) database. Calibrating this model consists of determining a set of model coefficients to optimize (minimize) the model prediction errors. The performance data in the PMS database measured faulting as percentage faulted transverse joint within a pavement section—which, when combined with the previously discussed varying section lengths and locations in the survey, resulted in data unsuitable for modeling. Caltrans built JPCP without dowels, except for a few test sections, from the late 1940s until 1998 and experienced faulting and poor ride quality on much of its concrete network until dowels were introduced.

A study in 1967, after Caltrans had switched to plant-mixed CTB with greater cement content to try and reduce faulting, showed that faulting still typically occurred within 4 million equivalent single axle loads of traffic after construction (13). (It is interesting to note that the same study showed a switch on test sections on US 101 from 97% transverse cracking and 3% longitudinal cracking with the less stiff pre-1967 CTB to 40% transverse cracking and 60% longitudinal cracking with the stiffer CTB, an early indication of the effects of changing from CTB to LCB seen in the previous chapter of this report). A survey of JPCP with high traffic levels in 1999 indicated that faulting was prevalent on the majority of the pavement surveyed (6).

Caltrans mandating the use of dowels in JPCP construction since 1998 has had a significant impact on mitigating the faulting distress in California. As a result, the roughness caused by faulting has ceased to be much of an issue on JPCP; the low IRI on doweled JPCP appears to be primarily controlled by construction smoothness (1,7).

The calibration of the *Pavement ME* faulting model in 2007 (3) on undoweled JPCP, using faulting measurements made by the University of California Pavement Research Center (UCPRC) with a high-speed profiler moving at slow speeds, showed that the national faulting model for undoweled pavement did a good job of predicting performance on California pavements. This is likely due in part to the fact that a large part of the calibration of that model was done on California sections, which were used because most other states had switched to using

dowels much earlier than California. For the following reasons only the transverse cracking model was calibrated in this study:

- There were not enough sections with good faulting history data (built prior to 1998), and there are generally no available faulting data on JPCP built since 1998, according to the Automated Pavement Condition Survey (APCS) data in the PaveM database.
- Caltrans constructs doweled JPCP exclusively, and faulting is not a major problem for it.
- The faulting model in the *Mechanistic-Empirical Pavement Design Guide (MEPDG)* matched well with Caltrans data in 2006 for undoweled concrete. The model coefficients have changed since a calibration study in 2007 (3); however, the current model predictions have changed very slightly since the last calibration.
- IRI on doweled concrete pavement is primarily a function of the IRI achieved in construction.

3.2 Traditional Pavement ME Calibration Process

The goal of transverse cracking model calibration is to find a set of model coefficients that minimizes the model prediction error. Traditionally, ME models, including the *Pavement ME* models, have been calibrated with a small number of JPCP sections (hundreds at the national level, tens at the state level) for which all the design and non-design (material properties) variables were known or collected. UCPRC calibrated the *MEPDG* in 2007 with 52 rigid and 43 crack, seat, and overlay sections (3). The national calibration of the *MEPDG* used data from fewer than 200 Long-Term Pavement Performance (LTPP) sections, with a total length of about 20 miles (1).

In the context of this report, *design variables* are those—such as portland cement concrete (PCC) slab thickness, PCC slab length, base type, shoulder type, traffic, and climate—that can be determined by the pavement designer prior to construction. The *non-design variables* are those—such as PCC compressive strength, PCC modulus of rupture, and PCC coefficient of thermal expansion—whose exact values are unknown to the designer at the time of design. Design and non-design variables were discussed in the *Pavement ME Sensitivity Analysis* (5). According to traditional *Pavement ME* calibration, data for all the design and non-design variables must be collected, either by extracting them from as-builts or coring specimens, by running laboratory tests, or by conducting field tests. Once these data are obtained, in the traditional *Pavement ME* calibration, the following steps are taken to calibrate the distress models (15):

1. Select hierarchical input level for each input parameter.
2. Develop local experimental plan and sampling template.
3. Estimate sample size for specific distress prediction models.
4. Select roadway segments.
5. Extract and evaluate distress and project data.

6. Conduct field and forensic investigations.
7. Assess local bias of global calibration factors.
8. Eliminate local bias of distress prediction models.
9. Assess the standard error of estimate (SEE).
10. Reduce the SEE.
11. Interpret results.

For a more detailed description of each step, refer to *Guide for the Local Calibration of the Mechanistic-Empirical Pavement Design Guide (15)*.

Pavement management systems have much more performance data than what has been used for traditional mechanistic-empirical model calibration. The Caltrans PaveM database used for the calibration of the *Pavement ME* transverse cracking model presented in this report consists of 30,155 pavement sections with a combined length of approximately 4,380 lane-miles and with 265,033 performance observations. This is 150 times more pavement sections and more than 200 times more lane-miles than those used for the national calibration.

Traditional *Pavement ME* calibration has limitations that do not allow the use of the kind of “big performance data” that was used in PaveM for the model calibration presented in this report. Specifically, the traditional calibration does not consider the variabilities involved in pavement performance and therefore may predict reasonable average performance while underestimating variability. (The variabilities involved in pavement performance will be explained in the following sections.) Another limitation of the traditional calibration procedure is the requirement to determine all inputs, including non-design variables. This means field sampling and material testing are needed to determine inputs, which limits the number of roadway segments that can be included in the calibration and therefore may lead to underestimation of model error and input error. The residual errors in past calibration efforts can be attributed to two causes: the model adopted has a significant amount of error and/or the inputs to the model have errors. To overcome these shortcomings, a new approach was developed to calibrate *Pavement ME* for this project. The new approach uses the big performance data from the Caltrans PaveM while accounting for the different sources of pavement performance variability.

In this chapter, the step-by-step procedure for *Pavement ME* calibration is discussed in detail, as well as the calibrated transverse cracking model coefficients obtained from the procedure. The calibrated model will be used to develop the Caltrans JPCP design catalog.

3.3 Variability Affecting Pavement Performance

Different sources of variability in pavements cause differences in their performance behaviors, such as their rates of section deterioration and crack progression. The sources of these performance variabilities may be due to variabilities in known design variables, external conditions such as traffic loads and climate, or unknown variables such as material properties. A good calibration process will take all these variabilities into account to render a more reliable calibration. However, before the new *Pavement ME* calibration procedure is presented, it is necessary to have a good understanding of the different components of the variabilities involved in pavement performance.

Like any other structure, pavements are not uniform. Theoretically, a pavement's performance is determined by external factors such as climate and traffic and by internal factors such as pavement structure and material properties. Each of these factors can be characterized as a random variable, and together they form a random vector. For ease of reference, the random vector can be designated as X , and it can be called *pavement variable inputs* because it is essentially a collection of the selected inputs believed to have significant effects on pavement performance.

The performance of a pavement regarding certain failure mechanisms can be expressed as the *time history* of the percentage of pavement failed by the mechanism under consideration. Consider, for example, a JPCP pavement condition survey that monitors percent slabs with transverse cracking. In the following equation, Y denotes transverse cracking—which is a function of pavement age (t) and input variable X —and can be expressed mathematically as:

$$Y = Y(t) = P(t_f \leq t|X) = Y(t; X) \quad (3.1)$$

where P is the probability of failure and t_f is the time to failure (when the slab is cracked transversely). $Y(t; X)$ is a function of time t with parameter X and is essentially the cumulative distribution function (CDF) of failure time t_f for a given performance input X . As shown in Equation 3.1, pavement performance is a time history affected by the input vector X . The variabilities in performance come from the variabilities in X .

For pavements in a large network (as in a PMS database), performance is understandably different. This is because the mean values of X are different between projects. This could be due to differences in PCC slab thickness, PCC slab length, PCC compressive strength, PCC coefficient of thermal expansion, and traffic load. The variability in pavement performance caused by a change in the mean value of X is referred to as *between-project variability* (BPV). The unexplained part of this variability (i.e., the part that cannot be explained by the model's inputs) is introduced as random effects in the mixed-effects cracking performance model used for this calibration.

Alternatively, consider a specific project in which X is nominally the same throughout. Of course, “nominally the same” does not mean “exactly the same.” Statistically, two variables are nominally the same when they have the same distribution. The following are some examples of variables that are nominally the same:

- Concrete materials are nominally the same if they are produced by the same plant following the same mix design, use the same sources for raw materials, and are placed by the same contractor. However, concrete properties such as modulus of rupture may vary in different locations of a single project, and this variation may cause different rates of deterioration—and hence different cracking performance—in different slabs within the project.
- PCC slab thicknesses are nominally the same in the overall project based on the design thickness. However, not all slabs are constructed with the exact same thickness. Their thicknesses may slightly vary over the project, which will eventually result in different cracking rates.
- Climate conditions are nominally the same if they are classified into the same climate zone, but temperature, humidity, and other climate conditions may differ for the project, and this variation may cause different cracking performance in the project.

Given the random nature of X , pavement distresses are expected to develop at different rates within the project even if X is nominally the same. This type of variability in pavement performance is referred to as *within-project variability* (WPV). In other words, a project can be divided into many segments, with each segment representing a random sample of X , and the values of X in the segments are likely to be different from each other. This results in different pavement performance.

There is a third type of variability that is caused by the change in the variability (standard deviation) of X . There are many scenarios in which the variability of X can change. However, changes in variability of X are typically accompanied by changes in its mean value as well. One scenario that can lead to minimal change in the mean value of X while allowing the variability of X to change is a change related to the contractor. Different contractors have different quality-control tolerances and hence different variability in X . For example, Contractor A may have rigorous quality control and produce a PCC whose flexural strength after 28 days has a mean value of 643 psi and a standard deviation of 25 psi, while Contractor B may not follow such rigorous quality control and produce a PCC with the same mean flexural strength (643 psi) but with much larger standard deviation (e.g., 60 psi). These two contractors will have different *between-contractor variability* (BCV) even if they are using the same materials at the same project location.

3.4 Effects of Different Variabilities on Pavement ME Transverse Cracking Transfer Function

To illustrate the effects of different variabilities on the *Pavement ME* transverse cracking transfer function, a simplified example of a project in which all the variables that have an effect on pavement performance (such as pavement structure, material properties, traffic loads, and climate) is considered. The only parameters that may change over the entire project are PCC modulus of rupture (MR) and the stress applied on the pavement under loading (σ). Further, to make the calculation simple, it is assumed that there is only bottom-up cracking and no top-down cracking. These simplifications are referred to as the *simple project assumption*.

It is assumed that both MR and σ are random variables that follow normal distributions (the exact type of distribution is irrelevant since it does not change the results). Together, MR and σ form the input random vector X discussed in the previous section.

According to the *Pavement ME* documentation, concrete fatigue life, N_f , is determined by the modulus of rupture, MR , and the applied tensile stress σ through the following equation:

$$\log_{10}(N_f) = C_1 \cdot \left(\frac{MR}{\sigma}\right)^{C_2} \quad (3.2)$$

where $C_1 = 2.0$ and $C_2 = 1.22$. The applied stress depends on various factors, such as traffic and structure. The fatigue damage DI_f , accumulated following Miner's Rule, is:

$$DI_f = \sum_{ijklmno} \frac{n_{ijklmno}}{N_{ijklmno}} \quad (3.3)$$

where the subscripts $ijklmno$ indicate the permutations of various factors affecting the applied stress, and $n_{ijklmno}$ is the number of traffic load applications corresponding to the stress level. Once the fatigue damage is known, the percent of slabs cracked, denoted as CRK , can be calculated using the following equation:

$$CRK = \frac{100}{1 + C_4(DI_f)^{C_5}} \quad (3.4)$$

C_4 and C_5 are the model coefficients that should be calibrated separately with each region's separate condition. The nationally calibrated values for these coefficients are $C_4 = 0.52$ and $C_5 = -2.17$. These values are used in this section to describe the effects of different variabilities on transverse cracking model predictions. Figure 3.1 illustrates the correlation between accumulated damage and the number of slabs cracked using Equation 3.4. This equation is called the *transfer function*. It converts mechanistic damage to pavement distress through an empirical correlation.

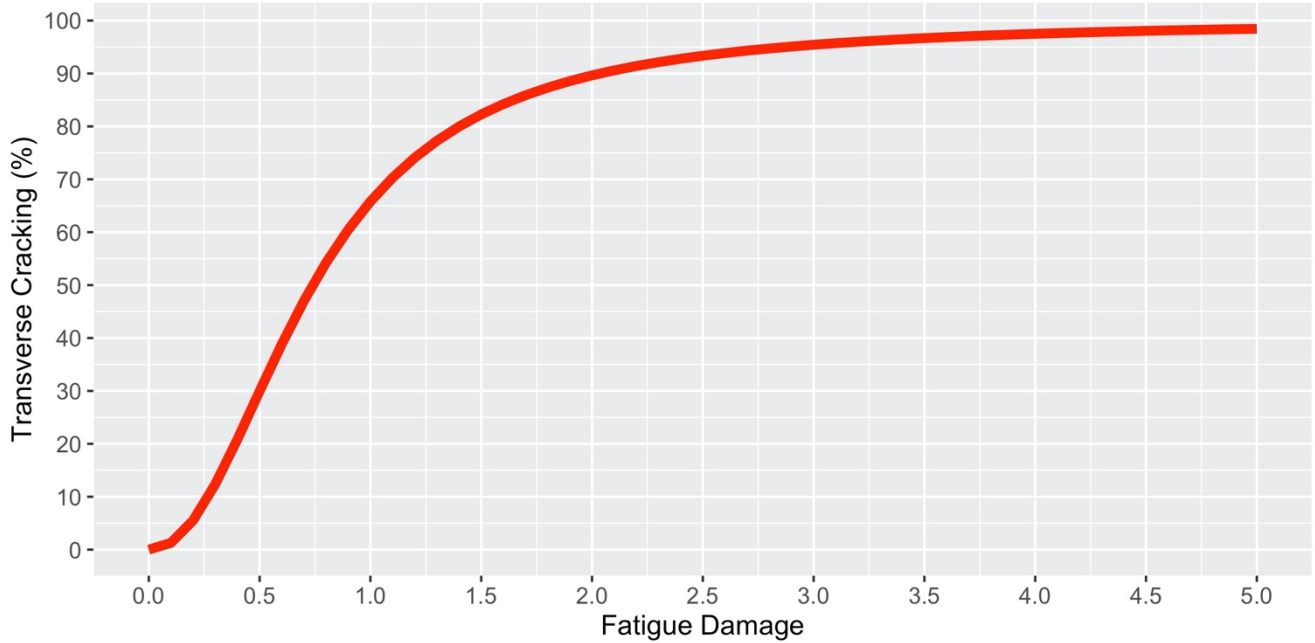


Figure 3.1: Pavement ME transverse cracking transfer function.

It is assumed that a project can be divided into contiguous segments in which the material properties (MR in this case) and loading (σ in this case) are uniform and constant along each individual segment. For simplicity, it is also assumed that the segments are equal in length. This scenario is referred to as the *uniform segmentation assumption*.

Within the uniform segmentation assumption, the values of MR and σ for any specific segment within a simple project are random samples of the corresponding distributions. The percent of slabs cracked in a particular segment can be calculated with Equation 3.2 to Equation 3.4. The percent of slabs cracked over the whole project is then the average of the values over all segments:

$$CRK_{project}(t) = \frac{1}{m} \sum_{i=1}^m CRK_i(t) = \frac{1}{m} \sum_{i=1}^m CRK(t; MR_i, \sigma_i) \quad (3.5)$$

where m is the number of equal-size segments within the simple project, MR_i and σ_i are the values of MR and σ , respectively, for segment i , and t is the time since the project opened to traffic. The value $CRK_{project}(t)$ represents the percent of slabs expected to have cracked at any given time t . In other words, Equation 3.5 calculates the probability that any slab will crack by time t . This suggests that $CRK_{project}(t)$ is the CDF of slab cracking life.

Similarly, the transfer function defined in Equation 3.4 represents the percent of slabs expected to have cracked for any given level of fatigue damage DI_f . Since DI_f is a monotonic function of time, the transfer function is also

a CDF of slab cracking life, albeit in the damage space. In other words, the link from damage to cracking is not deterministic. In fact, cracking can occur at any damage level, although more damage corresponds to a greater probability of cracking. This is why not all slabs within a segment crack at the same time even though their calculated damage is the same.

Following the simple project assumption and the uniform segmentation assumption, a project is made up of many uniform segments. Each segment is uniform in terms of the calculated fatigue damage, DI_f , if the same properties are assumed for all slabs in the segment. Therefore, each segment shows a different rate of cracking due to the variability in loading and material properties. These concepts and definitions will be used in the following sections of this chapter to show the effects of different variabilities on predicted transverse cracking and to explain how the different sources of variability can be accounted for in the calibration process. They will also be used in the development of the Caltrans JPCP design catalog and in the use of *Pavement ME* to design a pavement.

3.4.1 Monte Carlo Simulation Procedure

Following the simplified example introduced in the previous section of this chapter, a Monte Carlo simulation is used to illustrate the different types of variability involved in pavements. The steps below are followed for conducting a Monte Carlo simulation:

1. Determine the simulation duration in terms of maximum number of traffic loadings, N_{\max} .
2. Select a set of number of traffic applications and form an array $n = \{n_1, n_2, \dots, n_m\}$, where $n_i \in [0, N_{\max}]$. This array is referred to as the *traffic history array*. Each value in the array represents a point in time.
3. Determine the number of segments, n_{sg} , for the *simple project*.
4. Generate n_{sg} random samples for MR and σ independently and assign one set of values for each segment.
5. For each segment in the project:
 - a. Calculate the concrete fatigue life, N_f , using the MR and σ values corresponding to the current segment.
 - b. Calculate the damage history corresponding to the traffic history array, n , using Equation 3.3.
 - c. Convert the damage history into percent cracking history using Equation 3.4.
6. For every value in the traffic history array n , calculate the following statistics across all segments:
 - a. Average damage
 - b. Median damage
 - c. Average of percent slab cracked
 - d. Median of percent slab cracked

3.4.2 Within-Project Variability (WPV)

To illustrate the meaning of within-project variability (WPV), continuing with the simplified example presented above, a simple project is assumed with 1,000 segments of pavement. For the simplified pavement systems described in the previous sections, WPV comes from the random nature of both MR and σ . To illustrate WPV, it is assumed that MR in a project follows a normal distribution with a mean value of 5.5 MPa and a standard deviation of 0.5 MPa —i.e., $MR \sim N(5.5, 0.5)$ —where $N(\mu, \epsilon)$ indicates a random variable following the normal distribution with mean, μ , and standard deviation, ϵ . Similarly, it is assumed that the stress applied in a project follows a normal distribution with a mean value of 2.0 MPa and a standard deviation of 0.3 MPa —i.e., $\sigma \sim N(2.0, 0.3)$.

Figure 3.2 shows the histories of accumulated damages for the 1,000 segments as well as the overall average. As expected, different small segments show different rates for damage accumulation depending on the ratio between MR and σ . Damage accumulates rapidly in some segments and slowly in others. Due to the simple project assumption of the same randomly sampled stress being repeated in a given segment, damage always accumulates at a constant rate for a given segment, which results in straight lines for damage time histories.

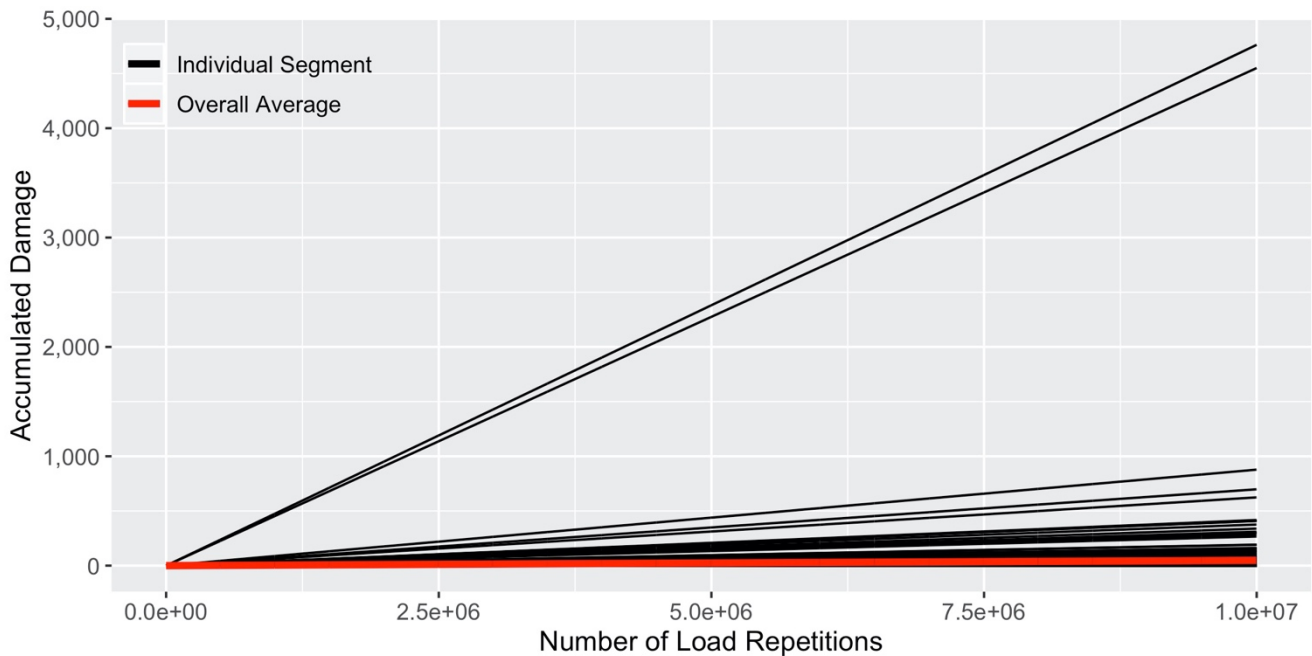


Figure 3.2: Accumulated damages versus number of load repetitions for 1,000 pavement segments

Figure 3.3 shows the percent transverse cracking histories for different segments within the simple project. Some segments reach 100% cracking very quickly while other segments last much longer. The large difference between

different segments of the project illustrates the WPV. As discussed earlier, the percent cracking history for each individual segment is the CDF of cracking life for that particular segment.

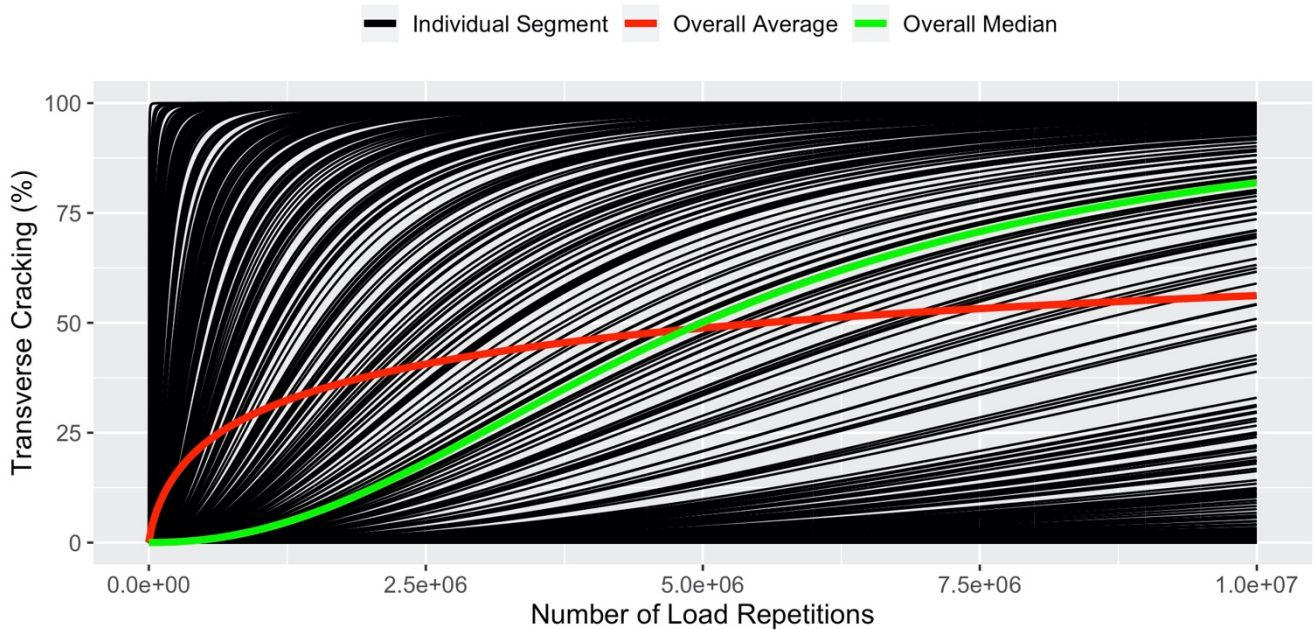


Figure 3.3: Transverse cracking (percent of slabs transverse cracked) versus number of load repetitions for 1,000 pavement segments.

In Figure 3.3, the history of overall average percent cracking is shown as a red curve. The overall average represents the aggregation over the 1,000 segments in the project as if pavement cracking data were collected from a series of pavement condition surveys. The overall average percent cracking history is the CDF of cracking life for any randomly selected segment within the project.

Figure 3.3 indicates that the shape of the percent cracking history for individual segments is very different from the one for the overall project (i.e., the overall average). This is expected because the shape of the overall average depends on the amount of WPV while the shape for any individual segment depends only on the specific value of X assigned to the segment. This is a very important observation because it means that trends observed from individual uniform segments are not applicable to the relatively long and non-uniform project.

In Figure 3.3, the overall median cracking curve for all the pavement segments is shown as a green curve. The overall median cracking curve is determined by finding the median of percent cracking among all segments at any given time. Unlike the overall average, the overall median has the same shape as the individual segments. This is because the histories for individual segments have the same shape and do not cross each other. This observation

is universally applicable because of some intrinsic properties of pavement systems. Namely, pavement performance is a monotonic function of different inputs. This property is referred to as the *monotonic property*.

In the case of the simple project under discussion here, the monotonic property refers to the fact that surface cracking is a monotonic function of both MR and σ . Specifically, surface cracking is a strictly decreasing function of MR and a strictly increasing function of σ . As a result, the cracking history that results from input of the median of MR and σ leads to the median of percent slabs cracking at any given time t (or, interchangeably, any number of traffic cycles applied n):

$$\overline{CRK}(t) = CRK(t; \overline{MR}, \overline{\sigma}) = \frac{100}{1 + C_4 \cdot [DI_f(t; \overline{MR}, \overline{\sigma})]^{C_5}} \quad (3.6)$$

where $\overline{(\cdot)}$ indicates taking the median value of a quantity. According to Equation 3.6, the overall median percent cracking history is determined by the median values of MR and σ , and therefore is essentially the CDF of cracking life for a segment with median input X and should have the same shape as the percent cracking history for each individual segment.

Equation 3.6 also suggests that the relation between overall median percent cracking, $\overline{CRK}(t)$, and overall median damage, $\overline{DI_f}(t)$, (which is equal to $DI_f(t; \overline{MR}, \overline{\sigma})$ due to the monotonic property) follows the transfer function.

Figure 3.3 shows that overall average and overall median are typically different when a project is non-uniform. However, overall average will converge to the overall median as the variabilities in MR and σ both decrease to zero. Figure 3.3 also shows an important finding: the overall average and overall median reach 50% at exactly the same time. This is not a coincidence. To explain this further, first denote the point of intersection as P_{50} . Given that the overall average cracking history represents the CDF of cracking life, the X -coordinate of this point represents the median cracking life, which depends only on the median values of MR and σ due to the monotonic property. In other words, although changing the variability of MR and σ will change their shape, all overall average curves will have to go through point P_{50} as long as the mean values for MR and σ are the same.

3.4.3 Between-Contractor Variability (BCV)

Between-contractor variability (BCV) can be illustrated through an example where the mean values of MR and σ are fixed at 5.5 MPa and 2.0 MPa, respectively, indicating the same material strength and same slab thickness, while their standard deviations are set to different values, indicating different contractor variability for material strength and slab thickness. Figure 3.4 shows the BCV caused by changing the standard deviation of MR from 0

to 0.4 MPa while keeping σ fixed at 2.0 MPa. Figure 3.5 shows the BCV caused by changing the standard deviation of σ from 0 to 0.01 MPa while keeping MR fixed at 5.5 MPa. Figure 3.6 shows the BCV caused by changing standard deviations for both MR and σ . In Figure 3.4 to Figure 3.6, the Y-axis shows the overall average of percent slabs with transverse cracking among all segments within a project.

Figure 3.4 to Figure 3.6 confirm that the time (or, interchangeably, the number of traffic cycles applied, n , in this case) needed for 50% of a pavement to reach cracking failure remains the same no matter what the standard deviations are for MR and σ .

As shown in Figure 3.4 to Figure 3.6, a higher standard deviation causes the curves to rise faster initially, but these curves flatten more after 50% cracking, which means that there are more slabs that have either very short or very long cracking lives. In other words, higher standard deviations of MR and σ cause slab cracking life to spread out more, which is expected. The range of this spread reflects the amount of BCV.

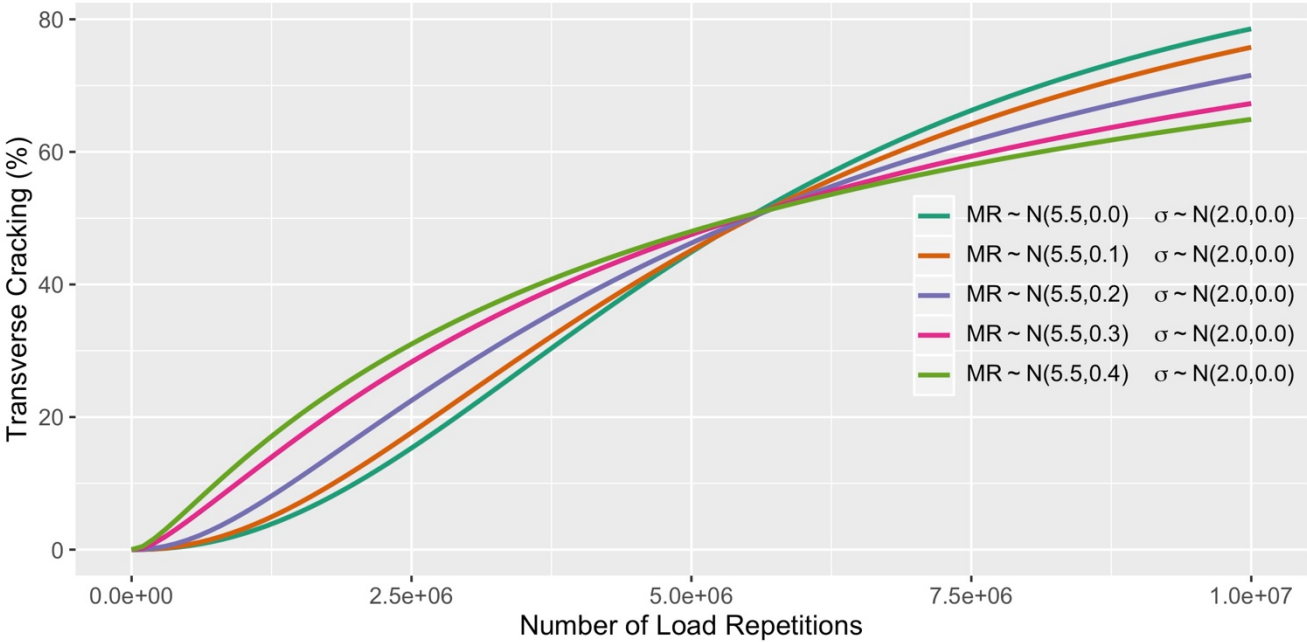


Figure 3.4: Transverse cracking histories for projects with different standard deviation in modulus of rupture.

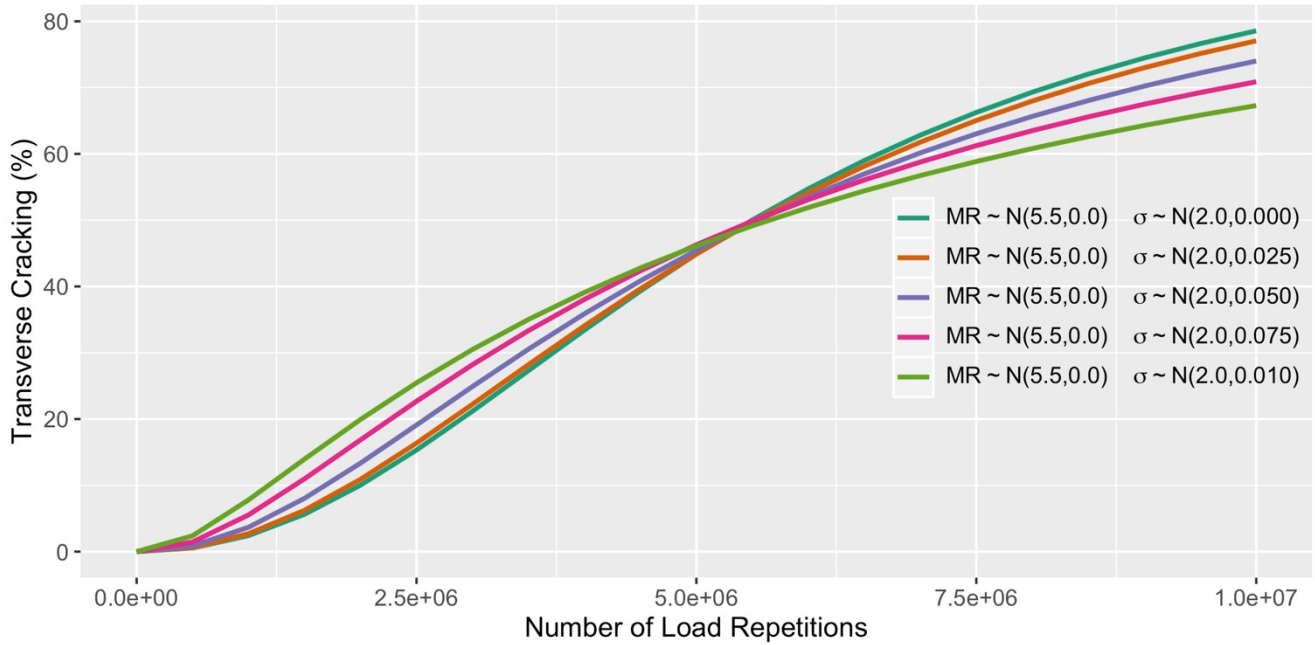


Figure 3.5: Transverse cracking histories for projects with different standard deviation in applied stress.

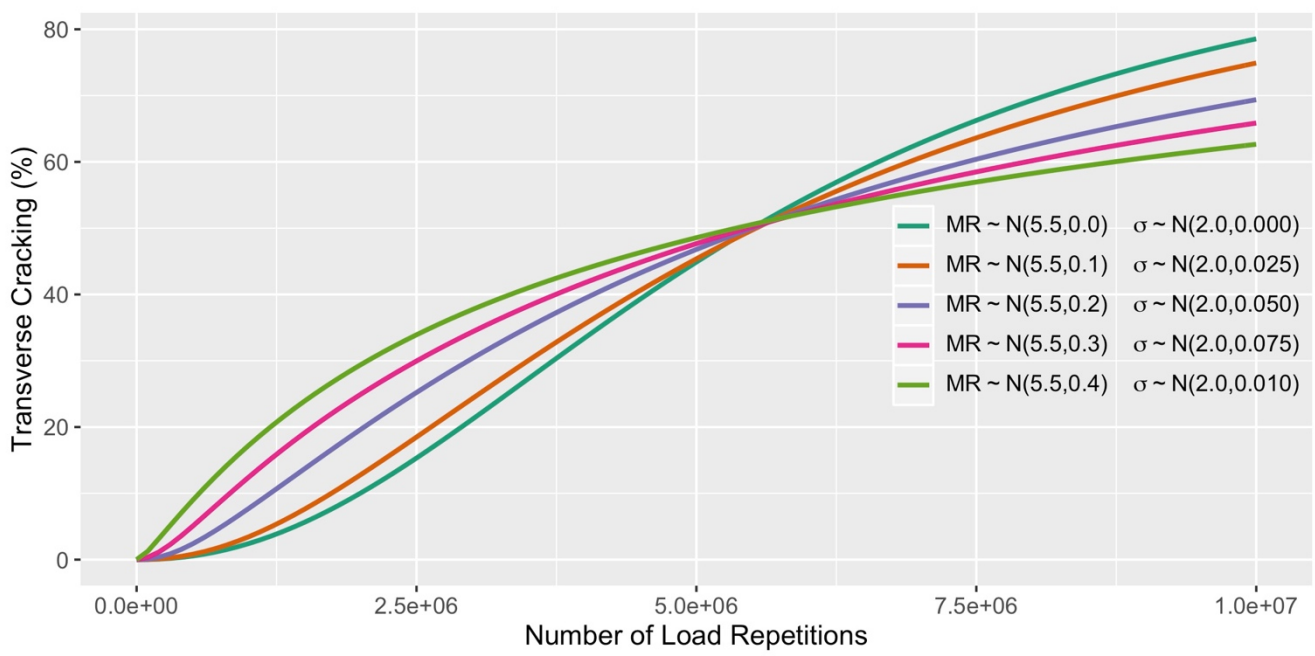


Figure 3.6: Transverse cracking histories for projects with different standard deviations in modulus of rupture and applied stress.

3.4.4 Between-Project Variability (BPV)

To illustrate between-project variability (BPV), Monte Carlo simulations were conducted by varying the mean values for MR or σ while keeping their standard deviations at zero. Results are shown in Figure 3.7. In this figure, the Y -axis shows the overall average of percent slab cracking. Despite the lack of variability in MR and σ , all segments within a project perform the same, and, as a result, the overall median and overall average are the same.

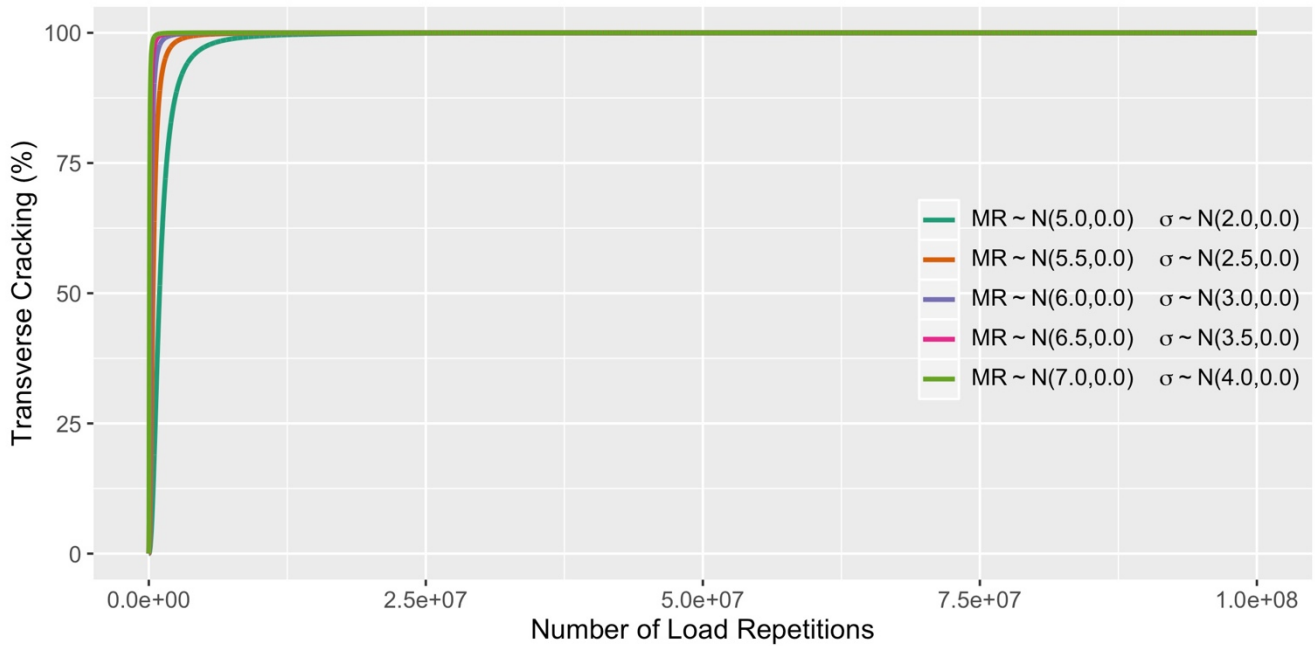


Figure 3.7: Transverse cracking histories for projects with different mean values and zero standard deviation in modulus of rupture and applied stress.

Figure 3.7 shows the percent cracking histories for projects with different mean values for both MR and σ . Figure 3.8 shows the same graph but with the X -axis in log scale to make the plot more readable. As expected, cracks develop faster as the ratio $\frac{\sigma}{MR}$ increases.

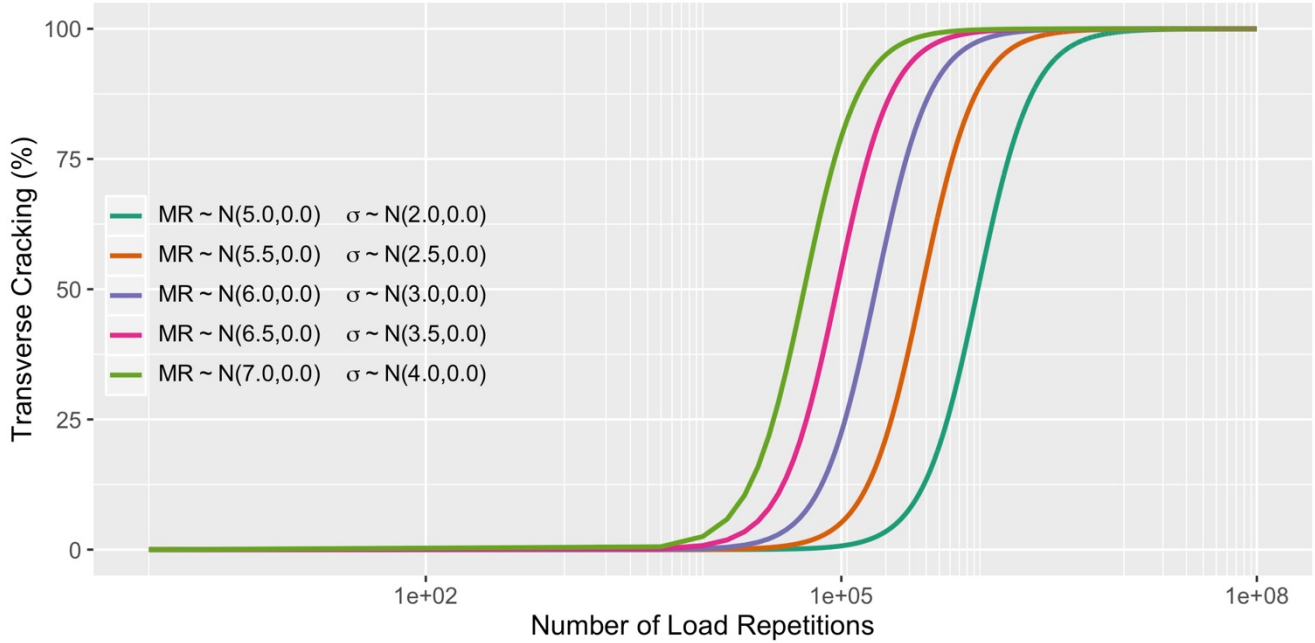


Figure 3.8: Transverse cracking histories for projects with different mean values in modulus of rupture and applied stress in a semi-log plot.

Figure 3.8 shows that the shapes of percent cracking histories are the same with the X -axis in log scale, and the differences between them can be removed by applying a project-dependent scale factor on the time axis. This observation is not a coincidence, and it is due to another fundamental property of pavement performance. Specifically, damage in a given pavement project follows the same pattern of damage versus time, regardless of the actual value of various factors affecting performance, but with the patterns shifted in time (the X -axis in Figure 3.8 when the mean values change). This is because the damage pattern is determined by traffic pattern (for traffic-induced damage), which is fixed for a given pavement project. Mathematically, this means:

$$DI_f(t; X_1) = DI_f(t; X_2) \cdot f(X_2, X_1) \quad (3.7)$$

where $DI_f(t; X)$ is the fatigue damage at time t for a given input X , and $f(X_2, X_1)$ is a function that depends only on inputs X_1 and X_2 . The proof for this equation is shown in the following.

According to Equation 3.3:

$$DI_f(t; X_1) = \sum_{ijklmno} \frac{n_{ijklmno}(t)}{N_{ijklmno}(X_1)} \quad (3.8)$$

This can be recast as:

$$DI_f(t; X_1) = N(X_1)^T n(t) \quad (3.9)$$

where N is a vector with $N_{ijklmno}$ as the elements and n is a vector with $n_{ijklmno}$ as the elements. Note that n represents the division of traffic into different traffic loading cases (such as combination of axle type, axle load, and tire pressure) and in general:

$$n(t) = n(t) \cdot \hat{n} \quad (3.10)$$

where \hat{n} is a unit vector representing the traffic load spectrum while $n(t)$ is the accumulated traffic volume at time t . With this, the following holds:

$$\frac{DI_f(X_1;t)}{DI_f(X_2;t)} = \frac{N(X_1)^T n(t)}{N(X_2)^T n(t)} = \frac{N(X_1)^T \hat{n}}{N(X_2)^T \hat{n}} \quad (3.11)$$

which means that Equation 3.7 holds. This feature of the transverse cracking model is referred to as the *scalability property*. It should be noted that no WPV has been included in the proving of the scalability property. Another way to think about this is to assume that Equation 3.7 to Equation 3.11 are being applied to a segment that has uniform inputs X .

The scalability property means that pavements will have the same shape of damage versus time (same damage rate with time) no matter how good or how bad their materials are, as long as their traffic histories (volumes and spectra) are the same. Although it requires the use of Miner's Rule to prove, the scalability property makes sense for pavement performance in general. For the projects used to illustrate BPV in this section, the scalability property is illustrated in Figure 3.9, which shows the accumulated damage histories for projects with different mean values for both MR and σ . As shown in the figure, the histories of accumulated damage are all straight lines in a log-log plot, indicating that their difference can be removed by applying a project-dependent scale factor on the Y-coordinate (i.e., accumulated damage).

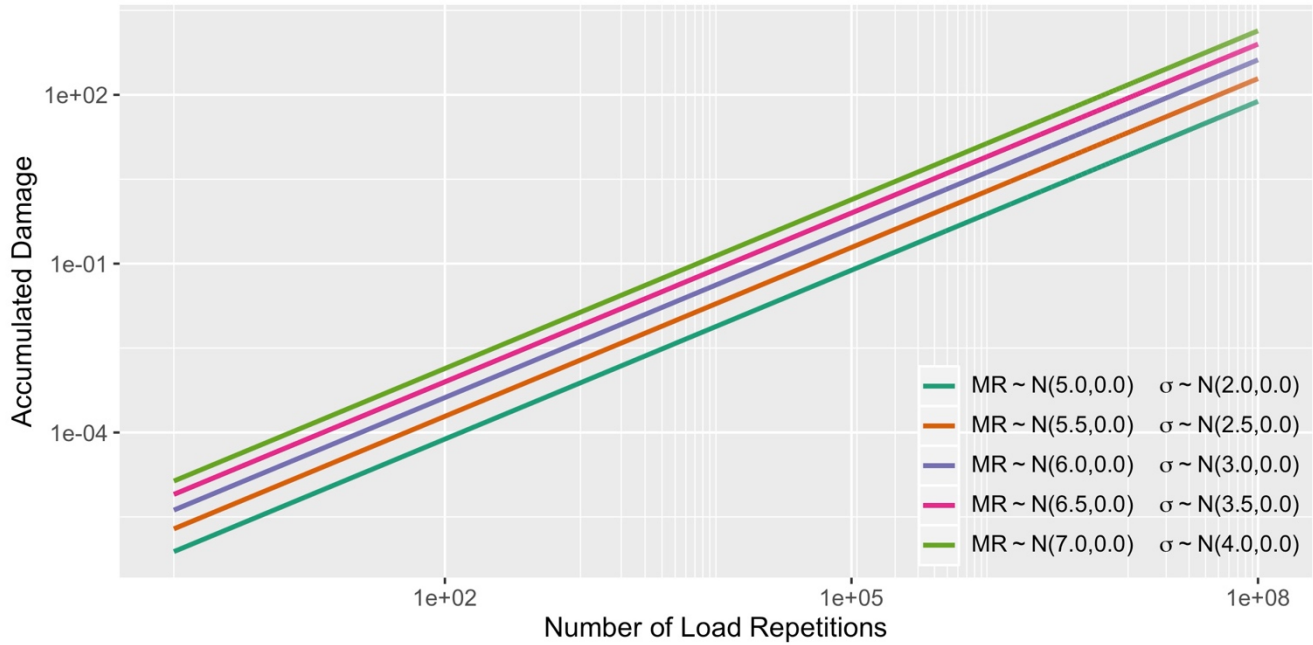


Figure 3.9: Accumulated damage histories for projects with different mean values in modulus of rupture and applied stress in a log-log plot.

The illustrations of WPV, BCV, and BPV in the above sections show how each source of variability affects pavement performance. To summarize:

- The amount of WPV affects the shape of the observed cracking history (i.e., overall average), but it does not affect the overall median cracking history.
- The amount of WPV determines the amount of deviation between overall average (mean) and overall median cracking. As WPV decreases to zero, the overall average converges to the overall median.
- The amount of BCV affects the range of variation of the overall average.
- BPV affects only the rate of damage accumulation versus time but not the shape of damage versus time.

All the findings in this section will be used in the next section to separate the three different variabilities.

3.5 Step-by-Step Procedure for Pavement ME Transverse Cracking Calibration Using Pavement Database

As discussed earlier, the new *Pavement ME* calibration procedure considers two properties of pavement systems:

- *Monotonic property*: pavement performance is monotonically related to various relevant factors. For example, pavement lasts longer if one increases MR of the concrete while keeping everything else equal.
- *Scalability property*: damage in a given pavement project shares the same relationship of damage versus time (or traffic loading) regardless of the actual value of various factors affecting performance. This is because the damage versus traffic relationship is determined by the traffic loading as expressed by the

axle load spectrum for traffic-induced damage, which is fixed for a given pavement project. In other words, any change in the traffic load spectrum will cause a change in the damage pattern. An increase or decrease in the amount of traffic will result in a shift in the relationship along the time axis. The same is true for environment-induced damage in terms of the temperature and shrinkage spectrum for concrete pavement.

The monotonic property implies that median inputs correspond to median performance. This allows for linking of at least one set of inputs—vector X —with its corresponding performance for the roadway network under calibration. Therefore, instead of sampling and testing each individual calibration segment, one needs only to determine the median input, vector X , for a given roadway network under calibration to produce the median performance, or the median input vector for a subset of the roadway network to produce the median performance for the subset, such as a subset with same median slab thickness, base type, shoulder type, and joint length.

The scalability property implies that one can use the median input—vector X —to determine the damage pattern over time. The true damage can be obtained by further applying a scale factor. The value of the scale factor reflects how different the actual input vector is from the median input vector. The distribution of the scale factor indicates the BPV of the road network.

Among all the variables included in input vector X , some are typically known to designers at the time of design while others are not. The known variables in this approach are referred to as *design inputs*, while the others are *non-design inputs*. Typical design inputs for rigid pavements include the following:

- Traffic (volume and spectrum)
- Climate
- PCC slab thickness
- PCC joint spacing
- Doweled/undoweled
- Base type (AB, HMA, LCB, CTB, etc.)
- Shoulder type (FLX, NA, RIG, WRF, etc.)

Typical non-design inputs include:

- Modulus of rupture (MR)
- Modulus of elasticity (E)
- Coefficient of thermal expansion (CTE) and other thermal properties

- Shrinkage properties
- Albedo

The division of design and non-design inputs may change from one road agency to another. For example, one agency might specify the maximum value for CTE and change it from a non-design input to a design input.

A design program needs to provide the performance estimation for a given set of design inputs while accounting for the uncertainties in the non-design inputs. If the known inputs for calibration do not match the given design inputs, the calibration models for transverse cracking can be adjusted by adding or removing BCV and BPV for non-overlapping inputs. For example, modulus of rupture (MR) is typically assumed to be a design input, yet in reality it is a non-design input because its actual value for any given project is typically unknown prior to construction of the project. The BPV of MR should be determined as part of the calibration to explain part of the variability in observed performance.

In *Pavement ME*, pavement distress prediction is a two-step process. In the first step, pavement damage is determined based on pavement response and damage accumulated over time. In the second step, the damage is converted into the corresponding pavement distress through an empirical correlation that is referred to as a *transfer function*. The first step is mechanistic, and the second step is empirical. The mechanistic step reflects the known factors about various pavement behaviors, while the empirical step reflects the unknown or unaccounted-for factors. It is assumed that the mechanistic step is more or less correct, and only the empirical step needs to be calibrated. The calibration procedure should determine how each uncertainty in various components of the pavement affects the empirical step. This is only partially true for the national calibration because its authors had no direct measurements of damage and were required to manually separate the calibration of the mechanistic component and the transfer function.

For the transverse cracking model, the corresponding pavement damage is denoted as DI_f . The objective of the calibration is to determine coefficients for the transfer function defined by Equation 3.4, namely C_4 and C_5 . The variabilities involved in pavement performance—namely, BPV, WPV, and BCV—should be accounted in the calibration process.

As stated in Section 3.4.4, BPV is caused by differences in average input variables—such as PCC modulus of rupture, PCC compressive strength, and PCC coefficient of thermal expansion—between different projects. BPV shifts the transverse cracking horizontally as shown in Figure 3.7 and Figure 3.8. In Equation 3.4, C_4 is responsible for BPV and shifts the transverse cracking in the horizontal direction. Figure 3.10 shows the effect of different C_4

values on the transfer function while keeping C_5 constant. As the C_4 value increases, the model shifts to the right and predicts less transverse cracking (note the damage corresponding to 50% cracking for different curves) for a given amount of accumulated damage. Therefore, the effect of BPV should be reflected in the C_4 coefficient.

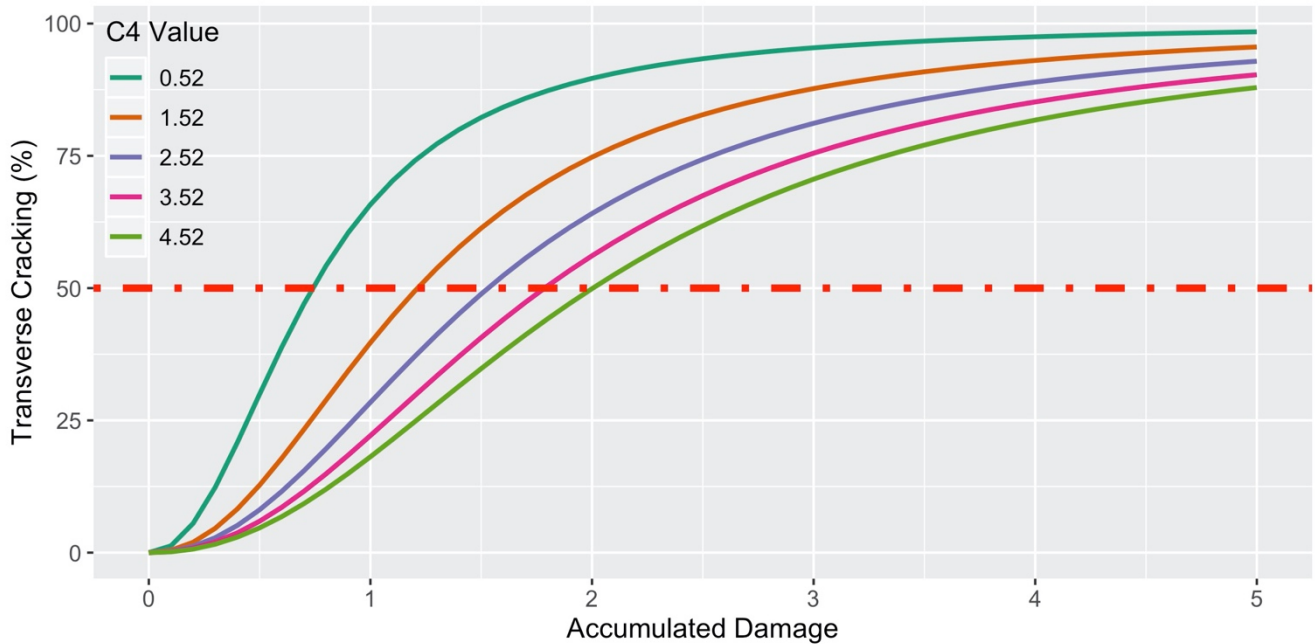


Figure 3.10: Effects of C_4 coefficient on *Pavement ME* transfer function.

Figure 3.11 is a schematic representation of transverse cracking for 50 different projects. Each black line represents the cracking performance of a single project. These projects show different cracking performances due to the differences in their nominal input variable values (those such as PCC compressive strength and PCC coefficient of thermal expansion that are unknown to the designer). Figure 3.11 illustrates that these projects show a wide range of cracking performance that is caused by BPV. The green line represents performance for 50% reliability, and the red line represents performance for 95% reliability.

Theoretically, calibrating the *Pavement ME* transverse cracking model to each of the black lines results in a distribution of C_4 values. Choosing 50 and 95 percentiles, C_4 values from that distribution correspond to the green and red lines, respectively. However, this is not a feasible action in this study since important non-design variables are not available for each project. In Sections 3.5.8 and 3.5.9, a detailed procedure showing how to account for BPV using the statistical random-effects performance model developed in Section 2.4 and how to obtain the C_4 values for 50% and 95% reliabilities will be explained.

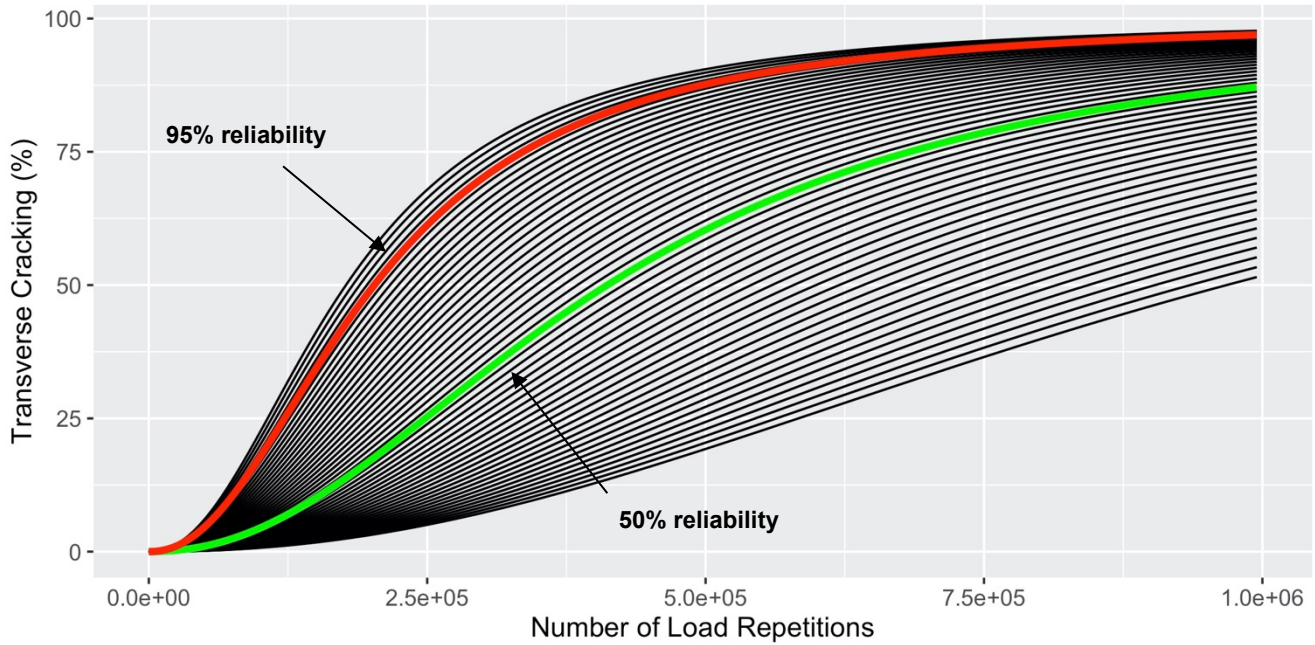


Figure 3.11: Schematic representation of BPV.

WPV and BPV are caused by variations in the standard deviation of average input variables such as PCC modulus of rupture, PCC compressive strength, and PCC coefficient of thermal expansion within each project. WPV and BCV affect the shape of transverse cracking curves as shown in Figure 3.4 to Figure 3.6. In Equation 3.4, C_5 is responsible for WPV and BCV and changes the shape of the transverse cracking curve. Figure 3.12 shows the effect of different C_5 values on the transfer function while keeping C_4 constant. As the C_5 value becomes more negative, the model predicts higher rates of cracking at the beginning, but the curve becomes flatter as more damage occurs. Figure 3.12 shows how C_5 values spread the curve and hence reflect the effects of WPV and BCV. In order to account for these variabilities in determining the C_5 value, a Monte Carlo simulation was performed on a set of important non-design variables that will be explained in detail in Section 3.5.7.

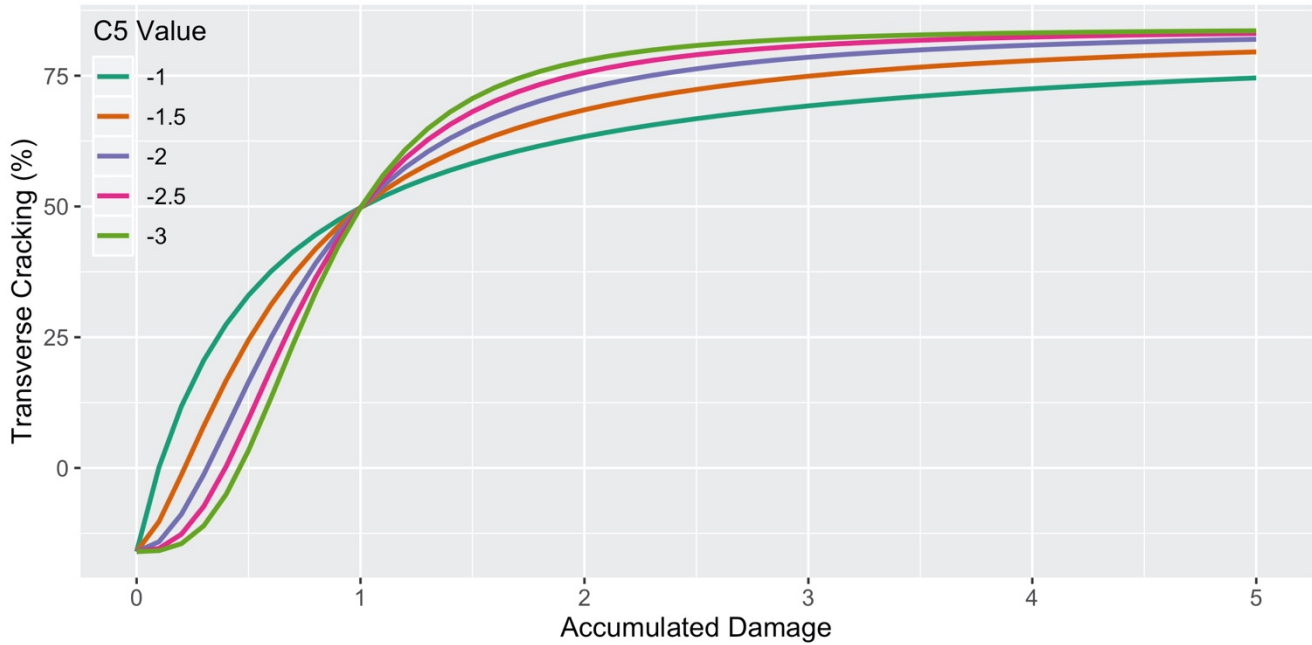


Figure 3.12: Effects of C_5 coefficient on *Pavement ME* transfer function.

The following sections of this chapter explain step-by-step the procedure for calibrating the transverse cracking model in *Pavement ME* using the PavEM database.

3.5.1 Step 1: Identify Roadway Segment

In Step 1, the criteria for identifying roadway segments for calibration outlined in *Guide for the Local Calibration of the Mechanistic-Empirical Pavement Design Guide* (hereafter referred to as the “local calibration guide”) should be followed (15). In general, there should be a reasonable amount of observed distress both in terms of number of observations and the extent of distress. In the local calibration guide, Step 4 discusses how roadway projects are selected while Step 7 discusses how to use the data from roadway segments to access local bias. There is no requirement on the length of roadway segments.

3.5.2 Step 2: Prepare PMS Data

In Step 2, anomalies and obvious measurement errors are removed from the condition survey data. Since the condition surveys collect first- and third-stage cracking, these measurements are converted to transverse cracking (the cracking type that *Pavement ME* predicts) using the model proposed in Chapter 2 of this report.

3.5.3 Step 3: Develop Statistical Performance Model

In addressing Step 3, performance data for an individual pavement project may be scattered. Since performance data are panel data and collected from different projects, a mixed-effects model that can capture the BPV is developed. The equation for the statistical performance model and a detailed discussion on its coefficients can be found in Chapter 2 of this report.

3.5.4 Step 4: Estimate Median Values for Non-Design Variables

As stated in Section 3.4, for variables unknown to the designer— variables also referred to as *non-design variables* in this report—the median value should be used for each of the inputs in order to predict median performance. The resulting set of inputs are referred to as the *golden reference inputs*. *Pavement ME Sensitivity Analysis (5)* discusses these variables and their effect on transverse cracking model predictions. The following is a list of unknown variables and their summary statistics. These distributions were obtained from previous tests carried out by the UCPRC as part of different projects funded by Caltrans.

- PCC compressive strength:
 - Mean: 4,539 *psi*
 - Median: 4,458 *psi*
 - Standard deviation of within-project standard deviation (BCV): 400 *psi*
- PCC coefficient of thermal expansion:
 - Mean: $4.91 \times 10^{-6} \text{ } ^\circ\text{F}^{-1}$
 - Median: $4.8 \times 10^{-6} \text{ } ^\circ\text{F}^{-1}$
 - Standard deviation of within-project standard deviation: $0.275 \times 10^{-6} \text{ } ^\circ\text{F}^{-1}$
- PCC density
 - Mean: 147 *pcf*
 - Median: 147 *pcf*
 - Standard deviation of within-project standard deviation: 1.64 *pcf*

Among the three variables shown above, PCC density does not have a significant effect on transverse cracking. Therefore, its effects on WPV and BCV will not be considered in Section 3.5.7.

3.5.5 Step 5: Run Pavement ME for Each Cell of Data

As stated in Section 2.4, a cell of data is a set of performance data that could be collected from different projects but that have the same values for all design variables. These variables are PCC slab thickness, PCC slab length,

base type, shoulder type, weigh-in-motion (WIM) spectra, average annual daily truck traffic (AADTT) lane, and climate. Figure 3.13 shows an example of performance data for a cell of data from the Pavem database.

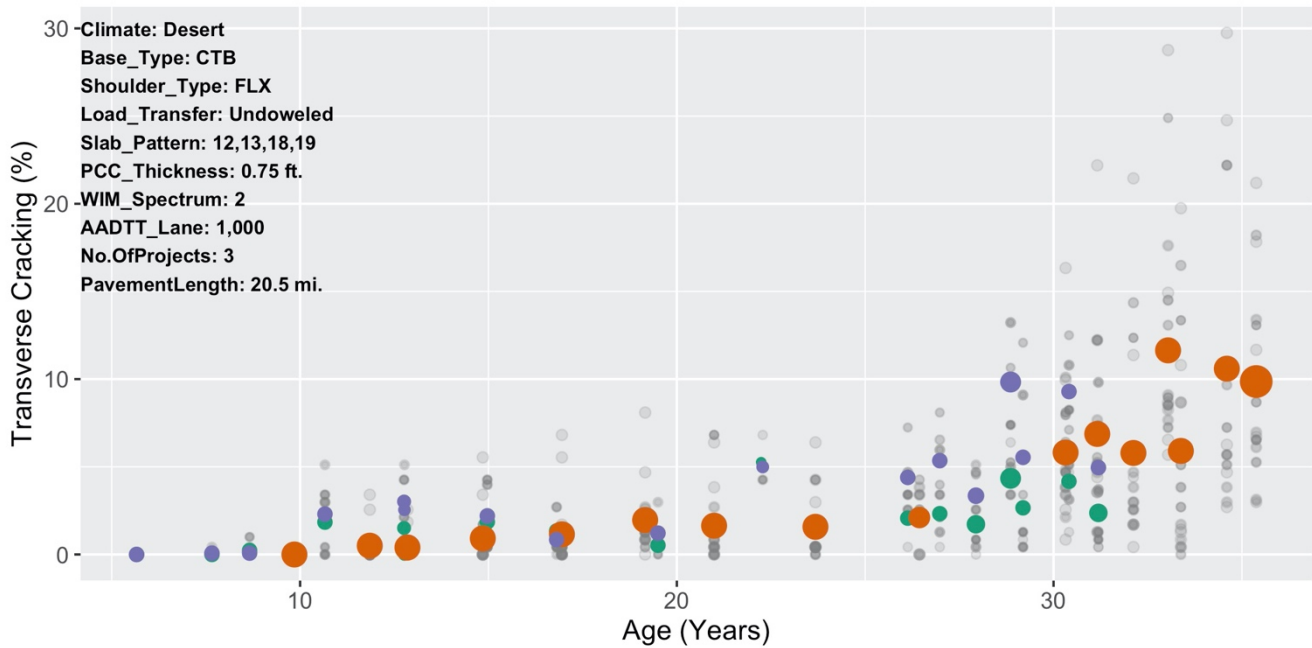


Figure 3.13: A cell of data of cracking performance used for *Pavement ME* calibration in Pavem database.

Figure 3.13 shows the amount of transverse cracking observed from three different projects that are in a cell of data. The *X*-axis represents the age of the pavement, and *Y*-axis represents the percent of transverse cracking. Each project is represented with a different color. The size of each data point indicates the amount of data (pavement lane-miles) available for that specific observation; the bigger the data point the more lane-miles of pavement data it represents. On the top-left corner, the variables corresponding to the cell of data are presented. The total length of pavement included in this graph is 20.5 lane-miles. The shaded gray points are the raw data from the Pavem database; after they were aggregated, these data became the colored data points that were used for the calibration. Figure 3.13 shows a clear increasing trend in the amount of transverse cracking for each project, which was expected.

Not all the cells in the Pavem database have multiple projects with this much data. For example, Figure 3.14 shows a cell of data with one project and 0.7 lane-miles of pavement.

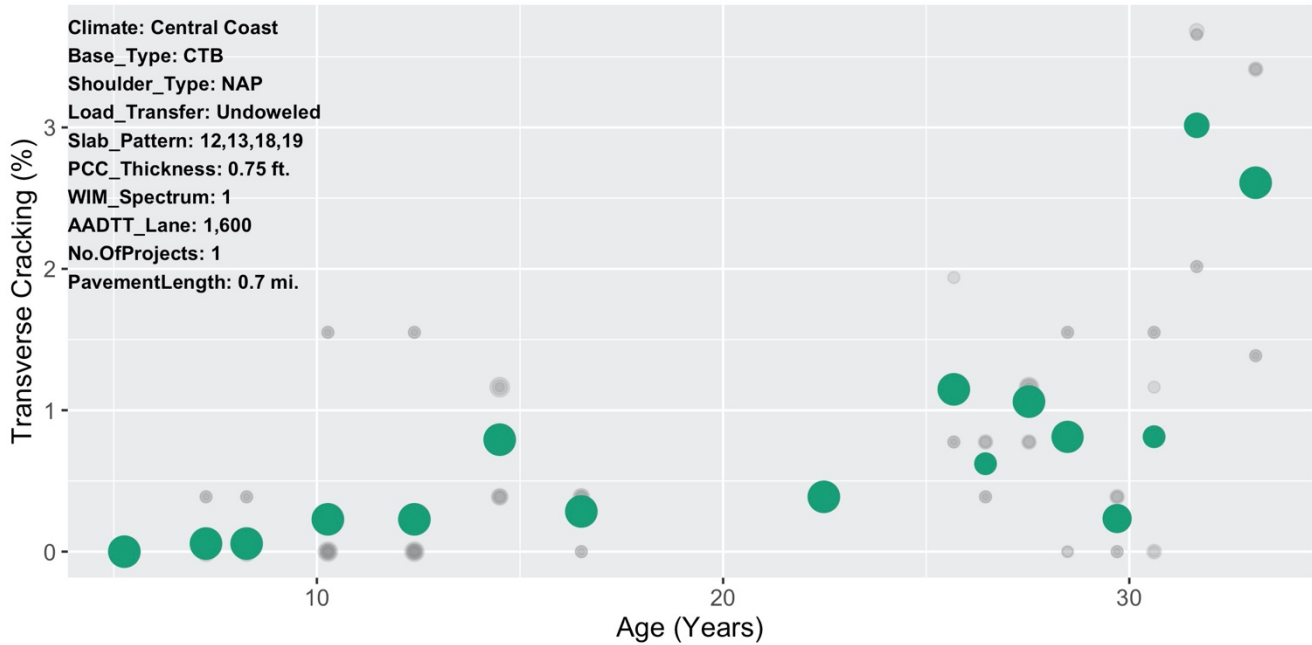


Figure 3.14: An example of a cell of data with limited observations.

There are 1,646 cells of data, corresponding to different combinations of design, climate, and traffic variables, available in the *PaveM* database. The factor levels of all variables that constitute the 1,646 cells of data are as follows:

- PCC thickness: 0.60 ft. to 1.2 ft. with 0.05 ft. increment
- Slab pattern: 12,13,14,15 ft. and 12,13,18,19 ft.
- Base type: aggregate base (AB), asphalt-treated permeable base (ATPB), hot mix asphalt (HMA), cement-treated base (CTB), and lean concrete base (LCB)
- Shoulder type: no shoulder (NAP), untied flexible (FLX), tied concrete (RIG), and widened concrete (WRF)
- Load transfer: doweled and undoweled
- WIM spectra: WIM_1, WIM_2, WIM_3, WIM_4, and WIM_5
- AADTT per lane: 100 to 13,200 in increments of 100
- Climate region: Central Coast, Desert, High Desert, High Mountain, Inland Valley, Low Mountain, South Coast, South Mountain

Pavement ME should be run for each of these cells. However, since the slab pattern is a categorical variable in the database with two levels—12,13,14,15 ft. and 12,13,18,19 ft.—a decision was made to run *Pavement ME* four times (once for each of the slab lengths within the slab pattern category) and use the average of the results for

calibration. For example, for a 12,13,14,15 ft. slab pattern, *Pavement ME* is run separately for 12 ft., 13 ft., 14 ft., and 15 ft. slab lengths, and the average predicted results of these runs are used for calibration. As a result, 6,584 ($1,646 \times 4$) *Pavement ME* runs are executed.

After running *Pavement ME* for each cell, the output files that contain the data pertaining to the amount of bottom-up and top-down damage versus age are stored separately, for use in the calibration.

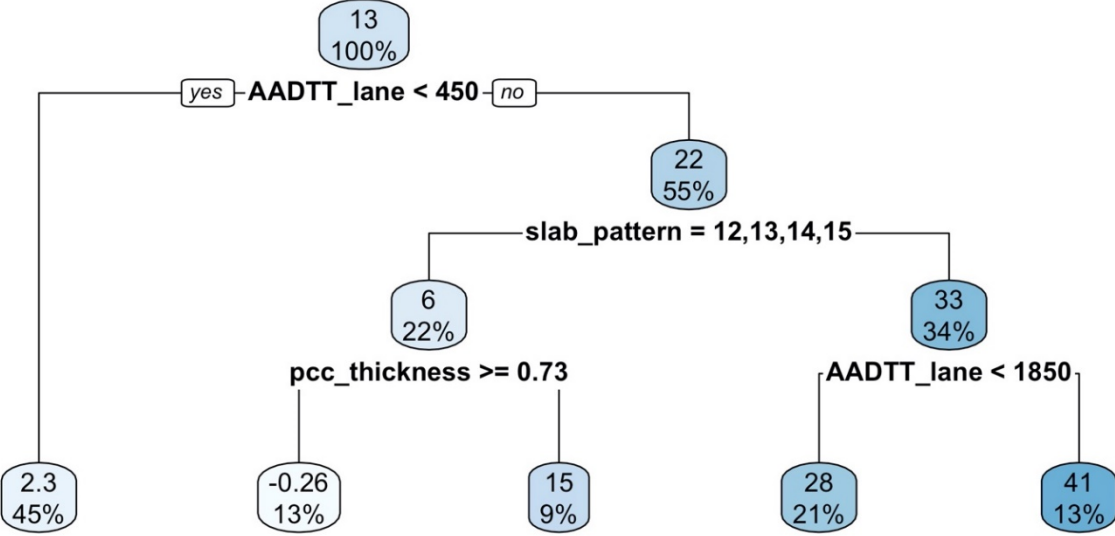
3.5.6 Step 6: Analyze Nationally Calibrated Model Error

Looking at the predictions of the *Pavement ME* transverse cracking model using the nationally calibrated coefficients $C_4 = 0.52$ and $C_5 = -2.17$, it was found that there is a significant difference between the amount of error for short (12,13,14,15 ft.) compared with (long 12,13,18,19 ft.) slab patterns. Figure 3.15 is a decision tree model fit on the errors made by the nationally calibrated *Pavement ME* transverse cracking model versus the Pavem performance data. In each blue box, the upper number is the bias (average error) of the national model compared to the California performance data in terms of the difference in percent slabs cracked between the model prediction and the performance data; the lower number is the portion of the total calibration data for that variable factor level.

The top blue box shows that, considering 100% of the data, the nationally calibrated model has a 13% overall bias. This indicates that on average the national model overpredicts the amount of transverse cracking in California projects by 13%. One of the goals of this calibration project is to reduce this number to as close to zero as possible. Going one level down, the branch on the right is divided by slab pattern, which indicates that the model prediction error is considerably different between two types of slab patterns. It shows that the national model on average makes a 6% error (overprediction) on shorter slabs, whereas it makes 33% error (overprediction) on longer slabs. This significant difference between model predictions for different slab patterns suggested that two sets of calibration coefficients were needed to handle the model errors properly. As shown in the following steps, the calibration was done for the two slab patterns separately and, as a result, there are two sets of calibrated C_4 s and C_5 s.

Figure 3.16 shows a decision tree model based on the errors made by the nationally calibrated *Pavement ME* transverse cracking model versus the Pavem performance data only for short slab pattern JPCPs. It shows that the nationally calibrated *Pavement ME* model overpredicts the amount of transverse cracking for the short slab pattern by 3.3%. Going down the tree, it shows that the model performs worse for PCC slabs thicker than 0.68 ft. compared to thinner ones.

Figure 3.17 and Figure 3.18 show examples of *Pavement ME* transverse cracking model predictions compared to actual data and their corresponding errors. The dashed line represents the nationally calibrated *Pavement ME* transverse cracking model prediction. Figure 3.17 shows that the model significantly overpredicts the amount of transverse cracking occurring in longer slabs, while in Figure 3.18 there is less overprediction for shorter slabs.



Note: in each blue box the upper number is the bias (average error) of the national model compared to the California performance data in terms of the difference in percent slabs cracked between the model prediction and the performance data; the lower number is the portion of the total calibration data for that variable factor level.

Figure 3.15: Decision tree fitted on the nationally calibrated *Pavement ME* transverse cracking model prediction error for all data.

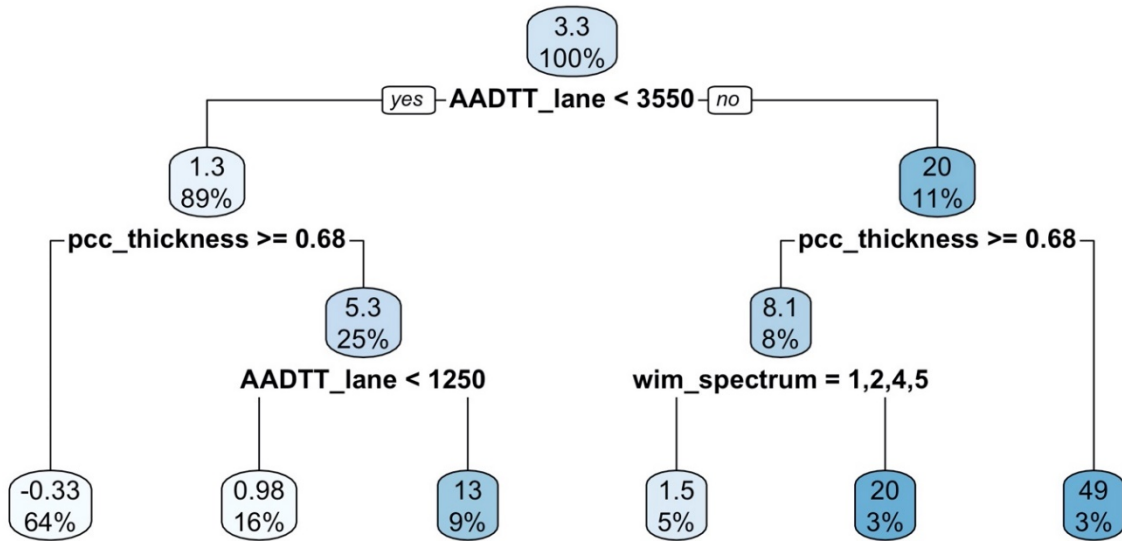


Figure 3.16: Decision tree fitted on the nationally calibrated *Pavement ME* transverse cracking model prediction error for only short slab pattern 12,13,14,15 ft.

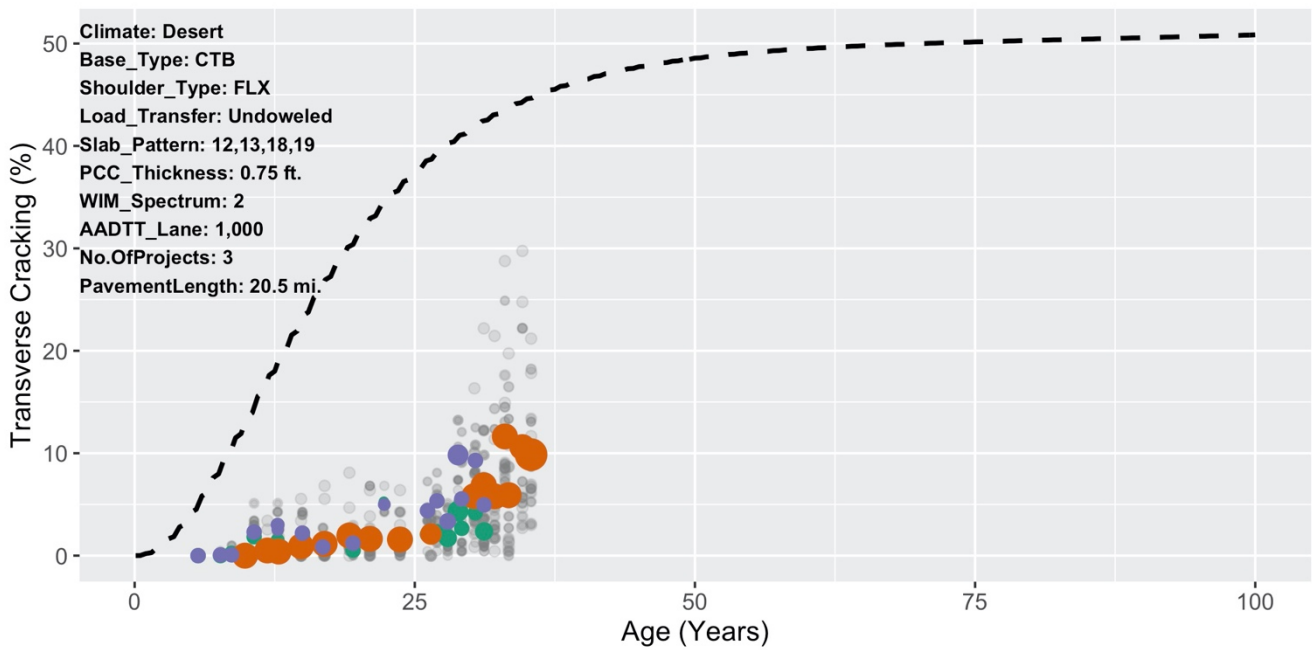


Figure 3.17: An example of long slab pattern performance data compared with *Pavement ME* transverse cracking model prediction showing overprediction error.

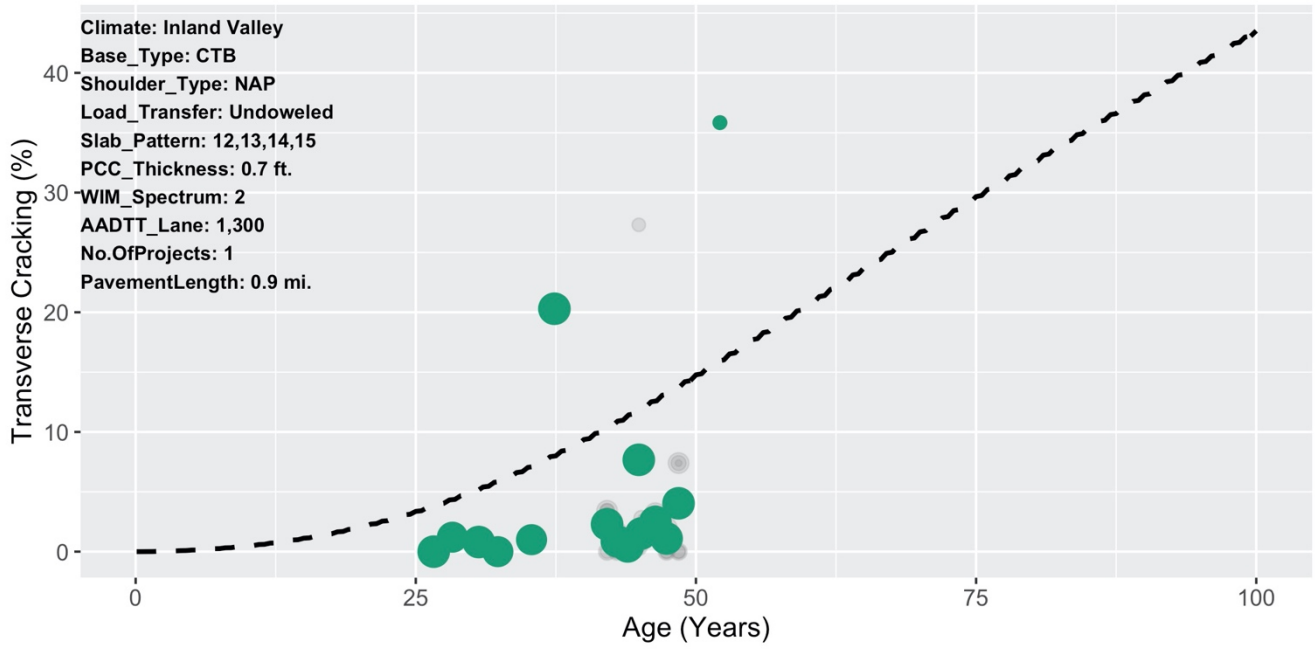


Figure 3.18: An example of short slab pattern performance data compared with *Pavement ME* transverse cracking model prediction showing overprediction error.

Figure 3.19 shows an example of *Pavement ME* transverse cracking model predictions for the short slab pattern that underpredicts the pavement performance.

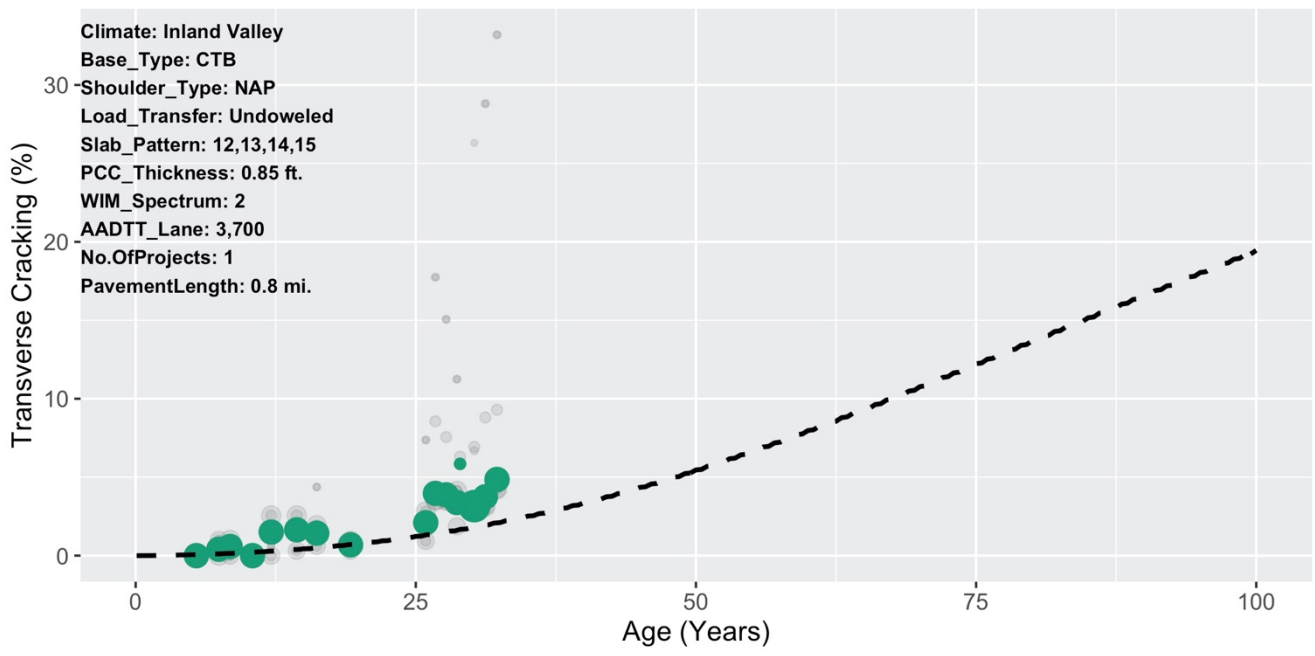


Figure 3.19: An example of short slab pattern performance data along with *Pavement ME* transverse cracking model prediction showing underprediction error.

3.5.7 Step 7: Identify WPV and BCV and Find Calibrated C_5

For determining WPV and BCV, those input variables that have significant effect on the transverse cracking prediction were used. Variables and their effects on the model prediction were investigated in the *Pavement ME Sensitivity Analysis (5)*. Three variables—PCC slab thickness, PCC compressive strength, and PCC coefficient of thermal expansion—that were believed to have a significant impact on the *Pavement ME* transverse cracking model prediction were selected to simulate WPV and BCV using the Monte Carlo simulation method discussed earlier in this chapter.

Based on the discussion in Section 3.4.1, a Monte Carlo simulation was performed on a few cells (not all cells, due to computational constraints) of data using variations in the three input variables mentioned above. The distributions for PCC compressive strength and PCC coefficient of thermal expansion were shown in Section 3.5.4. The standard deviation of within-project standard deviation for PCC slab thickness, SS_x , used to perform BCV is 0.03 ft. This variable was not discussed in Section 3.5.4 as it was not a non-design variable. However, it has variability in its measurements, and since it has significant effect on the *Pavement ME* transverse cracking model, it was included in the Monte Carlo simulation. For each variable two distributions were considered to choose random values as follows:

- $N(X, \sigma_x - SS_x)$
- $N(X, \sigma_x + SS_x)$

in which $N(\cdot)$ represents the normal distribution, X is the median of the variable under study, σ_x is the standard deviation of the variable representing WPV, and SS_x is the standard deviation of within-project standard deviation of the variable representing the BCV. Therefore, there will be eight combinations of variable distributions from which 100 (corresponding to 100 uniform segments) inputs are randomly drawn. Choosing randomly from these distributions simulates eight different projects that have the same median values for the variables of interests—which here are PCC compressive strength, PCC coefficient of thermal expansion, and PCC slab thickness—with different WPV.

Figure 3.20 shows an example of a Monte Carlo simulation performed on a cell of data. Each gray line represents the *Pavement ME* transverse cracking model prediction for randomly chosen values from eight combinations of input distributions mentioned above. The lines cover a wide range of performance due to WPV and BCV. Some segments show a rapid increase in the rate of cracking in the first few years of service life, whereas on the other side of spectrum some show barely any cracking in 100 years. The lines are shown with transparency to better illustrate their density.

In Figure 3.20, each line represents a specific slab length and input value. As mentioned earlier, 100 randomly selected sets of input variables were sampled from the distributions for concrete strength, CTE, and thickness as part of the Monte Carlo simulation; these correspond to 100 uniform segments of pavement. Taking the average performance from these 100 samples for each specific length and distribution, the expectation would be that they cross over the 50% cracking, as shown earlier in this chapter.

Figure 3.21 shows eight lines for each slab length, passing through 50% transverse cracking, after averaging the 100 runs. Each line corresponds to a combination of the three random input distributions used in this section to run Monte Carlo simulation. The pink, purple, orange, and green lines correspond to 15 ft., 14 ft., 13 ft., and 12 ft. slab lengths, respectively.

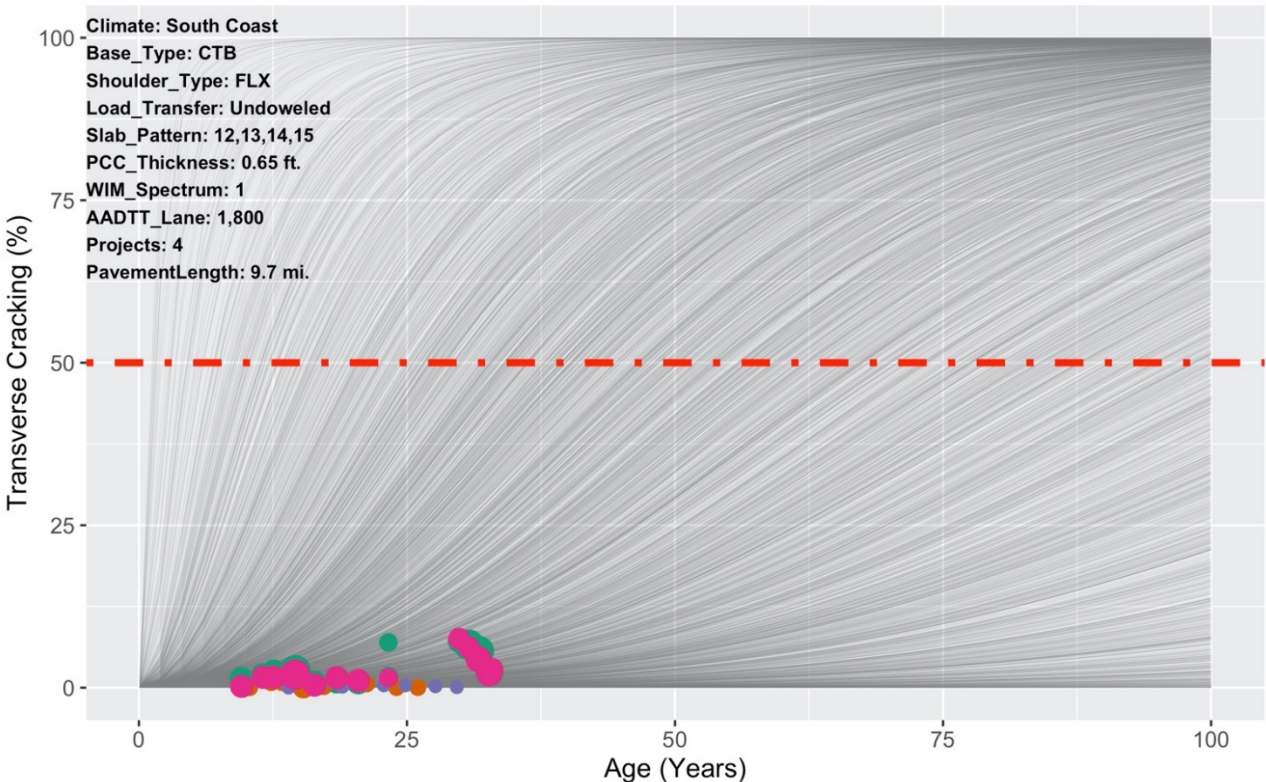


Figure 3.20: An example of a Monte Carlo simulation on a cell of data.

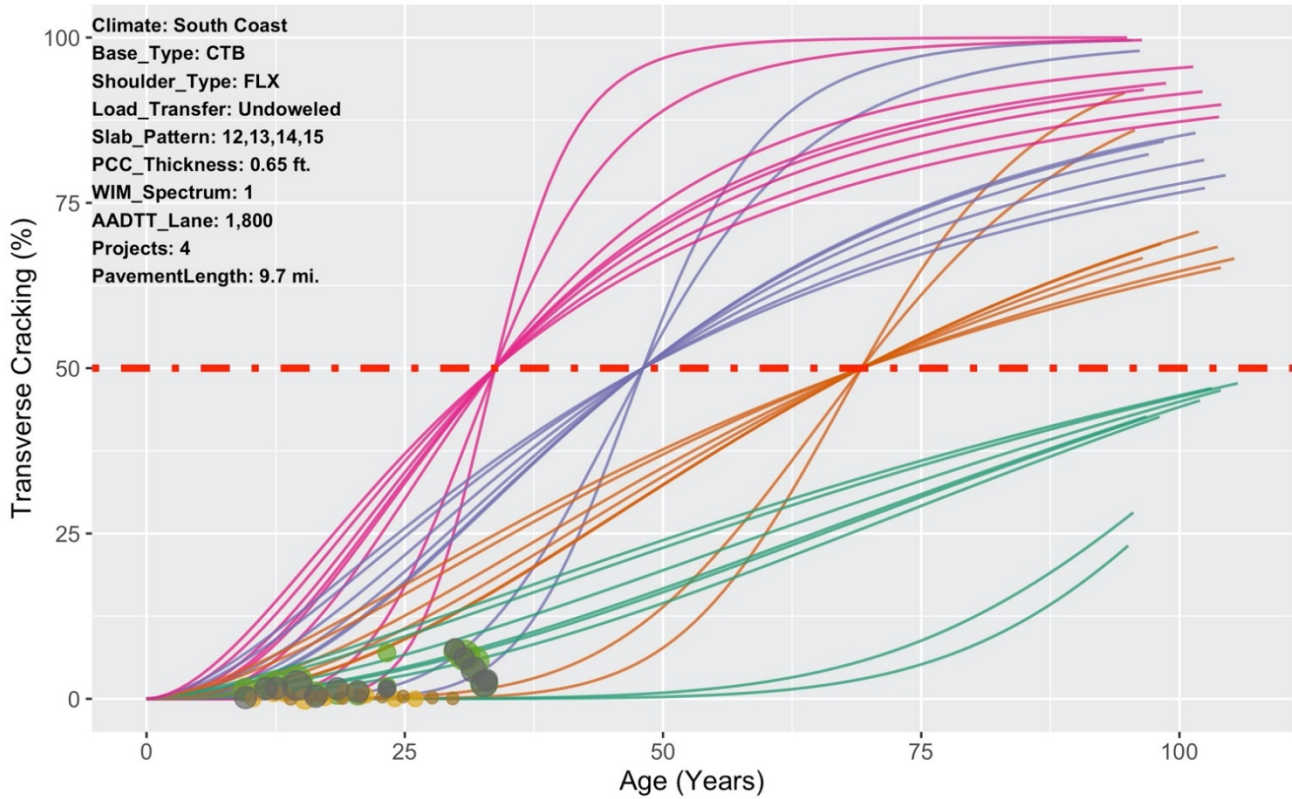


Figure 3.21: An example of Monte Carlo simulation on a cell of data grouped by slab length.

The C_5 coefficient directly affects the shape of the transfer function in *Pavement ME* and hence accounts for WPV and BCV. Therefore, running Monte Carlo simulations helps find the distribution for the C_5 values by using the median value as the calibrated coefficient. In order to find the distribution for the C_5 coefficient for each Monte Carlo run, the time to 50% cracking (t_{50}) is obtained using the damage calculated by *Pavement ME*. For each combination of input variables—PCC slab thickness, PCC coefficient of thermal expansion, and PCC compressive strength—100 input variables were chosen randomly. Therefore, there are 100 different t_{50} values corresponding to these runs. It is assumed that each run is a step function for a slab, and the t_{50} is the time that failure occurs, as shown in Figure 3.22. Each black line is a step function that shows the time at which the slab transversely cracked (corresponding to t_{50}). A logistic regression (which has an S shape) is fit to the data using t_{50} as a point on the logistic regression. The red line in Figure 3.22 is the logistic regression model fitted to the black step lines. Having this logistic regression, the C_5 coefficients and their distributions can be obtained by performing simple mathematical operations.

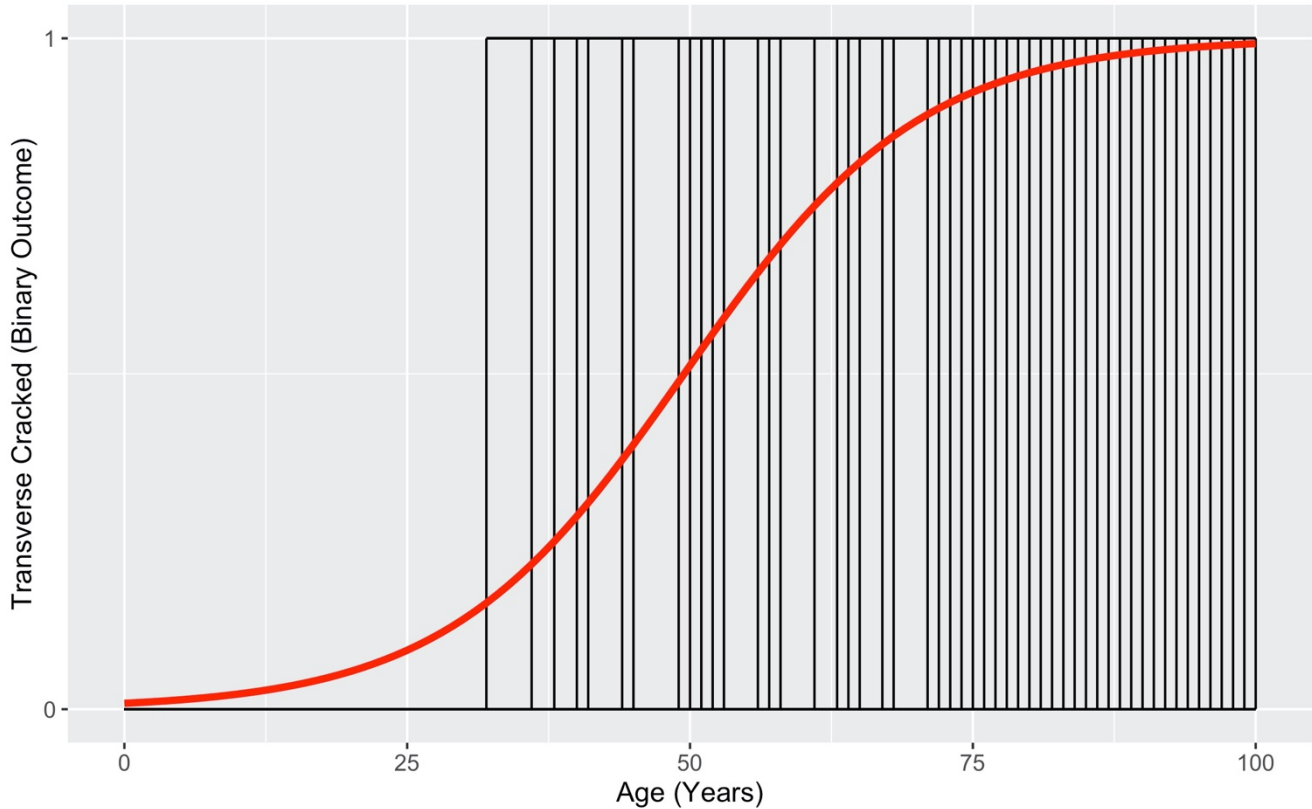


Figure 3.22: Schematic representation of cracked slabs and fitted logistic regression model.

Since *Pavement ME* has distinct predictions for short and long slab patterns, this procedure has been done separately for each slab pattern, and the C_5 distribution was obtained for both slab patterns as follows:

- Short slab pattern: $C_5 \sim N(-2.37, 2.18)$
- Long slab pattern: $C_5 \sim N(-2.56, 2.39)$

The C_5 coefficient for short slabs has a median of -2.37 and a standard deviation of 2.18, and the C_5 for long slabs a median of -2.56 and a standard deviation of 2.39. As these coefficients are fairly similar, a decision was made to use a single C_5 coefficient with a median of -2.37 for both slab patterns. This value is very close to -2.17, the nationally calibrated coefficient.

3.5.8 Step 8: Identify Between-Project Variability and Find Calibrated C_4

In Section 2.4, the statistical performance model and how it estimates between-project variability (BPV) were discussed. This statistical performance model will be used to account for BPV and to calibrate the *Pavement ME* transfer function for C_4 .

Figure 3.23 is repeated here from Chapter 2 (Figure 2.26) to illustrate the procedure followed to obtain the calibrated C_4 coefficient while accounting for BPV. Figure 3.23 is a cell of data that contains three different projects shown in different colors. It is clear that these projects have different cracking performance caused by errors in the estimation of the design variables and/or effects that cannot be explained with the design variables shown on the top left of the figure. This randomness in cracking performance is considered in developing the statistical model by assigning a random variable to each project and by estimating the random project variable by iteratively maximizing the log of likelihood. The colored lines are the statistical model predictions for each project considering the individual fit of the random effect between projects (BPV) due to some unknown variables (i.e., PCC compressive strength, PCC coefficient of thermal expansion, etc.) and the dashed line is the expected (average) behavior of a pavement section with this random effect (BPV) removed and replaced by the median value for those unknown variables. For the cell shown, all three projects had worse performance than when median properties are assumed for the unknown variables. Therefore, to account for BPV, this unknown source of randomness should be accounted for in C_4 calibration.

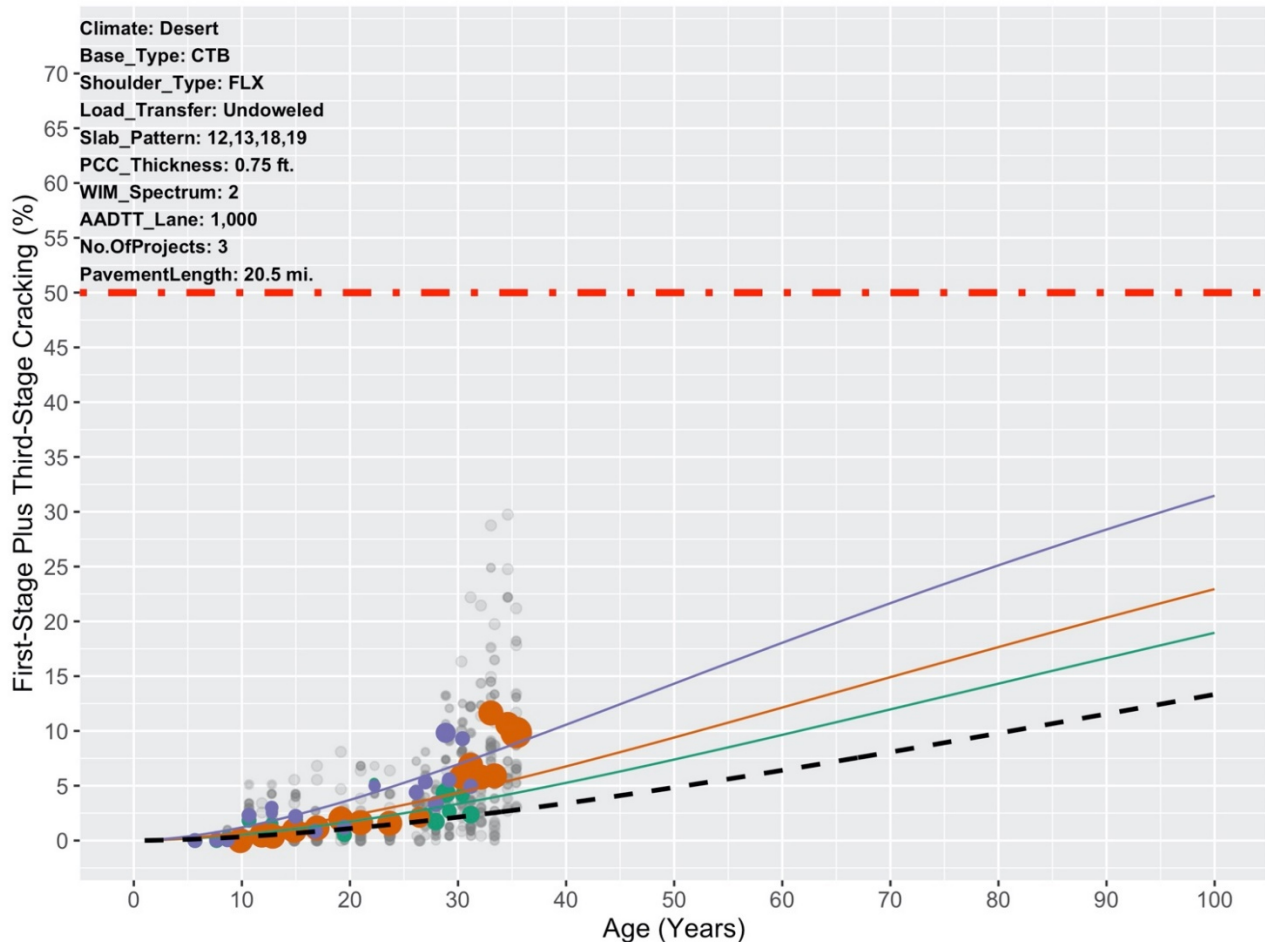


Figure 3.23: Mixed-effects cracking performance model predictions for a cell of data.

To achieve this goal, the colored lines should be shifted so that they lie on the dashed line. Therefore, time to 50% cracking ($t_{50-expected}$) as a reference point was calculated for the dashed line using the statistical model developed in Section 2.4. The same procedure was followed to find $t_{50-project}$ for each individual project. Having these values, the *scale factors* (the amount of shift specific to each project) are used to shift each individual project to match the expected performance using the median values for the unknown variables. The scale factors can be calculated as:

$$SC_i = \frac{t_{50-expected}}{t_{50-project_i}} \quad (3.12)$$

in which SC_i is the scale factor corresponding to project i ; $t_{50-expected}$ is the expected time (without BPV) to 50% cracking for a pavement with known variables such as PCC thickness, slab pattern, base type, shoulder type, AADTT per lane, and climate used in the statistical performance model; and $t_{50-project_i}$ is the time (with BPV) to 50% cracking for a pavement in project i .

For the data shown in Figure 3.23, $t_{50-expected}$ is about 190 years, and $t_{50-project_i}$ for the projects are about 90, 122, and 144 years. Using these numbers, the scale factors for these projects are 2.11, 1.55, and 1.31, respectively. These scale factors are used to account for BPV to shift each project performance to match the expected performance. Figure 3.24 shows the performance data after BPV adjustment. It shows that all the data along with colored lines (statistical model performance prediction with BPV) are shifted and lie along the expected performance prediction (dashed line).

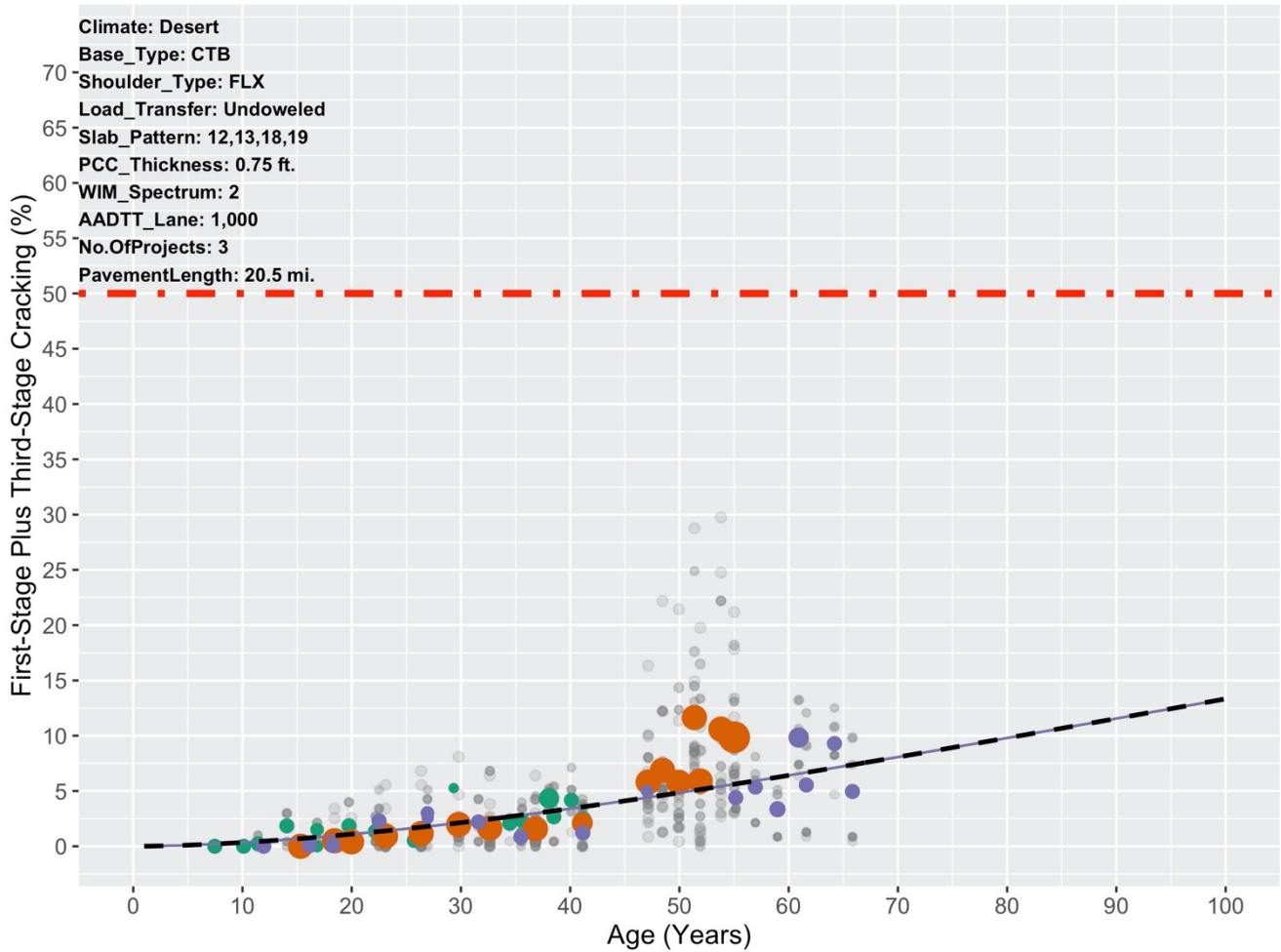


Figure 3.24: The expected (average) performance of the pavement after removing BPV.

Using this process, BPV has been removed from the data, which is a preliminary step for C_4 calibration. One should note that the C_4 obtained through this process corresponds to 50% reliability, as the scale factors shift the data to the expected (average) performance using the statistical model. With BPV removed, the data will be used to minimize the *Pavement ME* transverse cracking model prediction bias shown below:

$$\text{Bias} = \Sigma(y_i - \hat{y}_i) \tag{3.13}$$

in which y_i is the actual transverse cracking percentage measured from the field (PaveM data) and \hat{y}_i is the predicted transverse cracking value by *Pavement ME* model.

As stated earlier, two sets of calibrated C_4 are computed for the two slab patterns due to the significant difference in their transverse cracking performance. Table 3.1 shows the C_4 coefficients calculated corresponding to 50% reliability.

Table 3.1: Calibrated C_4 for 50% Reliability

Slab Pattern	Calibrated C_4 for 50% Reliability
12,13,14,15 ft.	4.129
12,13,18,19 ft.	468.755

3.5.9 Step 9: Find C_4 Corresponding to 95% Reliability

Looking at the statistical model developed in Chapter 2 and shown in Equation 2.2, the $u(project_i)$ is the between-project variability (BPV) assigned to each project in the model. In fitting the model, this random effect is assumed to have a normal distribution $u(project_i) \sim N(0, \sigma)$. The standard deviation was calculated to be 1.15.

In the previous step, to account for BPV, all individual project data were shifted to the average (expected value) performance. Applying the expected value function ($E(.)$) to Equation 2.2 also resulted in the average performance. This is because the $E(u(project_i)) = 0$; therefore, randomness is accounted for in the calibration process and the resulting function corresponds to 50% reliability.

To find the C_4 that corresponds to 95% reliability, the performance data should be adjusted (shifted) to a project such that 95% of projects had better cracking performance. This was done by looking at the distribution of BPV ($u(project_i)$) in the statistical model and using the value that 95% of the random effect variables fall below. Figure 3.25 shows the distribution of this variable obtained from the statistical model.

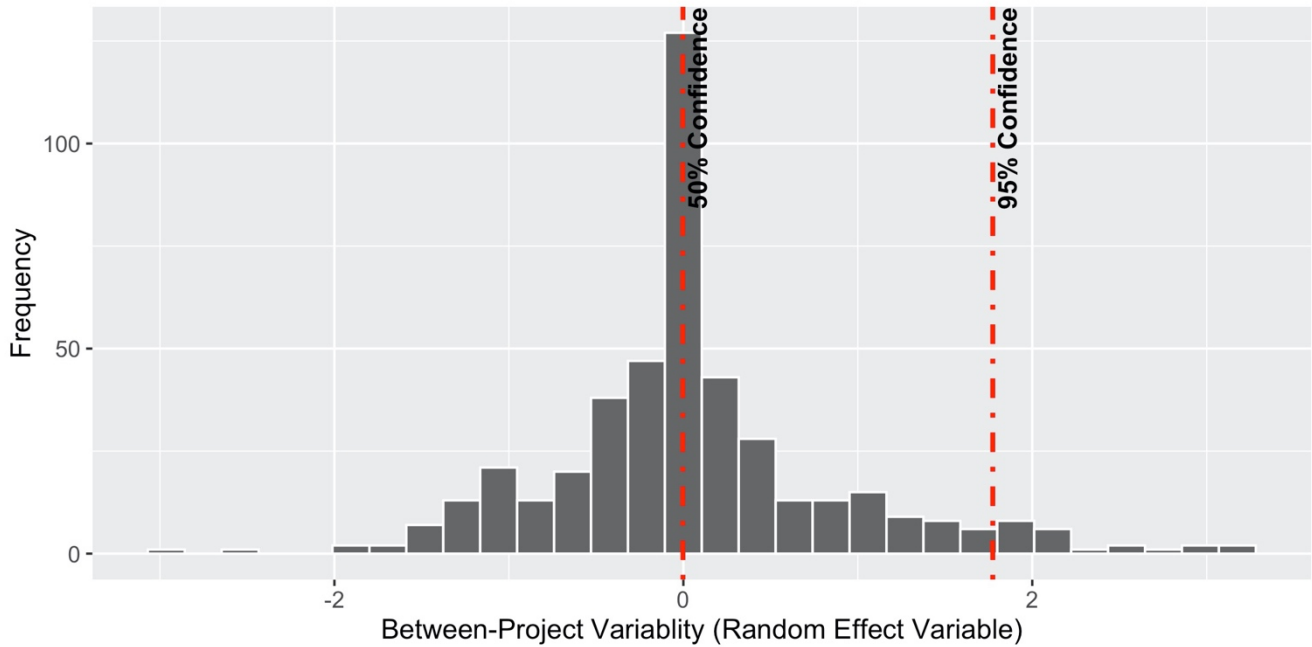


Figure 3.25: Distribution of random effect variable in mixed-effects cracking performance model.

Having BPV correspond to the project at which 95% of the projects in the PavEM database had better performance, the $t_{50-95\%conf}$ for each cell of data can be calculated using the first- and third-stage cracking performance model.

Using $t_{50-95\%conf}$, the scale factor equation becomes:

$$SC_i = \frac{t_{50-95\%conf}}{t_{50-project_i}} \quad (3.14)$$

in which $t_{50-95\%conf}$ is the time to 50% cracking for the project that performed worse than 95% of the rest of the projects in the PavEM database. Using this scale factor, the rest of the calibration process for 95% reliability is the same as the previous step. The following are the C_4 coefficients calculated corresponding to 95% between-project reliability.

Table 3.2: Calibrated C_4 for 95% Between-Project Reliability

Slab Pattern	Calibrated C_4 for 95% Between-Project Reliability
12,13,14,15 ft.	0.217
12,13,18,19 ft.	33.172

Figure 3.26 shows that a *Pavement ME* prediction for a 50% reliability nationally calibrated model (dashed line) and for 50% (solid black line) and 95% (red line) reliability locally calibrated models, for one specific Pavem long slab cell of data.

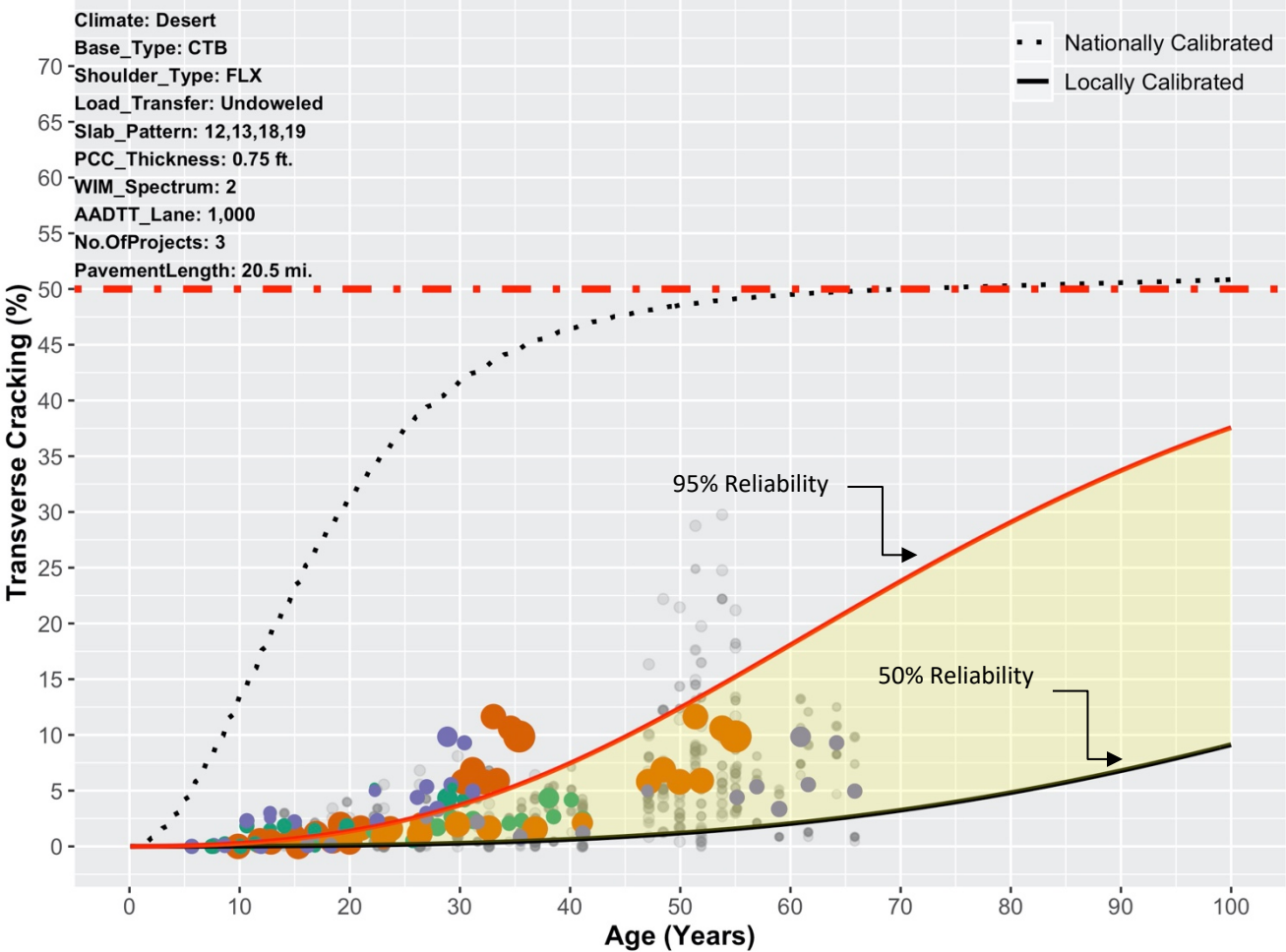


Figure 3.26: Example of locally calibrated *Pavement ME* transverse cracking model prediction with 50% and 95% reliabilities for long slab pattern for one cell.

Figure 3.27 shows an example of *Pavement ME* calibrated model prediction for short slab pattern.

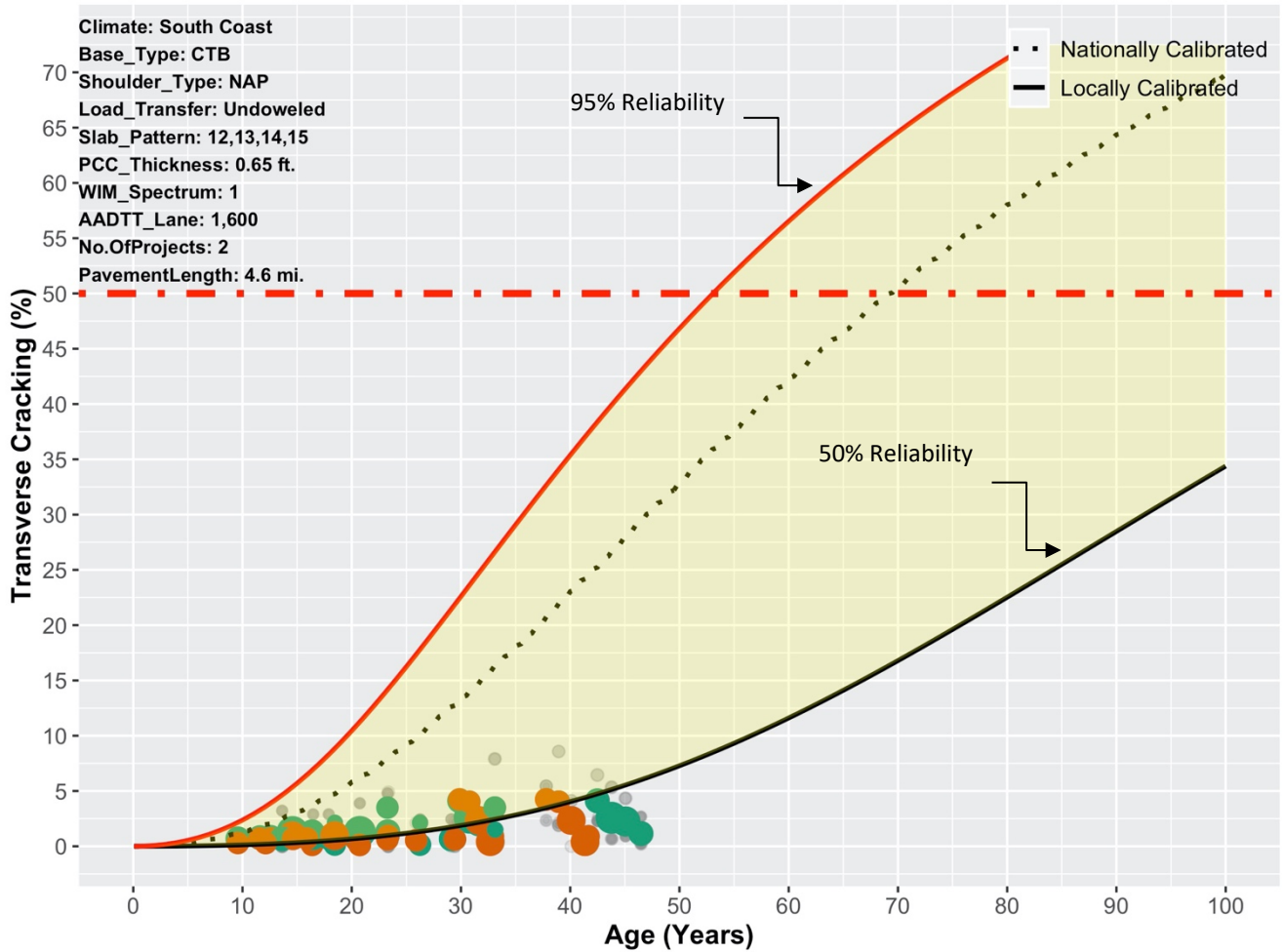


Figure 3.27: Example of locally calibrated *Pavement ME* transverse cracking model prediction with 50% and 95% reliabilities for short slab pattern for all cells as seen applied to one cell.

3.5.10 Step 10: Analyze Calibrated Model Error

Figure 3.28 and Figure 3.29 show the *Pavement ME* transverse cracking predictions (50% reliability) against the actual data collected from the field. The size of each data point represents the amount of data it contains in lane-miles. It is clear that the nationally calibrated *Pavement ME* tends to overpredict the amount of transverse cracking, as most of the data lies above the line of equality (red line). After calibration the bias has decreased from 13.3% to 0.039%, and it can be seen in Figure 3.29 that the data is now well distributed around the equality line. The standard error has also significantly decreased from 23.03% to 5.62%.

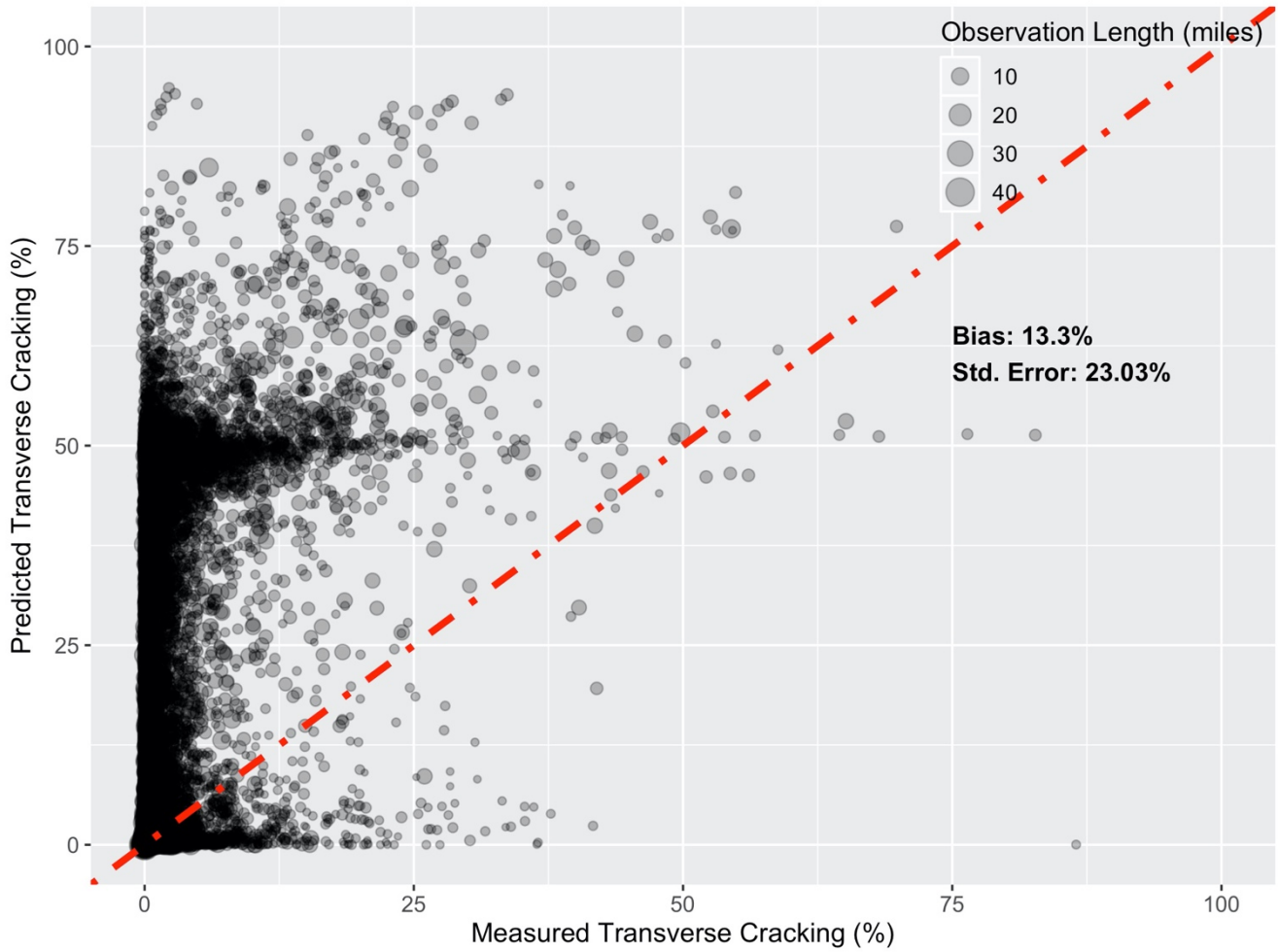


Figure 3.28: Predicted transverse cracking from nationally calibrated *Pavement ME* transverse cracking model versus measured transverse cracking.

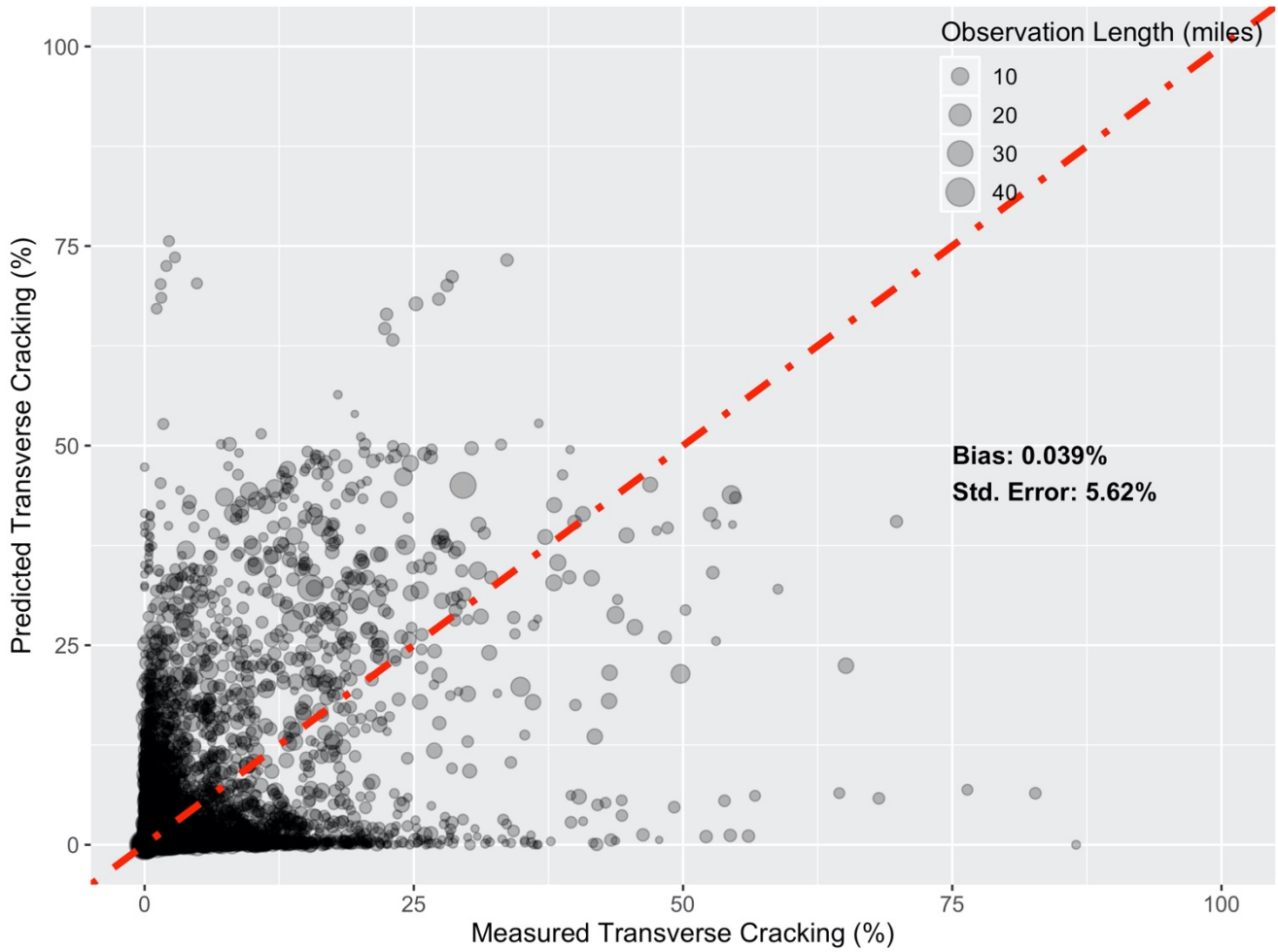


Figure 3.29: Predicted transverse cracking from locally calibrated *Pavement ME* transverse cracking model versus measured transverse cracking.

4 SUMMARY, CONCLUSIONS, AND RECOMMENDATIONS

4.1 Summary

In this study, the *Pavement ME* (V2.5.5) transverse cracking model for jointed plain concrete pavements was calibrated. A very large performance database with data collected from California's highway network as part of the annual condition survey was used for the calibration.

The calibration of the *Pavement ME* faulting model in 2007 (3) on undoweled jointed plain concrete pavements (JPCP) and using faulting measurements made by the University of California Pavement Research Center (UCPRC) with a high-speed profiler moving at slow speeds showed that the national faulting model for undoweled pavement did a good job of predicting performance on California pavements. This is likely due in part to the fact that a large part of the calibration of that model was done on California sections, which were used because most other states had switched to using dowels much earlier than California. For the following reasons, only the transverse cracking model was calibrated in this study:

- There were not enough sections with good faulting history data (built prior to 1998), and JPCP built since 1998 generally does not have faulting according to the Automated Pavement Condition Survey (APCS) data in the Pavem pavement management system (PMS) database.
- Caltrans constructs doweled JPCP exclusively, and faulting is not a major problem for these pavements.
- The faulting model in *Mechanistic-Empirical Pavement Design Guide (MEPDG)* matched well with Caltrans data in 2006 for undoweled concrete. The model coefficients have changed since a calibration study in 2007 (3); however, the current model predictions have changed very slightly since the last calibration.
- International Roughness Index (IRI) on doweled concrete pavement is primarily a function of the IRI achieved in construction.

Historically, Caltrans collected first- and third-stage cracking data as part of its manual pavement condition surveys. Caltrans defines first-stage cracking as a single crack that divides a slab into two pieces. This crack can be either transverse or longitudinal. Third-stage cracking is defined as a state of cracking that divides a slab into three or more pieces. Almost all third-stage cracking in California consists of either two transverse cracks or a transverse and a longitudinal crack. The *Pavement ME* transverse cracking model predicts only the amount of transverse cracking that will occur in JPCP. Therefore, a model was needed to predict the portion of first-stage cracking that is transverse cracking.

The APCS 2010–2011 has per-slab information on first-stage, transverse, and longitudinal cracking data. A model was developed based on this dataset to predict the transverse cracking percentage of pavements with first-stage cracking. Using this model, the amount of transverse cracking could be computed from first-stage cracking data. The computed transverse cracking will be added to third-stage cracking (which has at least one transverse crack) to calculate total transverse cracking. Total transverse cracking data will be used to calibrate the *Pavement ME* transverse cracking model.

In addition to the first-stage-to-transverse cracking model, a performance model was developed to predict the amount of first- and third-stage cracking. This model was used to account for variabilities involved in JPCP performance, and these variabilities were used in the new calibration approach.

The goal of the *Pavement ME* transverse cracking model calibration was to find a set of model coefficients that minimizes model prediction error with observed cracking data. Traditionally, *Pavement ME* models have been calibrated with a small number of JPCP sections (hundreds) for which all the design and non-design variables were known (or collected). Design variables are those such as portland cement concrete (PCC) slab thickness, PCC slab length, base type, and shoulder type that can be determined by the pavement designer prior to construction. Non-design variables such as PCC compressive strength, PCC modulus of rupture, and PCC coefficient of thermal expansion are those that are unknown to the designer.

Traditional *Pavement ME* calibration has limitations that do not permit the use of very large performance databases from pavement management systems such as California's *PaveM*. It does not include consideration of the independent variabilities between projects and within projects of pavement performance, and therefore the traditionally calibrated models predict reasonable average performance while they underestimate the variability. Another limitation of the traditional calibration procedure is the requirement of using project-specific inputs that in practice are not known to the designer and are not present in the pavement management system database. This means field sampling and material testing are needed to determine inputs. This limits the number of roadway segments that can be included in the calibration and therefore may lead to underestimation of model error and input error. Despite the use of design variable inputs, large residual errors are typically encountered in past calibration efforts. These large errors may be attributed to two reasons: (1) the model adopted has significant amount of error and/or (2) the inputs to the model have errors. Both reasons seem highly likely. With these challenges, and the very large dataset that Caltrans has built into *PaveM*, a new calibration approach was introduced in this study that uses the extensive Caltrans performance database while accounting for the variabilities caused by unknown (non-design) variables.

The new approach considers the variabilities involved in JPCP performance—such as between-project variability, within-project variability, and between-contractor variability—to produce more reliable results. These variabilities will be used in the *Pavement ME* transverse cracking model predictions in the forthcoming Caltrans JPCP design catalog. After calibrating the *Pavement ME* transverse cracking model, the model’s average error for the percent of slabs cracked has been reduced from 13.3 to 0.039 for predicted versus observed transverse cracking.

An updated design catalog will be developed based on the design variable factorial that will be determined by consulting with Caltrans to meet its future JPCP design needs. The design catalog will use calibrated *Pavement ME* transverse cracking model predictions with 50% and 95% reliabilities.

4.2 Conclusions

During development of a first- and third-stage cracking performance model, the following were found from the performance data:

- JPCP with thicker and shorter slabs performs much better than JPCP with thinner and longer slabs, as was previously known and expected.
- Neither the presence nor the absence of dowels in a JPCP impacts its cracking performance.
- Among JPCP base types, lean concrete base (LCB) has the poorest cracking performance, and cement-treated base (CTB) and hot mix asphalt (HMA) have the best.
- JPC pavements with untied flexible (FLX) shoulders and with no shoulders (NAP) show more cracking than JPCPs with tied concrete shoulders (RIG). JPCP with widened concrete shoulders (WRF) do not perform well, and the statistical model predicts performance similar to FLX shoulders. This is due to the fact that widened shoulders used to be constructed in 14 ft. slabs, which are susceptible to longitudinal cracking.
- The JPCP in the Inland Valley, High Mountain, and South Mountain climate regions have the worst performance among all the California climate regions. The best JPCP performance occurs in the South Coast, Central Coast, High Desert, and Desert regions. The Low Mountain region falls between the two.
- The weigh-in-motion (WIM) spectra effect does not follow the expected trend of higher WIM levels causing more cracking. WIM Spectra 3 and 4 cause more cracking than WIM Spectra 5.
- The model predicts more cracking under higher average annual daily truck traffic (AADTT) per lane, as expected.
- The *Pavement ME* transverse cracking model tends, in general, to overpredict the amount of transverse cracking by about 13%. This bias is 19% for JPCPs with the long slab pattern but just 3.3% for those with

the short slab pattern. Therefore, due to these distinct trends in *Pavement ME* transverse cracking model predictions, two separate sets of model coefficients were obtained for the different slab patterns.

4.3 Recommendations

There are two important variables—PCC coefficient of thermal expansion and PCC compressive strength—that were not available for calibration and that had a significant impact on the *Pavement ME* transverse cracking model prediction. The designer of a JPCP project does not know these variables prior to construction; the designer only knows the minimum specified values. Use of the minimum specified values will tend to impart additional unquantifiable conservatism into the designs. The distribution of measured strengths, translated to flexural strengths, was considered in the calibration and will be considered in the updated Caltrans JPCP design catalog. The new approach presented in this study accounts for the uncertainties produced by these unknown factors by incorporating different types of variabilities in the calibration process and hence different levels of reliabilities in the model predictions. However, having better data for these variables from projects in California in the future will definitely reduce the calibrated model errors for future calibrations.

The WIM spectra that were believed to have a significant impact on JPCP performance (i.e., higher level WIM Spectra 4 and 5 cause less cracking) were found to have an opposite effect in first- and third-stage cracking performance model development. This data should be fixed in the Pavem database for better future performance model development and *Pavement ME* calibrations.

5 REFERENCES

1. National Cooperative Highway Research Program. 2003. *Guide for Mechanistic-Empirical Pavement Design of New and Rehabilitated Pavement Structures*. Washington, DC: National Cooperative Highway Research Program.
2. Kannekanti, V., and Harvey, J. 2006. *Sensitivity Analysis of 2002 Design Guide Rigid Pavement Distress Prediction Models* (Design Guide: UCPRC-DG-2006-01). Davis and Berkeley, CA: University of California Pavement Research Center. <https://escholarship.org/uc/item/0zw2b8n4>.
3. Kannekanti, V. and Harvey, J.T. 2007. *Field Calibration of MEPDG JPCP Distress Prediction Models* (Research Report: UCPRC-RR-2007-02). Davis and Berkeley, CA University of California Pavement Research Center.
4. Kannekanti, V., and Harvey, J. 2006. *Sample Rigid Pavement Design Tables Based on Version 0.8 of the Mechanistic-Empirical Pavement Design Guide* (Technical Memorandum: UCPRC-TM-2006-04). Davis and Berkeley, CA: University of California Pavement Research Center. https://escholarship.org/uc/item/21g3r9rz_
5. Saboori, A., Harvey, J. T., Lea, J. D., Lea, J., Wu, R., and Mateos, A. 2020. *Pavement ME Sensitivity Analysis (Version 2.5.3)* (Research Report: UCPRC-RR-2019-02). Davis and Berkeley, CA: University of California Pavement Research Center. <https://escholarship.org/uc/item/6bv7d7t6>.
6. Harvey, J., Roesler, J., Farver, J., and Liang, L. 2000. *Preliminary Evaluation of Proposed LLPRS Rigid Pavement Structures and Design Inputs* (Paper No.: FHWA/CA/OR-2000/02). Berkeley, CA: Pavement Research Center and Institute of Transportation Studies, University of California at Berkeley. <https://escholarship.org/uc/item/933855pc>.
7. Lea, J.D. Forthcoming. Development of a Comprehensive Set of Performance Models for the Caltrans PMS: Part B. Davis and Berkeley, CA: University of California Pavement Research Center.
8. Kim, C., Lea, J.D., Kannekanti, V., and Harvey, J.T. 2018. *Updating Weigh-in-Motion (WIM) Spectra in Pavem* (Technical Memorandum: UCPRC-TM-2018-01). Davis and Berkeley, CA: University of California Pavement Research Center.
9. Saboori, A., Lea, J.D., Kannekanti, V. Saboori, A., and Harvey, J.T. 2018. “Development of a Cracking Performance Prediction Model for Replaced Concrete Slabs in California.” Presented at Transportation Research Board Annual Meeting, Washington, DC, January 7–11, 2018.
10. Tseng, E. 2012. “The Construction of Pavement Performance Models for Flexible Pavement Wheelpath Cracking and IRI for the California Department of Transportation New Pavement Management System.” Master’s thesis, University of California, Davis.
11. Christensen, R.H.B. n.d. “ordinal: Regression Models for Ordinal Data.” Regression Models for Ordinal Data, R package version 2015.6-28. <https://cran.r-project.org/web/packages/ordinal/index.html>.

12. Lederle, R.E. 2014. "Development of a Longitudinal Cracking Fatigue Damage Model for Jointed Plain Concrete Pavements Using the Principles of Similarity." PhD dissertation., University of Minnesota. <https://conservancy.umn.edu/handle/11299/170149>.
13. Macleod, D.R., and Monismith, C.L. 1979. *Performance of Portland Cement Concrete Pavement*. Berkeley, CA: Department of Civil Engineering, Institute of Transportation Studies, University of California, Berkeley.
14. Rezaei, A., and Harvey, J. 2013. *Investigation of Tire/Pavement Noise for Concrete Pavement Surfaces: Summary of Four Years of Measurements* (Research Report: UCPRC-RR-2013-12). Davis and Berkeley, CA: University of California Pavement Research Center. <https://escholarship.org/uc/item/99h8c6gp>.
15. American Association of State Highway Transportation Officials. 2010. *Guide for the Local Calibration of the Mechanistic-Empirical Pavement Design Guide*. Washington, DC: American Association of State Highway Transportation Officials.